IEC 61788-7

Edition 3.0 2020-03
REDLINE VERSION

INTERNATIONAL STANDARD

colour inside

Superconductivity –
Part 7: Electronic characteristic measurements – Surface resistance of high-temperature superconductors at microwave frequencies

IEC 61788-7:2020-03 RLV (en)

IEC Central Office
3, rue de Varembé
CH-1211 Geneva 20
Switzerland

Tel.: +41 22 919 02 11
info@iec.ch
www.iec.ch

About the IEC
The International Electrotechnical Commission (IEC) is the leading global organization that prepares and publishes International Standards for all electrical, electronic and related technologies.

About IEC publications
The technical content of IEC publications is kept under constant review by the IEC. Please make sure that you have the latest edition, a corrigendum or an amendment might have been published.

IEC publications search - webstore.iec.ch/advsearchform
The advanced search enables to find IEC publications by a variety of criteria (reference number, text, technical committee,…). It also gives information on projects, replaced and withdrawn publications.

IEC Just Published - webstore.iec.ch/justpublished
Stay up to date on all new IEC publications. Just Published details all new publications released. Available online and once a month by email.

IEC Customer Service Centre - webstore.iec.ch/csc
If you wish to give us your feedback on this publication or need further assistance, please contact the Customer Service Centre: sales@iec.ch.

Electropedia - www.electropedia.org
The world's leading online dictionary on electrotechnology, containing more than 22 000 terminological entries in English and French, with equivalent terms in 16 additional languages. Also known as the International Electrotechnical Vocabulary (IEV) online.

IEC Glossary - std.iec.ch/glossary
67 000 electrotechnical terminology entries in English and French extracted from the Terms and Definitions clause of IEC publications issued since 2002. Some entries have been collected from earlier publications of IEC TC 37, 77, 86 and CISPR.

IEC 61788-7

Edition 3.0 2020-03
REDLINE VERSION

INTERNATIONAL STANDARD

Superconductivity –
Part 7: Electronic characteristic measurements – Surface resistance of high-temperature superconductors at microwave frequencies

INTERNATIONAL
ELECTROTECHNICAL
COMMISSION

ICS 17.220.20; 29.050

ISBN 978-2-8322-7917-5

Warning! Make sure that you obtained this publication from an authorized distributor.

CONTENTS

INTERNATIONAL ELECTROTECHNICAL COMMISSION

SUPERCONDUCTIVITY –

Part 7: Electronic characteristic measurements – Surface resistance of high-temperature superconductors at microwave frequencies

FOREWORD

1) The International Electrotechnical Commission (IEC) is a worldwide organization for standardization comprising all national electrotechnical committees (IEC National Committees). The object of IEC is to promote international co-operation on all questions concerning standardization in the electrical and electronic fields. To this end and in addition to other activities, IEC publishes International Standards, Technical Specifications, Technical Reports, Publicly Available Specifications (PAS) and Guides (hereafter referred to as "IEC Publication(s)"). Their preparation is entrusted to technical committees; any IEC National Committee interested in the subject dealt with may participate in this preparatory work. International, governmental and non-governmental organizations liaising with the IEC also participate in this preparation. IEC collaborates closely with the International Organization for Standardization (ISO) in accordance with conditions determined by agreement between the two organizations.
2) The formal decisions or agreements of IEC on technical matters express, as nearly as possible, an international consensus of opinion on the relevant subjects since each technical committee has representation from all interested IEC National Committees.
3) IEC Publications have the form of recommendations for international use and are accepted by IEC National Committees in that sense. While all reasonable efforts are made to ensure that the technical content of IEC Publications is accurate, IEC cannot be held responsible for the way in which they are used or for any misinterpretation by any end user.
4) In order to promote international uniformity, IEC National Committees undertake to apply IEC Publications transparently to the maximum extent possible in their national and regional publications. Any divergence between any IEC Publication and the corresponding national or regional publication shall be clearly indicated in the latter.
5) IEC itself does not provide any attention of conformity. Independent certification bodies provide conformity assessment service and, in some areas access to IEC marks of conformity. IEC is not responsible for any services carried out by independent certification bodies.
6) All users should ensure that they have the latest edition of this publication.
7) No liability shall attach to IEC or its directors, employees, servants or agents including individual experts and members of its technical committees and IEC National Committees for any personal injury, property damage or other damage of any nature whatsoever, whether direct or indirect, or for costs (including legal fees) and expenses arising out of the publication, use of, or reliance upon, this IEC Publication or any other IEC Publications.
8) Attention is drawn to the normative references cited in this publication. Use of the referenced publications is indispensable for the correct application of this publication.
9) Attention is drawn to the possibility that some of the elements of this IEC Publication may be the subject of patent rights. IEC shall not be held responsible for identifying any or all such patent rights.

This redline version of the official IEC Standard allows the user to identify the changes made to the previous edition. A vertical bar appears in the margin wherever a change has been made. Additions are in green text, deletions are in strikethrough red text.

International Standard IEC 61788-7 has been prepared by IEC technical committee 90: Superconductivity.

This third edition cancels and replaces the second edition, published in 2006. This edition constitutes a technical revision.

This edition includes the following significant technical changes with respect to the previous edition:

a) informative Annex B, relative combined standard uncertainty for surface resistance measurement has been added;
b) precision and accuracy statements have been converted to uncertainty;
c) reproducibility in surface resistant measurement has been added.

The text of this International Standard is based on the following documents:

FDIS	Report on voting
90/447/FDIS	90/452/RVD

Full information on the voting for the approval of this International Standard can be found in the report on voting indicated in the above table.

This document has been drafted in accordance with the ISO/IEC Directives, Part 2.

A list of all parts of the IEC 61788 series, published under the general title *Superconductivity*, can be found on the IEC website.

The committee has decided that the contents of this document will remain unchanged until the maintenance result date indicated on the IEC web site under "http://webstore.iec.ch" in the data related to the specific publication. At this date, the document will be

- reconfirmed;
- withdrawn;
- replaced by a revised edition, or
- amended.

IMPORTANT – The 'colour inside' logo on the cover page of this publication indicates that it contains colours which are considered to be useful for the correct understanding of its contents. Users should therefore print this document using a colour printer.

INTRODUCTION

Since the discovery of some Perovskite-type Cu-containing oxides, extensive research and development (R & D) work on high-temperature oxide superconductors (HTS) has been, and is being, done worldwide, and its application to high-field magnet machines, low-loss power transmission, electronics and many other technologies is in progress.

In various fields of electronics, especially in telecommunication fields, microwave passive devices such as filters using oxide superconductors HTS are being developed and are undergoing on-site testing [1][2][1].

Superconductor materials for microwave resonators [3], filters [4],, antennas [5] and delay lines [6] have the advantage of very low loss characteristics. The parameters of superconductor materials needed for the design of microwave low loss components are the surface resistance, (R_s) and the temperature dependence of the R_s. Knowledge of this parameter is of primary importance for the development of new materials on the supplier side and for the design of superconductor microwave components on the customer side.

Recent advances in high Tc superconductor (HTS) thin films with R_s R_s of high quality HTS films is generally several orders of magnitude lower than that of normal metals [7] [8] [9] [10], have which has increased the need for a reliable characterization technique to measure this property [3,4]. Traditionally, the R_s of niobium or any other low-temperature superconducting material was measured by first fabricating an entire three-dimensional resonant cavity and then measuring its Q-value [11]. The R_s could be calculated by solving the electro-magnetic field (EM) distribution inside the cavity. Another technique involves placing a small sample inside a larger cavity. This technique has many forms but usually involves the uncertainty introduced by extracting the loss contribution due to the HTS films from the experimentally measured total loss of the cavity.

The best HTS samples are epitaxial films grown on flat crystalline substrates and no high-quality films have been grown on any curved surface so far. What is needed is a technique that: can use these small flat samples; requires no sample preparation; does not damage or change the film; is highly repeatable; has great sensitivity (down to 1/1 000 the R_s of copper); has great dynamic range (up to the R_s of copper); can reach high internal powers with only modest input powers; and has broad temperature coverage (4,2 K to 150 K).

The dielectric resonator method is selected among several methods [5,6,7] to determine the surface resistance at microwave frequencies because it is considered to be the most popular and practical at present. Especially, the sapphire resonator is an excellent tool for measuring the R_s of HTS materials [8,9] [12] [13] [14].

The test method given in this document can also be applied to other superconductor bulk plates including low T_c materials.

This document is intended to provide an appropriate and agreeable technical base for the time being to engineers working in the fields of electronics and superconductivity technology.

The test method covered in this document is based on the VAMAS (Versailles Project on Advanced Materials and Standards) pre-standardization work on the thin film properties of superconductors.

1 Numbers in square brackets refer to the bibliography.

SUPERCONDUCTIVITY –

Part 7: Electronic characteristic measurements – Surface resistance of high-temperature superconductors at microwave frequencies

1 Scope

This part of IEC 61788 describes measurement of the surface resistance (R_s) of superconductors at microwave frequencies by the standard two-resonator method. The object of measurement is the temperature dependence of R_s at the resonant frequency.

The applicable measurement range of R_s for this method is as follows:

– Frequency: 8 GHz < f < 30 GHz

– Measurement resolution: 0,01 mΩ at 10 GHz

The R_s data at the measured frequency, and that scaled to 10 GHz, assuming the f^2 rule for comparison, is reported.

2 Normative references

The following documents are referred to in the text in such a way that some or all of their content constitutes requirements of this document. For dated references, only the edition cited applies. For undated references, the latest edition of the referenced document (including any amendments) applies.

IEC 60050-815, *International Electrotechnical Vocabulary (IEV) – Part 815: Superconductivity*

3 Terms and definitions

For the purposes of this document, the terms and definitions given in IEC 60050-815 apply.

ISO and IEC maintain terminological databases for use in standardization at the following addresses:

- IEC Electropedia: available at http://www.electropedia.org/
- ISO Online browsing platform: available at http://www.iso.org/obp

~~In general, surface impedance Z_s for conductors, including superconductors, is defined as the ratio of the electric field E_t to the magnetic field H_t, tangential to a conductor surface:~~

$$Z_s = E_t / H_t = R_s + jX_s$$

~~where R_s is the surface resistance and X_s is the surface reactance.~~

4 Requirements

The R_s of a superconductor film shall be measured by applying a microwave signal to a dielectric resonator with the superconductor film specimen and then measuring the attenuation of the resonator at each frequency. The frequency shall be swept around the resonant frequency as the centre, and the attenuation–frequency characteristics shall be recorded to obtain the Q- value, which corresponds to the loss.

The target ~~precision~~ relative combined standard uncertainty of this method ~~is a coefficient of variation (standard deviation divided by the average of the surface resistance determinations) that~~ is less than 20 % for the measurement temperature range from ~~30~~ 20 K to 80 K.

It is the responsibility of the user of this document to ~~consult and~~ establish appropriate safety and health practices and to determine the applicability of regulatory limitations prior to use.

Hazards exist in this type of measurement. The use of a cryogenic system is essential to cool the superconductors to allow transition into the superconducting state. Direct contact of skin with cold apparatus components can cause immediate freezing, as can direct contact with a spilled cryogen. The use of an RF generator is also essential to measure high-frequency properties of materials. If its power is too high, direct contact to human bodies can cause an immediate burn.

5 Apparatus

5.1 Measurement system

Figure 1 shows a schematic diagram of the system required for the microwave measurement. The system consists of a network analyzer system for transmission measurement, a measurement apparatus, and a thermometer for monitoring the measuring temperature.

An incident power generated from a suitable microwave source such as a synthesized sweeper is applied to the dielectric resonator fixed in the measurement apparatus. The transmission characteristics are shown on the display of the network analyzer. The measurement apparatus is fixed in a temperature-controlled cryocooler.

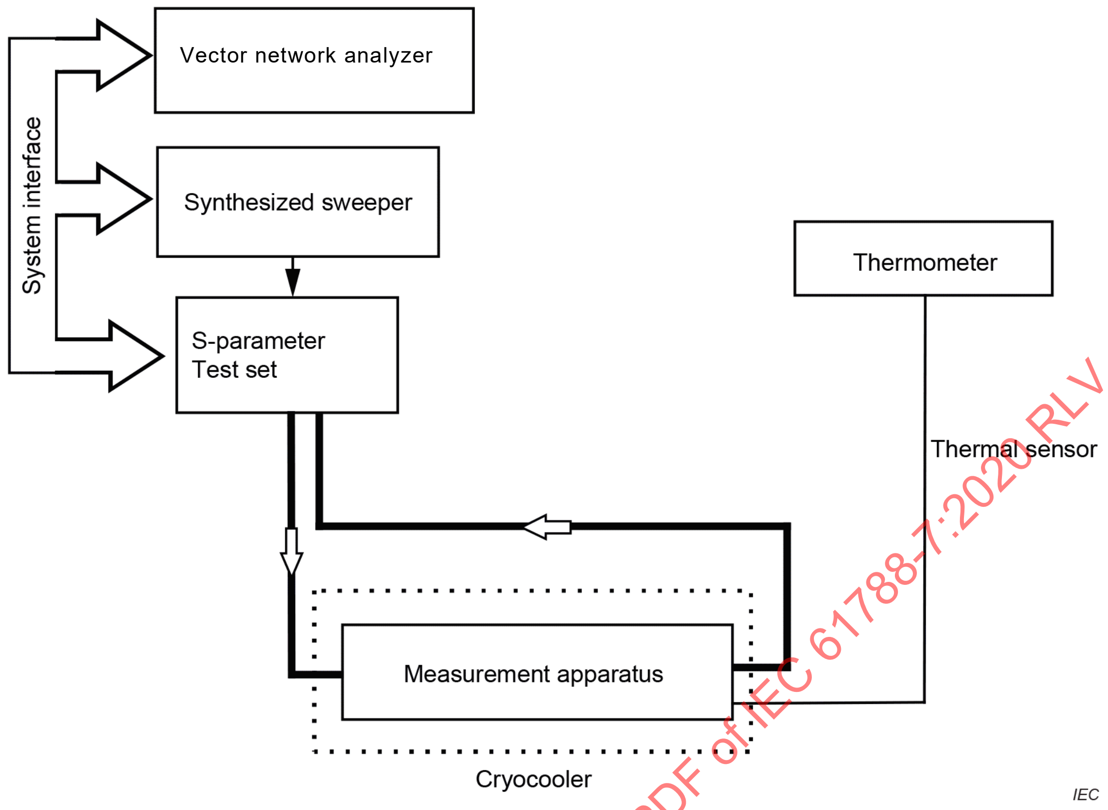

Figure 1 – Schematic diagram of measurement system for temperature dependence of R_s using a cryocooler

~~The measurement apparatus is fixed in a temperature-controlled cryocooler.~~

For the measurement of R_s for superconductor films, a vector network analyzer is recommended. A vector network analyzer has better measurement accuracy than a scalar network analyser due to its wide dynamic range. The performance requirements of the vector network analyzer are specified in 7.1.

5.2 Measurement apparatus for R_s

Figure 2 shows a schematic of a typical measurement apparatus (closed type resonator) for the R_s of ~~superconductor~~ HTS films deposited on a substrate with a flat surface. The upper ~~superconductor~~ HTS film is pressed down by a spring, which is made of phosphor bronze. The plate type spring ~~is recommended to~~ should be used for the improvement of measurement ~~accuracy~~ uncertainty. This type of spring reduces the friction between the spring and the other part of the apparatus, and allows the smooth movement of superconductor films due to the thermal expansion of the dielectric rod. In order to minimize the measurement ~~error~~ uncertainty, the sapphire rod and the copper ring shall be ~~set in coaxial~~ arranged coaxially.

Two semi-rigid cables for measuring transmission characteristics of the resonator shall be attached on both sides of the resonator in an axial symmetrical position (ϕ = 0 and π, where ϕ is the rotational angle around the central axis of the sapphire rod). Each of the two semi-rigid cables shall have a small loop at the ends. The plane of the loop shall be set parallel to that of the superconductor films in order to suppress the unwanted Transverse Magnetic Wave Modes (TM_{mn0} modes). The coupling loops shall be carefully checked for cracks in the spot weld joint that may have developed upon repeated thermal cycling. These cables can move right and left to adjust the insertion attenuation (IA). In this adjustment, coupling of unwanted cavity modes to the interested dielectric resonance mode shall be suppressed. Unwanted, parasitic coupling to the other modes reduces the high Q-value of the Transverse Electro-Magnetic Mode (TE mode) resonator. For suppressing the parasitic coupling, special attention shall be paid to designing high-Q resonators. Two other types of resonators along with the closed type shown in Figure 2 can be used. They are explained in A.4.

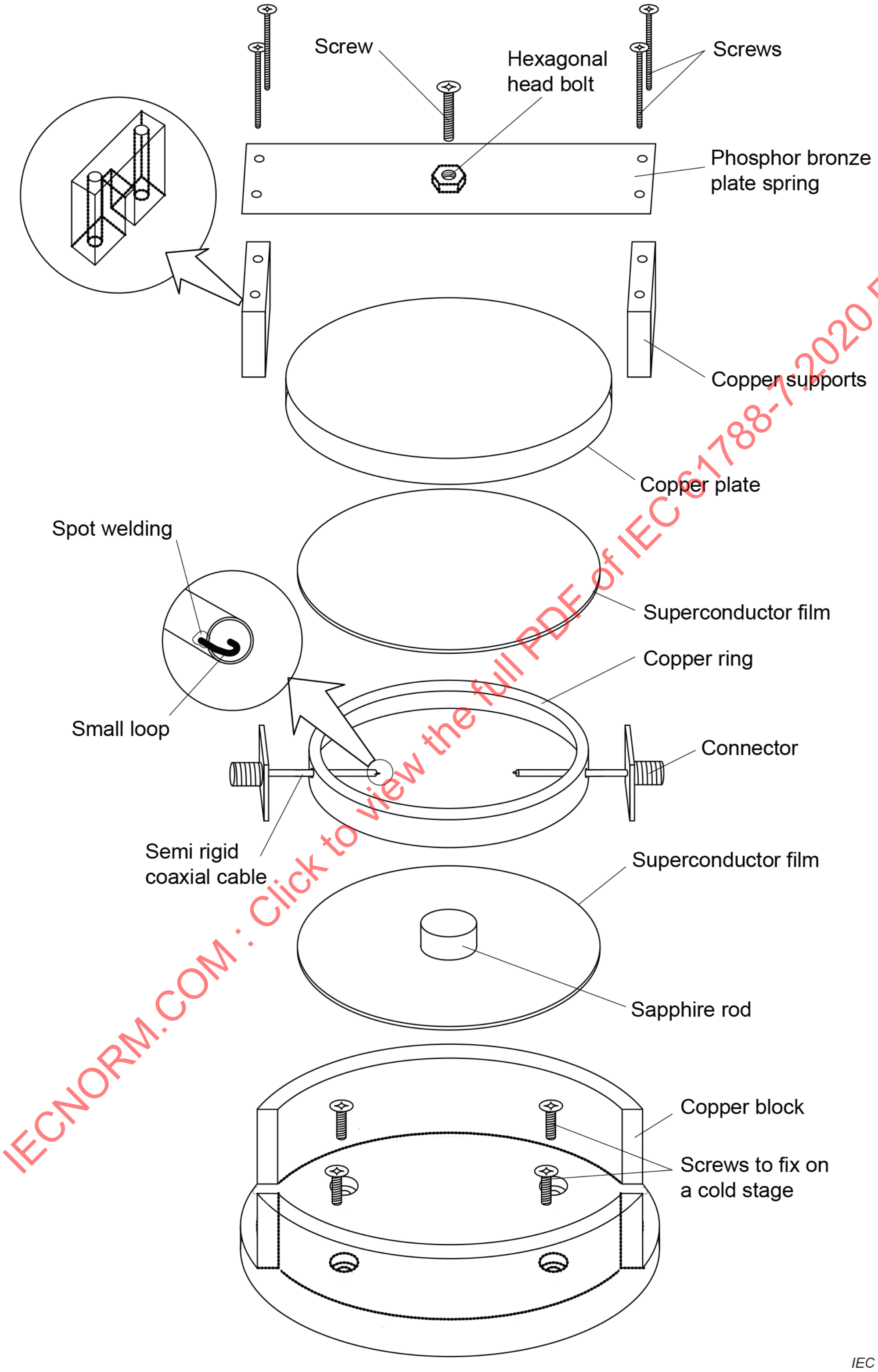

Figure 2 – Typical measurement apparatus for R_s

A reference line made of a semi-rigid cable shall be used to measure the full transmission power level, i.e. the reference level. This cable has a length equal to the sum of the two cables of the measurement apparatus. Semi-rigid cable with an outer diameter of 1,20 mm is recommended.

In order to minimize the measurement ~~error~~ uncertainty, two superconductor films shall be set to be parallel to each other. To ensure that the two superconductor films remain in tight contact with the ends of the sapphire rod, without any air gap, both of the surfaces of the films and the ends of the rod shall be cleaned carefully.

5.3 Dielectric rods

Two dielectric rods with the same relative permittivity, ε', and loss factor, tan δ, preferably cut from one cylindrical dielectric rod, are required. These two rods, standard dielectric rods, shall have the same diameter but different heights: one ~~has a~~ shall have height three times longer than the other.

It is preferable to use ~~standard~~ dielectric rods with low tan δ to achieve the requisite measurement ~~accuracy~~ uncertainty on R_s. Recommended dielectric rods are single-crystal sapphire rods with tan δ less than ~~10^{-6}~~ 2×10^{-7} at 77 K. Specifications on the sapphire rods are described in 7.1. In order to minimize the measurement error in R_s of the superconductor films, both ends of the sapphire rods shall be polished parallel to each other and perpendicular to the axis. Specifications for the sapphire rods are given in Clause 7.

The diameter and the heights of the standard sapphire rods shall be carefully designed so that the TE_{011} and TE_{013} modes do not couple to other TM, HE and EH modes, since the coupling between TE mode and other modes causes the degradation of unloaded Q. A design guideline for the standard sapphire rods is described in Clause A.5. Table 1 shows typical examples of dimensions of the standard sapphire rods for 12 GHz, 18 GHz, and 22 GHz resonance. ~~At higher frequencies the unloaded Q value will be lower, which makes the measurement easier, and the error will be lower.~~ In the R_s measurement at 22 GHz, the required film diameter can be set to 20 mm, and the measured Q_L is small, therefore the effect of the dielectric loss of sapphire rod can be reduced.

Table 1 – Typical dimensions of pairs of ~~standard~~ single-crystal sapphire rods for 12 GHz, 18 GHz and 22 GHz

~~Frequency~~ ~~GHz~~		~~Diameter~~ ~~d~~ ~~mm~~	~~Height~~ ~~h~~ ~~mm~~
~~12~~	~~Short rod (TE_{011} resonator)~~	~~11,4~~	~~5,7~~
	~~Long rod (TE_{013} resonator)~~	~~11,4~~	~~17,1~~
~~18~~	~~Short rod (TE_{011} resonator)~~	~~7,6~~	~~3,8~~
	~~Long rod (TE_{013} resonator)~~	~~7,6~~	~~11,4~~
~~22~~	~~Short rod (TE_{011} resonator)~~	~~6,2~~	~~3,1~~
	~~Long rod (TE_{013} resonator)~~	~~6,2~~	~~9,3~~

Frequency GHz		**Diameter, d** mm	**Height, h** mm
12	Short rod (TE_{011} resonator)	11,40 ± 0,05	5,70 ± 0,05
	Long rod (TE_{013} resonator)	11,40 ± 0,05	17,10 ± 0,05
18	Short rod (TE_{011} resonator)	7,60 ± 0,05	3,80 ± 0,05
	Long rod (TE_{013} resonator)	7,60 ± 0,05	11,40 ± 0,05
22	Short rod (TE_{011} resonator)	6,20 ± 0,05	3,10 ± 0,05
	Long rod (TE_{013} resonator)	6,20 ± 0,05	9,30 ± 0,05

6 Measurement procedure

6.1 Specimen preparation

From ~~error~~ uncertainty estimation, the film diameter shall be about three times larger than that of the sapphire rods. In this configuration, the ~~reduction~~ increase in ~~precision~~ uncertainty of R_s due to the different radiation losses between TE_{011} and TE_{013} mode can be considered negligible, given the target ~~precision~~ relative combined standard uncertainty of 20 %. The film thickness shall be about ~~three~~ two times larger than the ~~London~~ magnetic-field penetration depth value at ~~each~~ the maximum temperature in the measurement temperature range. If the film thickness is much less than ~~three~~ two times the ~~London~~ magnetic-field penetration depth, the measured R_s should mean the effective surface resistance.

Table 2 shows dimensions of the superconductor films recommended for the standard sapphire rods of 12 GHz, 18 GHz, and 22 GHz.

Table 2 – Dimensions of superconductor film for 12 GHz, 18 GHz, and 22 GHz

~~Standard dielectric rod~~		~~Superconductor film~~	
~~Frequency~~ ~~GHz~~	~~Diameter~~ ~~*d*~~ ~~mm~~	~~Diameter~~ ~~*d'*~~ ~~mm~~	~~Thickness~~ ~~µm~~
~~12~~	~~11,4~~	~~>35~~	~~≅0,5~~
~~18~~	~~7,6~~	~~>25~~	~~≅0,5~~
~~22~~	~~6,2~~	~~>20~~	~~≅0,5~~

c-cut single-crystal sapphire rod		Superconductor film	
Frequency GHz	Diameter, *d* mm	Diameter, *d'* mm	Thickness µm
12	11,40 ± 0,05	> 35	≅ 0,5
18	7,60 ± 0,05	> 25	≅ 0,5
22	6,20 ± 0,05	> 20	≅ 0,5

In case of using closed type resonators, the dimensions of the superconductor films shall also be designed taking into account the dimension of the copper cylinder between the superconductor films. A design guideline for the dimension of the copper cylinder of the closed type resonator is described in Clause A.6.

6.2 Set-up

Set up the measurement equipment as shown in Figure 1. All of the measurement apparatus, standard sapphire rods, and superconductor films shall be kept in a clean and dry state as high humidity may degrade the unloaded Q-value. The specimen and the measurement apparatus shall be fixed in a temperature-controlled cryocooler. The specimen chamber shall be ~~generally~~ totally evacuated. The temperatures of the superconductor films and standard sapphire rods shall be measured by a diode thermometer, or a thermocouple. The temperatures of the upper and lower superconductor films and standard sapphire rods ~~must be kept as close as possible~~ shall not differ by more than 0,5 K. This can be achieved by covering the measurement apparatus with aluminium foil or filling the specimen chamber with helium gas.

6.3 Measurement of reference level

The level of full transmission power (reference level) shall be measured first. Fix the output power of the synthesized sweeper below 10 mW because the measurement ~~accuracy~~ uncertainty depends on the measuring signal level. Connect the reference line of semi-rigid cable between the input and output connectors. Then, measure the transmission power level over the entire measurement frequency and temperature range. The reference level can change several decibels when temperature of the apparatus is changed from room temperature to the lowest measurement temperature. Therefore, the temperature dependence of the reference level must be taken into account.

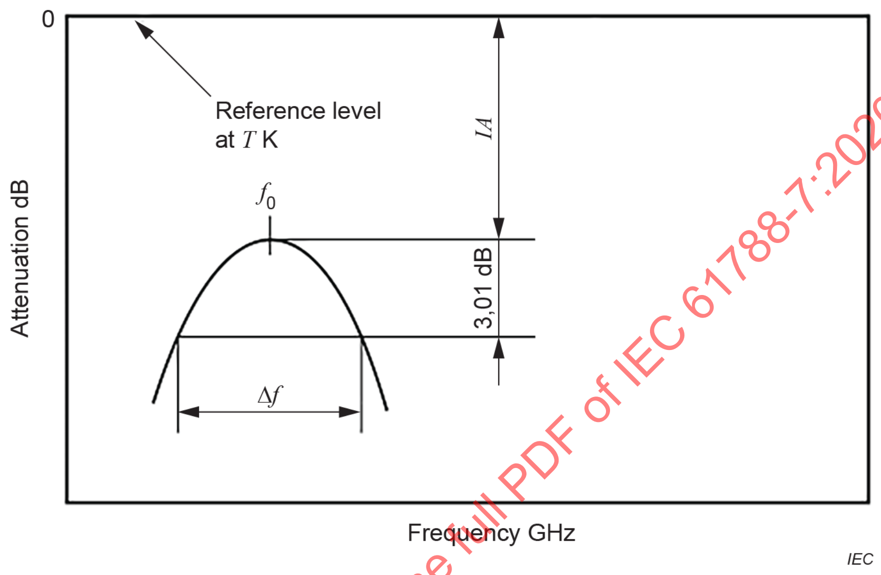

Figure 3 – Insertion attenuation, IA, resonant frequency, f_0, and half power bandwidth, Δf, measured at T kelvin

6.4 Measurement of the frequency response of resonators

The temperature dependence of the R_s can be obtained through the measurements of resonant frequency, f_0, and unloaded quality factor, Q_u, for TE_{011} and TE_{013} resonators, which shall be measured as follows.

a) Connect the measurement apparatus between the input and output connectors (Figure 1). Insert the standard short sapphire rod near the centre of the lower superconductor film and fix the distance between the rod and each of the loops of the semi-rigid cables to be equal to each other, so that this transmission-type resonator can be under-coupled equally to both loops. Put down the upper superconductor film gently to touch the top face of the rod. Be careful not to damage the surface of the superconductor films by excessive pressure. Evacuate and cool down the specimen chamber below the critical temperature.

b) Find the TE_{011} mode resonance peak of this resonator at a frequency nearly equal to the designed value of f_0.

c) Narrow the frequency span on the display so that only the resonance peak of TE_{011} mode can be shown (Figure 3). Confirm that the insertion attenuation, IA, of this mode is larger than 20 dB from the reference level, which depends strongly on the temperature.

d) Measure the temperature dependence of f_0 and the half power band width Δf. The loaded Q-value, Q_L, of the TE_{011} resonator is given by

$$Q_L = \frac{f_0}{\Delta f} \qquad (1)$$

e) The unloaded Q-value, Q_u, shall be extracted from the Q_L by at least one of the two following techniques.

1) One technique for extracting the unloaded Q-value involves measuring the insertion attenuation IA. Q_u is given by

$$Q_u = \frac{Q_L}{1 - A_t}, \; A_t = 10^{-IA[\mathrm{dB}]/20} \tag{2}$$

The IA of each temperature is determined as follows. In the R_s measurement system shown in Figure 2, a semi-rigid cable is connected instead of the measurement apparatus, and the measurement system is short-circuited to determine the reference level. Measure the reference level at each temperature and use it to determine IA at each temperature.

This technique of using insertion attenuation assumes that the coupling on both sides of the resonator is identical. The coupling loops are difficult to fabricate, the orientation of the loop is difficult to control, and any movement of the sapphire rod during measurement is not known. These assembly-dependent effects are also temperature dependent. This potential asymmetry in coupling can result in large errors in calculating the coupling factor if the coupling is strong (IA <~ 10 dB). If the coupling is weak enough (IA > 20 dB), asymmetry in the coupling becomes less important.

2) Another technique for extracting the unloaded Q-value involves measuring the reflection scattering parameters at the resonant frequency of both sides of the resonator.

$$Q_u = Q_L (1 + \beta_1 + \beta_2) \tag{3}$$

$$\beta_1 = \frac{1 - |S_{11}|}{|S_{11}| + |S_{22}|} \tag{4}$$

$$\beta_2 = \frac{1 - |S_{22}|}{|S_{11}| + |S_{22}|} \tag{5}$$

In ~~the above equations~~ Equations (4) and (5), S_{11} and S_{22} are the reflection scattering parameters as shown in Figure 4, and are measured in linear units of power, not relative dB. β_1 and β_2 are the coupling coefficients.

This technique of using the reflection scattering parameters has two advantages. It does not require the additional step of calibration of the reference level and it gives a measurement of the coupling values for both sides of the resonator. This also has two disadvantages. It only works for a narrow band resonance (which is fortunately the case) and is limited by the dynamic range of the network analyzer in measuring the reflection coefficients [15] [16].

A combination of the two techniques is ~~an excellent “double” check and is therefore recommended~~ useful for a "double" check.

f) The f_0 and Q_u measured for this short rod are denoted as f_{01} and Q_{u1} for TE_{011} mode resonance. By slowly changing the temperature of the cryocooler the temperature dependence of f_{01} and Q_{u1} shall be measured.

g) After the temperature dependence measurement of f_{01} and Q_{u1} is finished, the measurement apparatus shall be heated up to room temperature.

h) Then, replace the TE_{011} resonator in the apparatus with the TE_{013} resonator at room temperature, cool down the apparatus to a temperature lower than the critical temperature, and measure the temperature dependence of f_0 and Q_u of its TE_{013} resonance mode, denoted as f_{03} and Q_{u3}, in a similar way to the TE_{011} resonator case. When the length of the sapphire rod of the TE_{013} resonator is precisely three times longer than that of the TE_{011} resonator, the f_{03} of the TE_{013} resonator must coincide with f_{01} of the TE_{011} resonator. If carefully designed, the difference between f_{01} and f_{03} is usually very small (<~ 0,25 %). We can ~~treat as $f_0 = f_{01} = f_{03}$ in the calculations of 6.5~~ consider that the f_0 in equation (9) can be replaced by f_{01} or f_{03}.

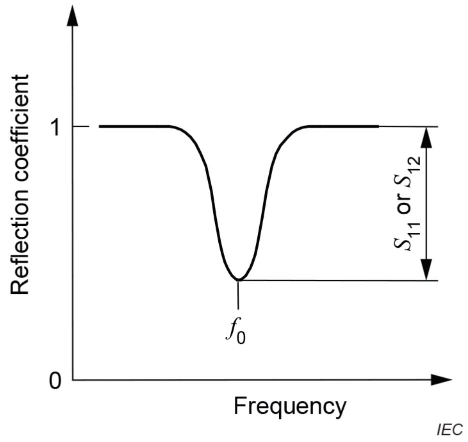

Figure 4 – Reflection scattering parameters (S_{11} and S_{22})

6.5 Determination of surface resistance of the superconductor and ε' and tan δ of the standard sapphire rods

~~Calculate the temperature dependence of the surface resistance R_s of the superconductor films, and ε' and tan δ of the standard sapphire rods using the temperature dependence of f_{01}, Q_{u1}, f_{03}, and Q_{u3} from Equations (6), (7) and (8).~~

Calculate the temperature dependence of the R_s of the superconductor films, and ε' and tan δ of the standard sapphire rods using the temperature dependence of Q_{u1} and Q_{u3}. Q_{u1} and Q_{u3} can be calculated using equations (1) and (2). If the measured temperatures for Q_{u3} appear to be slightly different from those for Q_{u1}, interpolation can be used for preparing adjusted temperature values for the former at the same temperatures for the later. Equations (6) to (12) are established in the open type cavity, but when the superconductor film size is three times larger than sapphire rod diameter, these equations can be used for closed type cavity.

$$R_s = \frac{30\pi^2 \times 3}{(3-1)} \left(\frac{2h_0}{\lambda 0} \right)^3 \frac{\varepsilon' + W}{1+W} \left(\frac{1}{Q_{u1}} - \frac{1}{Q_{u3}} \right) \quad (6)$$

$$\varepsilon' = \left(\frac{\lambda 0}{\pi d} \right)^2 \left(u^2 + v^2 \right) + 1 \quad (7)$$

$$\tan \delta = \frac{1 + \frac{W}{\varepsilon'}}{(3-1)} \left(\frac{3}{Q_{u3}} - \frac{1}{Q_{u1}} \right) \quad (8)$$

where

$$\lambda_0 = \frac{c}{f_0} \tag{9}$$

$$W = \frac{J_1^2(u)}{K_1^2(v)} \frac{K_0(v)K_2(v) - K_1^2(v)}{J_1^2(u) - J_0(u)J_2(u)} \tag{10}$$

~~$$v^2 = \left(\frac{\pi d}{\lambda_0}\right)^2 \left[\left(\frac{\lambda_0}{2h_0}\right)^2 -1\right] \tag{11}$$~~

$$v^2 = \left(\frac{\pi d}{\lambda_0}\right)^2 \left[\left(\frac{3\lambda_0}{2h_0}\right)^2 -1\right] \tag{11}$$

$$u\frac{J_0(u)}{J_1(u)} = -v\frac{K_0(v)}{K_1(v)} \tag{12}$$

In the equations, λ_0 is the free space resonant wavelength, c is the ~~velocity~~ speed of light in vacuum (c = 2,997 9 × 10^8 m/s), h_0 is the height of the short standard dielectric rod. The value u^2 is given by the transcendental Equation (12) using the value of v^2, where $J_n(u)$ is the Bessel function of the first kind, and $K_n(v)$ is the modified Bessel function of the second kind. The derivations of the equations are described in Clause A.3.

Generally the thermal expansion coefficient of the rods must be known to determine the temperature dependence of their sizes. However, the thermal expansion effect of the sapphire rods can be neglected for the target ~~precision of the~~ relative standard uncertainty of R_s (20 %).

It is noted that the measured R_s means the effective surface resistance if the film thickness is ~~not much larger~~ less than two times the temperature-dependent penetration depth.

7 ~~Precision and accuracy~~ Uncertainty of the test method

7.1 Surface resistance

The surface resistance (R_s) shall be determined from the Q-value measured with a dielectric resonator technique.

A vector network analyser as specified in Table 3 shall be used to record the frequency dependence of attenuation. The resulting record shall allow the determination of Q to a relative uncertainty of 10^{-2}.

Table 3 – Specifications for vector network analyzer

Dynamic range of S_{21}	above 60 dB
Frequency resolution	below 1 Hz
Attenuation uncertainty	below 0,1 dB
Input power limitation	below 10 dBm

The dielectric resonators shall be provided with two dielectric rods with low tan δ of less than ~~10^{-6}~~ 2×10^{-7} at 77 K and a radius less than 1/3 of the superconducting specimen's radius. The best candidate for the rods is sapphire as specified in Table 4. Term definitions in Table 4 are shown in Figure 5.

Table 4 – Specifications for sapphire rods

Diameter	±0,05 mm
Height	±0,05 mm
Flatness	below 0,005 mm
Surface roughness	top and bottom surface: below 10 nm RMS cylindrical surface: below 0,001 mm RMS
Perpendicularity	within 0,1 degree
Axis	parallel to *c*-axis within 0,3°

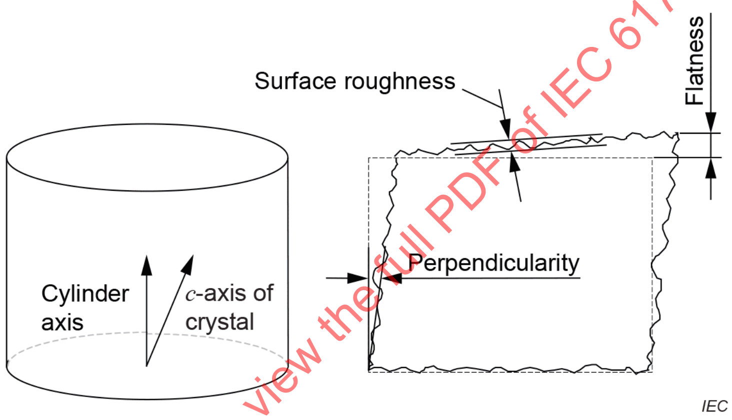

Figure 5 – Term definitions in Table 4

The technique as described assumes that single- and triple-height sapphire rods can be fabricated with the same tan δ. However, the variation of the tan δ between nominally identical rods, cut from the same boule and polished by the same technique, may be as large as two orders of magnitude. To date, the smallest variation in tan δ between nominally identical sapphire rods has been a factor of four ~~[9]~~. Therefore, the uncertainty in the measured tan δ is large. The variation of tan δ of the present sapphire rod causes an additional uncertainty up to at least 10 % in the surface resistance measurement. This limits the target ~~precision~~ uncertainty of the present technique at ~~20~~ 5 %. If reproducibility of sapphire rods is improved, or a selection method for standard sapphire rods is established, a target ~~precision~~ uncertainty can be improved.

7.2 Temperature

The measurement apparatus is cooled down to the specified temperature by any means during testing. An easy choice would be to immerse the apparatus into a liquid cryogen. This technique is quick and simple and yields a known and stable temperature. Unfortunately, most HTS materials are damaged by the condensation of moisture that occurs when removing the sample from the cryogen. In addition, uncertainties generated by the presence of a gas/liquid mixture within the cavity, and the inability to measure R_S as a function of temperature support the use of other cooling methods. These limitations can be circumvented by the immersion of a vacuum can into a liquid cryogen. If the vacuum can is backfilled with gas, then rapid cooling and uniform temperatures occur. If heaters are attached to the apparatus, then the temperature dependence of the HTS material can be measured. A third and equally good choice is the use of a cryocooler. In this case, the resonator is under vacuum and cooled by conduction through the metallic package. ~~Care must be taken to avoid~~ Temperature gradients with the apparatus shall be avoided.

A cryostat shall be provided with the necessary environment for measuring R_s and the specimen shall be measured while in a stable and isothermal state. The specimen temperature is assumed to be the same as the sample holder temperature. The holder temperature shall be reported to an accuracy of ±0,5 K, measured by means of an appropriate temperature sensor.

The difference between the specimen temperature and the holder temperature shall be minimized by using shields with good thermal conductivity.

7.3 Specimen and holder support structure

The support structure shall provide adequate support for the specimen. ~~It is imperative that~~ The two films shall be parallel and mechanically stable throughout the measurement, especially in a cryocooler and over a wide temperature range. The parallelism of the two films can be achieved by using a sapphire rod satisfying the specifications described in Table 4.

7.4 Specimen protection

Condensation of moisture and scratching of the film deteriorate superconducting properties. Some protection measures should be provided for the specimens. Polytetrafluoroethylene (PTFE) or polymethylmethacrylate (PMMA) coating does not affect the measurements, thus they can be used for protection. A coating material thickness of less than several micrometers is recommended.

7.5 Uncertainty of surface resistance measured by standard two-resonator method

For the dielectric resonance method, tan δ of the TE_{011} mode and TE_{013} mode sapphire rods are assumed to be absolutely equal. If tan δ of two sapphire rods is different, it is not possible to calculate the surface resistance using Equation (6). The effect of tan δ deviation on surface resistance was checked (see Annex B). Uncertainty in the microwave surface resistance of superconductors by dielectric resonator method depends on size, dielectric constant, tan δ of sapphire rods and uncertainty in measured Q of the resonator. The relative combined standard uncertainty is less than 20 % (see Annex B)

8 Test report

8.1 Identification of test specimen

The test specimen shall be identified, if possible, by the following:

a) name of the manufacturer of the specimen;

b) classification and/or symbol;

c) lot number;

d) chemical composition of the thin film and the substrate;

e) thickness and roughness of the thin film;

f) manufacturing process technique.

8.2 Report of R_s values

The R_s values at the measured frequency, and that scaled to 10 GHz, together with their corresponding f_{01}, f_{03}, Q_{u1}, Q_{u3}, IA and/or (β_1, β_2), ε' and tan δ values, and their temperature dependence shall be reported.

8.3 Report of test conditions

The following test conditions shall be reported:

a) test frequency and resolution of frequency;

b) test maximum RF power;

c) test temperature, accuracy of temperature and temperature difference in two plates;

d) sample history with temperature variation.

Annex A
(informative)

Additional information relating to Clauses 1 to 8

A.1 Scope

A.1.1 General

The establishment of the standard measurement method is needed to evaluate film quality of high Tc superconductor (HTS) films having low surface resistance, R_s, values such as 0,1 mΩ at 10 GHz. Several resonance methods as shown in Figure A.1 have been proposed so far to measure them in microwave and millimetre wave range. These resonator structures are grouped into six types (see A.1.2 to A.1.7).

A.1.2 Cylindrical cavity method [1][2] [10] [17]

Figure A.1 a) shows a cavity structure using the TE_{011} mode, which is constructed from a copper cylinder and two HTS films. In the microwave range below 30 GHz, the R_s measurement precision of this method is rather low, because the R_s value of the copper cylinder is 100 times higher than that of HTS films. This method is suitable in the millimetre wave region, because the R_s values increase with f^2 of HTS films and $f^{½}$ for copper.

A.1.3 Parallel-plates resonator method [2] [18] [19]

Figure A.1 b) shows a structure of a parallel-plates resonator using the TM_{nm0} mode, which is constructed by inserting a thin low loss dielectric spacer between two rectangular HTS films. This method offers the possibility of measuring extremely small R_s values, but from the viewpoint of the absolute estimation of R_s there are some problems, such as low measurement precision of thickness and tan δ of the dielectric spacer, uncertain estimations of radiation loss and an air-gap effect between the plates and the spacer, and critical excitation technique of the resonance modes.

A.1.4 Microstrip-line resonance method [1], [3] [20] [21]

Figure A.1 (c) shows a structure of a microstrip-line resonator using the TEM_n TE_{0mp} mode, which is fabricated by a pattern fabrication process and is close to the real microwave passive devices. However, this method is not suitable for the HTS film estimation because it includes an uncertain influence of the pattern fabrication process.

A.1.5 Dielectric resonator method [4], [5]-[7] [22] [23] [24] [25]

Figure A.1 d) shows a structure of a dielectric resonator using a TE_{011} mode, where a low loss sapphire rod is placed between two parallel HTS films. For the TE_{0mp} mode, we can eliminate the air-gap effects, because the normal component of electric field does not exist on the HTS films. In this method the R_s values of the HTS films have been measured by ignoring the effect of tan δ on the assumption of tan $\delta < 1 \times 10^{-8}$ for single-crystal sapphire [4] [24]. However, the tan δ values measured for sapphire at 10 GHz and near 50 K, as is well known, take values between 10^{-6} to 10^{-8} due to quantity of lattice defect. Therefore, preparation of very-low-loss sapphire rods with tan δ $< 1 \times 10^{-8}$ $< 2 \times 10^{-7}$ (at 80 K and at 10 GHz) is essential for this method.

[2] Numbers in brackets in this annex refer to the reference documents in Clause A.9

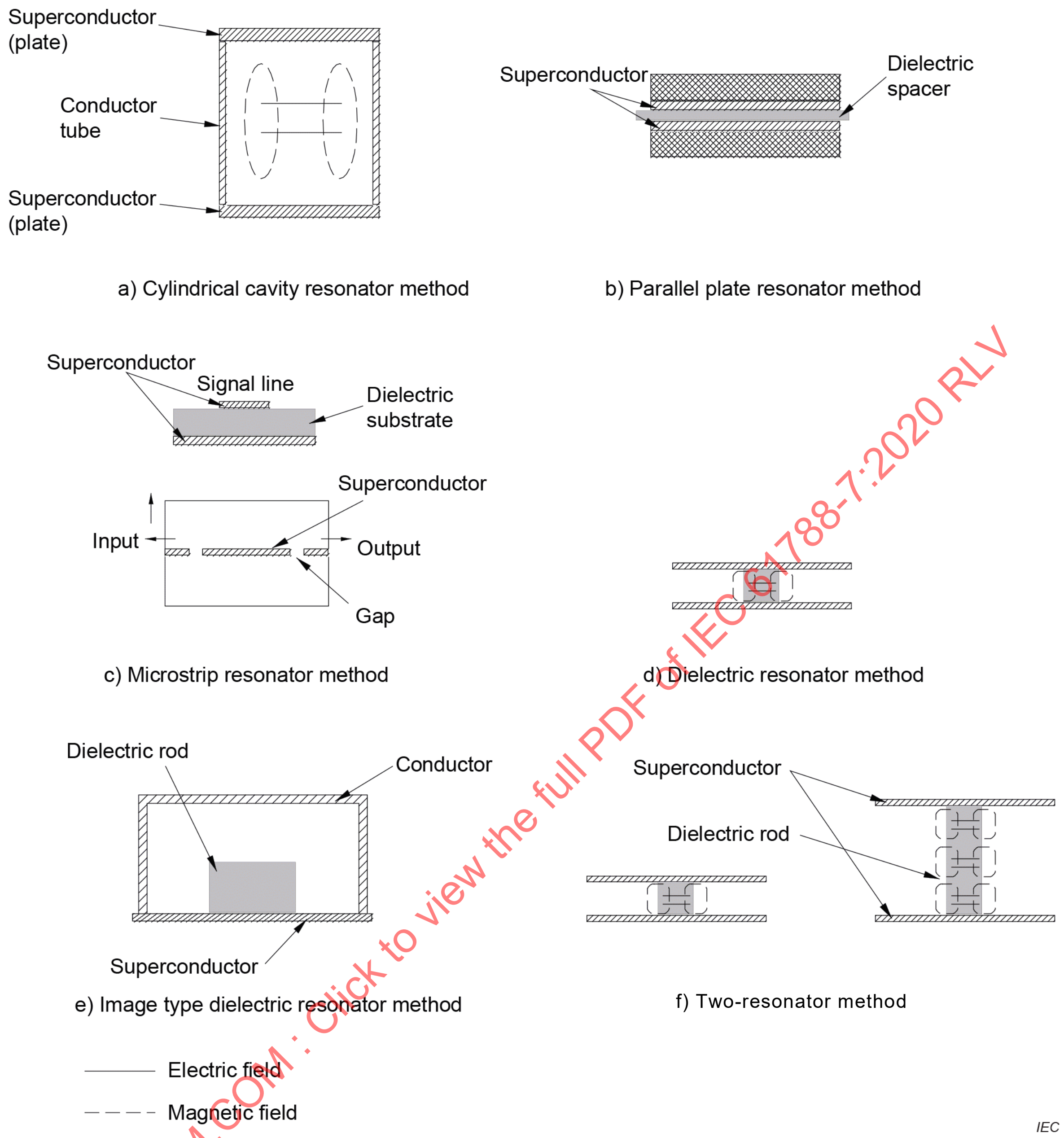

Figure A.1 – Schematic configuration of several measurement methods for the surface resistance

A.1.6 Image-type dielectric resonator method ~~[8]~~ [26] [27]

Figure A.1 e) shows a structure of an image-type dielectric resonator using the $TE_{01\delta}$ mode. This structure is available to measure only one HTS film. However, preparation of very-low-loss sapphire rods is essential also for this method, because the R_s is measured by ignoring the effect of tan δ.

~~In addition, complicated and tedious numerical calculations are needed to determine the R_s values from the measured resonant frequency and unloaded Q.~~

In an improved image-type sapphire rod resonator method, R_s can be obtained with simple calibration process. In this method, the exact R_s of a single HTS film can be obtained by one measurement under the 20 % limitation of variation coefficient.

A.1.7 Two-resonator method ~~[9],[10]~~ [28] [29]

In this method, two sapphire rod resonators with the same tan δ values are used; one is a TE_{011} mode resonator and the other is a TE_{013} mode resonator, as shown in Figure A.1 f). Similarly to the dielectric resonator method, the air-gap effects can be eliminated in this method. The tan δ value of the sapphire rods and the R_s value of the HTS films can be determined separately from the resonant frequencies and unloaded ~~Q's~~ Q-values measured for these resonators by using simple formulas derived from the rigorous analysis based on the mode matching method. Thus this method can eliminate the ambiguity of the tan δ affected to the R_s measurements. Actually, the results of R_s measured for six YBCO films with R_s = 0,1 mΩ at 12 GHz have verified that the measurement ~~precision~~ uncertainty of ~~10~~ 20 % is realized by this method ~~[10]~~ [22]. However, if there is a difference between two tan δ values (Δtan δ), the ~~errors of~~ uncertainty in R_s due to Δtan δ must be taken into account. This effect ~~will~~ can be estimated from results of the inter-laboratory round robin test of the same HTS films by this method. Recently, the R_s of YBCO film was measured three times and its deviation was less than 20 % (see Figure A.11).

As a result of comparisons among the six methods described above, the two-resonator method is recommended as the standard measurement method of R_s of HTS films, due to the following two advantages:

– absolute measurement of R_s is possible;

– the numerical treatment is simple and easy.

A.2 Requirements

Higher measurement frequencies are desirable for determination of lower R_s because R_s of superconductor films increases with the frequency according to the f^2 rule. The size of the resonators also can be made smaller by using higher measurement frequencies. However, it becomes difficult to set up a microwave measurement system as the measurement frequency becomes higher.

For the measurement temperatures of below ~~30~~ 10 K or above 80 K, this test method is sufficiently applicable, where some new cooling techniques may be required.

A.3 Theory and calculation equations

Figure A.2 shows the configuration of the ~~TE_{0mp}~~ TE_{0mn} mode resonator, which is used to eliminate the air-gap effects. A cylindrical dielectric rod with diameter, d, and height, h, is short-circuited at both ends by surfaces of two parallel superconductor films deposited on dielectric substrates with diameter, d', thus constituting a resonator. These superconductor films are required to have the same value of R_s. The value of R_s is calculated from the measured resonant frequency f_0 and unloaded quality factor Q_u for the ~~TE_{0mp}~~ TE_{0mn} resonance mode. When the two superconductor films have different values of R_s, the measured R_s value corresponds to the average value of these two films.

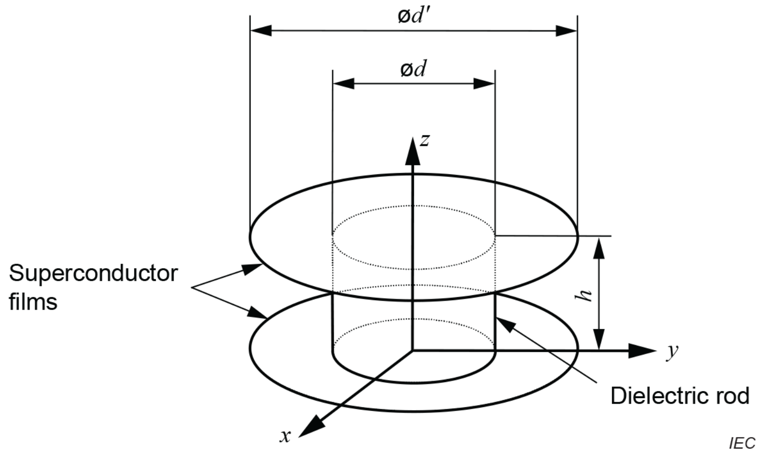

Figure A.2 – Configuration of a cylindrical dielectric rod resonator short-circuited at both ends by two parallel superconductor films deposited on dielectric substrates

The value of R_s is given by [25]

$$R_s = \frac{1}{B}\left(\frac{A}{Q_u} - \tan\delta\right) \tag{A.1}$$

where

$$A = 1 + \frac{W}{\varepsilon'} \tag{A.2}$$

$$B = p^2\left(\frac{\lambda_0}{2h}\right)^3 \frac{1+W}{30\pi^2\varepsilon'},\ p = 1,2,\ldots, \tag{A.3}$$

$$\lambda_0 = \frac{c}{f_0} \tag{A.4}$$

$$W = \frac{J_1^2(u)}{K_1^2(v)}\,\frac{K_0(v)K_2(v) - K_1^2(v)}{J_1^2(u) - J_0(u)J_2(u)} \tag{A.5}$$

~~$$v^2 = \left(\frac{\pi d}{\lambda_0}\right)^2\left[\left(\frac{p\lambda_0}{2h}\right)^2 - 1\right] \quad \text{(A.6)}$$~~

$$v^2 = \left(\frac{\pi d}{\lambda_0}\right)^2\left[\left(\frac{3\lambda_0}{2h}\right)^2 - 1\right] \tag{A.6}$$

$$u\frac{J_0(u)}{J_1(u)} = -v\frac{K_0(v)}{K_1(v)} \tag{A.7}$$

In Equations (A.1) and (A.2), ε' and tan δ are the relative permittivity and the loss factor of the dielectric rod, respectively. In Equations (A.3) and (A.4), λ_0 is the free space resonant wavelength, and c is the ~~velocity~~ speed of light in vacuum (c = 2,9979 × 10^8 m/s). The function W/ε' equals the ratio of electric-field energy stored outside to that stored inside the dielectric rod. If all of the electric field is concentrated inside the dielectric rod, the value W equals zero.

The value u^2 is given by the transcendental Equation (A.7) using the value of v^2, where $J_n(u)$ is the Bessel function of the first kind and $K_n(v)$ is the modified Bessel function of the second kind~~, respectively~~. For any value of v, the m-th solution u exists between u_{0m} and u_{1m}, where $J_0(u_{0m})$ = 0 and $J_1(u_{1m})$ = 0. The first solution (m = 1), which is used for easy mode identification, is shown in Figure A.3 by curve (A). The computed result of the W-v relation for m = 1 of TE_{0mp} resonance mode is shown in Figure A.3 by curve (B).

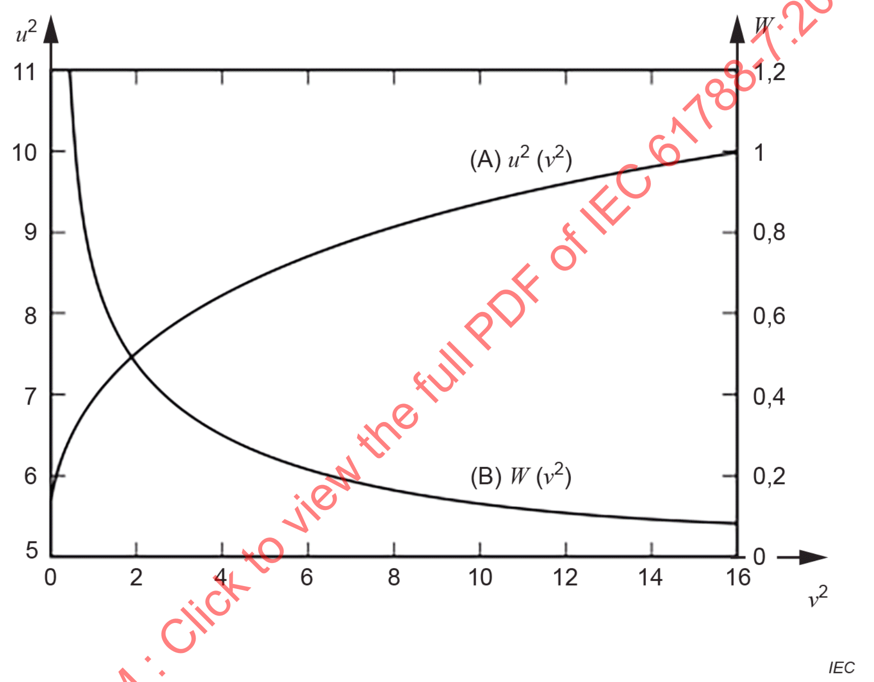

Figure A.3 – Computed results of the u-v and W-v relations for TE_{01p} mode

The value of ε' is given by

$$\varepsilon' = \left(\frac{\lambda_0}{\pi d}\right)^2 \left(u^2 + v^2\right) + 1 \quad \text{(A.8)}$$

using the value of v^2 and u^2.

In the two-resonator method, a pair of dielectric rods, which are called "standard dielectric rods", are used. These two rods have the same diameter but have different heights. The rod heights are such that one rod is p times the height of the other; p is commonly set equal to three. They are required to have the same values of ε' and tan δ.

Figure A.4 shows the configuration of the standard dielectric rods in the case of p = 3. To avoid confusion, the height of the short standard dielectric rod is denoted by h_0. Each resonator is called "TE_{011} resonator" and "TE_{013} resonator", respectively. The same superconductor films are used in these resonators. The values of f_0 and Q_u for the TE_{011} mode are measured using the TE_{011} resonator, and those for the TE_{01p} mode are measured using the TE_{01p} resonator. We denote the f_0 and Q_u for each resonator by using the subscripts 1 and p, respectively: f_{01} and Q_{u1} for TE_{011} resonator, and f_{0p} and Q_{up} for TE_{01p} resonator.

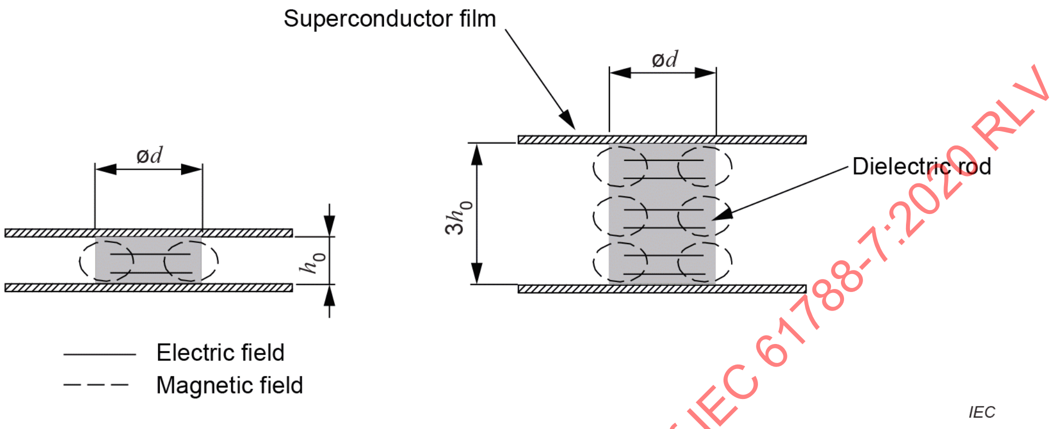

Figure A.4 – Configuration of standard dielectric rods for measurement of R_s and tan δ

The value of tan δ is given from the measured values of Q_u. When the TE_{01p} resonator is precisely p times longer than the TE_{011} resonator, f_{0p} coincides with f_{01}. However, Q_{up} is higher than Q_{u1} according to the different magnitude of the electric field energy stored in the two resonators. Because both dielectric rods are short-circuited at both ends by the same superconductor films, Equation (A.1) yields

$$\tan\delta = \frac{A}{(p-1)}\left(\frac{p}{Q_{up}} - \frac{1}{Q_{u1}}\right) \tag{A.9}$$

$$\tan\delta = \frac{A}{(3-1)}\left(\frac{3}{Q_{up}} - \frac{1}{Q_{u1}}\right) \tag{A.9}$$

As an alternative method, the value of R_s of superconductor films can be directly measured by

$$R_s = \frac{30\pi^2 p}{(p-1)}\left(\frac{2h_0}{\lambda 0}\right)^3 \frac{\varepsilon' + W}{1+W}\left(\frac{1}{Q_{u1}} - \frac{1}{Q_{up}}\right) \tag{A.10}$$

$$R_s = \frac{30\pi^2 \times 3}{(3-1)}\left(\frac{2h_0}{\lambda 0}\right)^3 \frac{\varepsilon' + W}{1+W}\left(\frac{1}{Q_{u1}} - \frac{1}{Q_{up}}\right) \tag{A.10}$$

where Equation (A.10) is derived by substituting Equation (A.9) into Equation (A.1).

A.4 Apparatus

Unwanted parasitic coupling to the other mode reduces the high Q-value of the TE mode resonator. For suppressing the parasitic coupling, special attention is paid to design high Q-value resonators. Three types of resonators are proposed and shown in Figure A.5.

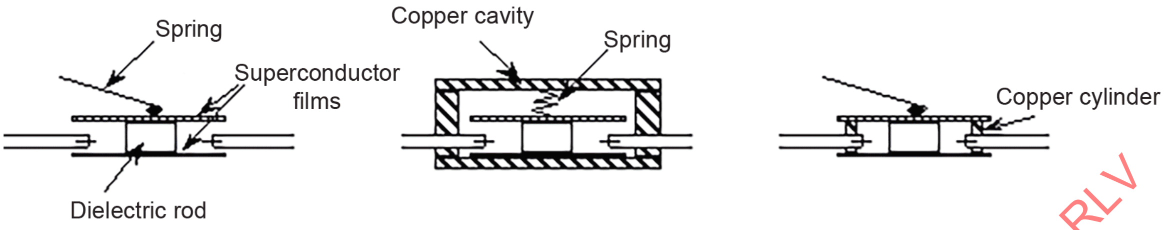

a) Open type resonator b) Cavity type resonator c) Closed type resonator

IEC

Figure A.5 – Three types of dielectric resonators

a) Open type resonator: a low loss dielectric rod is placed between two parallel superconductor films. Two semi-rigid cables for the RF input and output magnetic dipole coupling are attached on both sides of the resonator. In this configuration, the vertical position of the coupling cables should be carefully designed so as to prevent the radiation loss propagating along the coupling cables, which degrades the high Q-value of the TE_{0mp} mode and causes the increase in error for the R_s measurements. The coupling cables should be set as close as possible to the lower superconductor film.

b) Cavity type resonator: the open type resonator shown in a) is placed in a conductor (copper) cavity.

c) Closed type resonator: conductor (copper) cylinder is put between the superconductor films. In this configuration, the radiation loss along the coupling cable is strongly blocked by the copper cylinder. The vertical position of the coupling cables (z) at the highest z-axis magnetic field component (H_z), i.e. $z = h/2$, is recommended.

The measuring apparatus on the cryocooler is protected from mechanical and thermal disturbances, and installed in an X-Y and/or Z-axial manipulator for adjusting sample positions in the range of approximately ±1 mm.

A loop length of the antenna is designed on the basis of the quarter-wavelength rule for achieving the maximum measuring sensitivity.

A.5 Dimensions of the standard sapphire rods

Figure A.6 and Figure A.7 show the mode charts for designing the TE_{011} and TE_{013} mode resonators, respectively, short-circuited at both ends by parallel superconductor films, in which a uniaxial-anisotropic characteristic of the relative permittivity of the sapphire rod is taken into consideration ~~[11]~~ [28]. ε_z is the relative permittivity in the direction of the c-axis, ε_r is that in the plane perpendicular to the c-axis, d is the diameter of the sapphire rod, h is the height of the sapphire rod, and λ_0 is the free space resonant wavelength. As shown in Figure A.6 and Figure A.7, TE_{013} resonance mode is apt to be affected by TM or HE mode in comparison with TE_{011} resonance mode. Since the coupling between TE mode and other modes causes the degradation of unloaded Q, the (d/h) of the sapphire rods shall be selected so as to avoid the unwanted couplings.

As shown in Figure A.7, the value $(d/h)^2$ for the TE_{013} resonator is selected from 0,24 to 0,46 in order that the TE_{013} resonance mode is not affected by the other modes. This value

$(d/h)^2$ = 0,24 to 0,46 leads to a value of $(d/h)^2$ = 2,2 to 4,1 for the TE_{011} resonator. The TE_{011} resonance mode does not also couple with other modes when the value $(d/h)^2$ is in the region of 2,2 to 4,1 as shown in Figure A.6.

As the resonant frequency of TE mode is a function of relative permittivity and dimensions of the sapphire rod, its diameter and height are selected so that the desired f_0 is obtained.

From the curve of TE_{011} mode in Figure A.6, the value of $\varepsilon_r (d/\lambda_0)^2$ can be determined for each $(d/h)^2$ value. When the value $(d/h)^2$ equals 4,0, for example, the value of $\varepsilon_r (d/\lambda_0)^2$ equals 1,92. Thus, the resonant frequency of TE_{011} mode for the sapphire rod with dimension of $(d/h)^2$ = 4,0 is calculated from Equation (A.11) by specifying d and ε_r of the sapphire rod:

$$\varepsilon_r (d / \lambda_0)^2 = \varepsilon_r (d \times f_0 / c)^2 = 1{,}92 \quad \text{(A.11)}$$

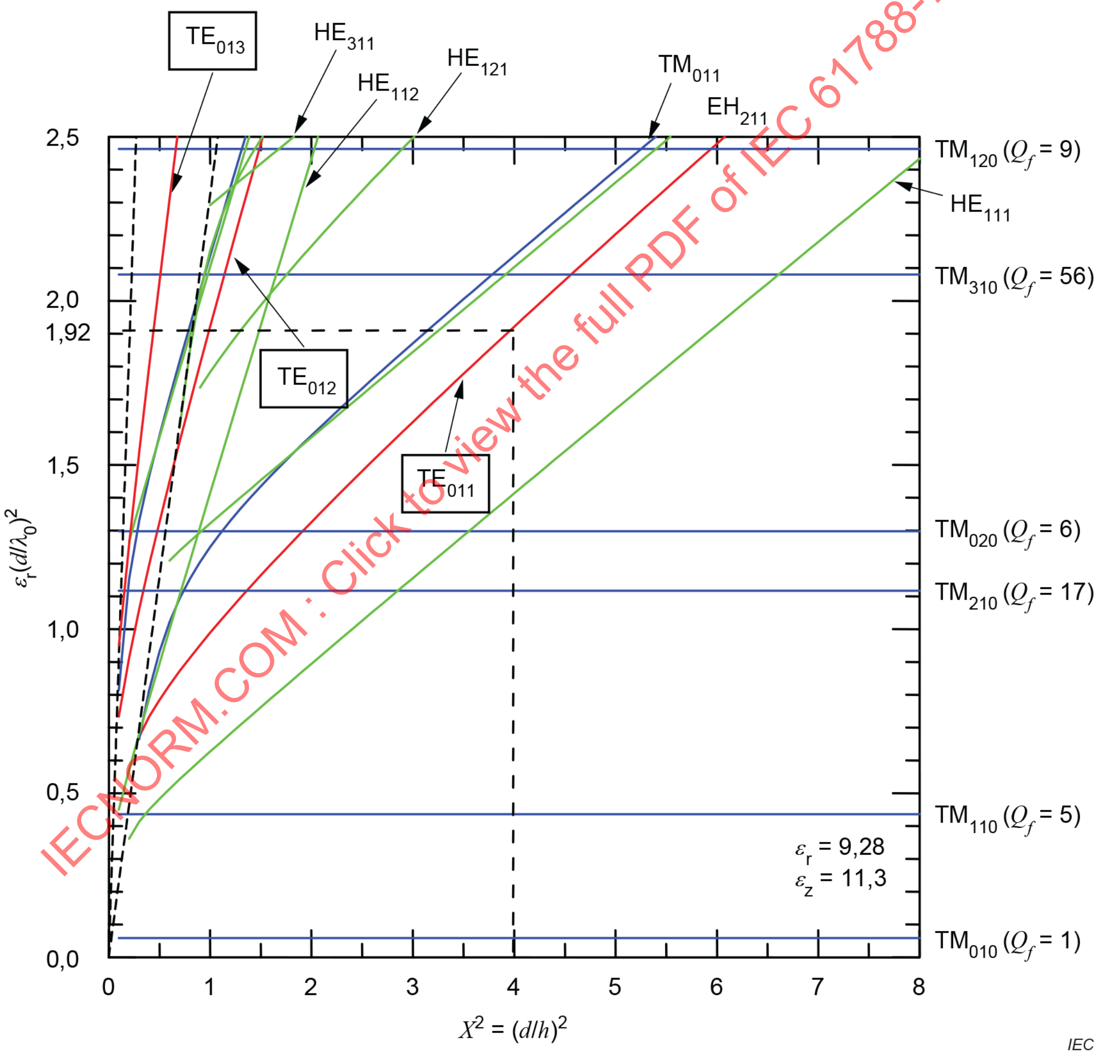

Figure A.6 – Mode chart to design TE_{011} resonator short-circuited at both ends by parallel superconductor films ~~[11]~~ [28]

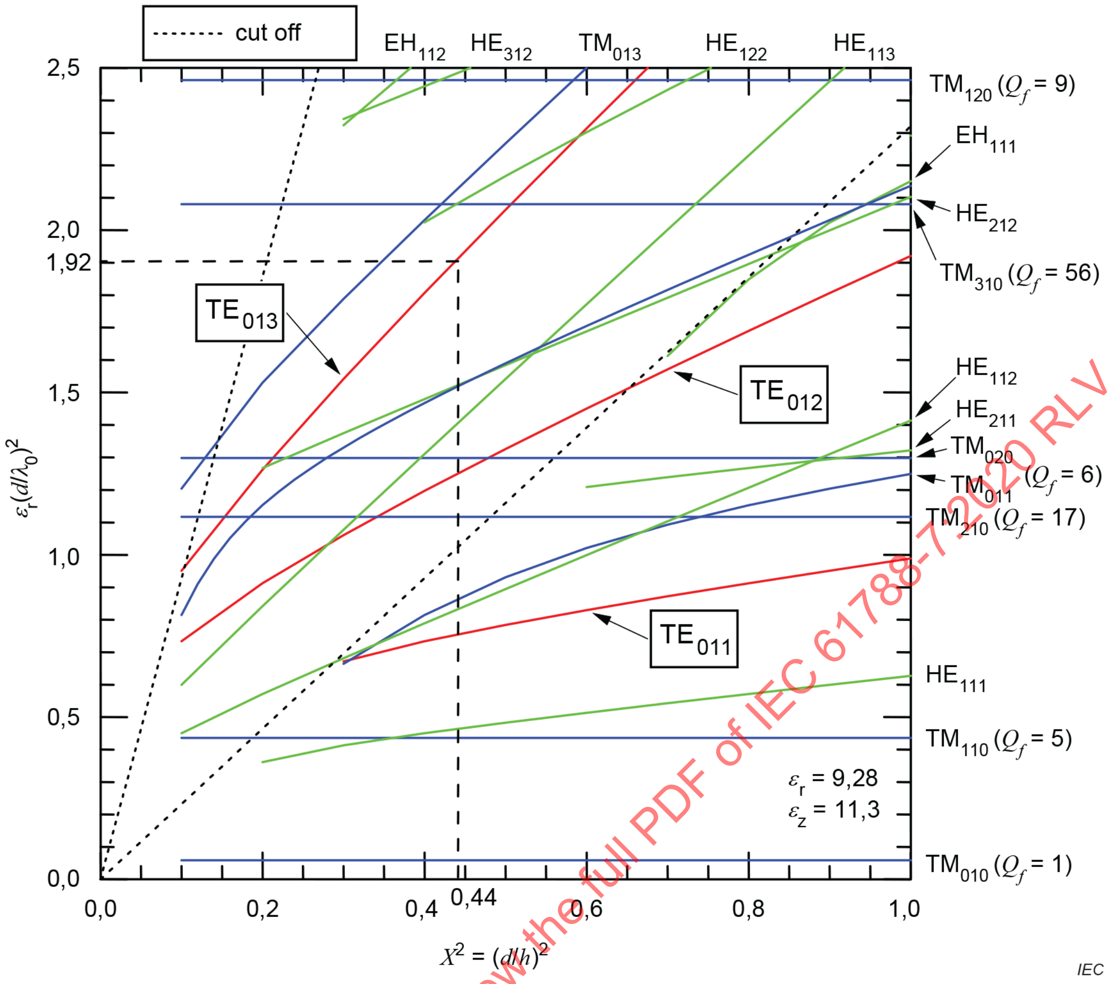

Figure A.7 – Mode chart to design TE_{013} resonator short-circuited at both ends by parallel superconductor films ~~[11]~~ [28]

A.6 Dimension of the closed type resonator

In the closed type resonator, a copper cylinder is put between the superconductor films and a sapphire rod is placed in the center of the copper cylinder (Figure A.5 c)). The resonant frequency of each mode changes with the inner diameter of the copper cylinder, D. Therefore, D shall be selected so as to avoid the unwanted coupling with the other modes. In Figure A.8 and Figure A.9, mode charts of the closed type resonators are shown for the short sapphire rod ($(d/h)^2 = 4$) and the long sapphire rod ($(d/h)^2 = 0{,}44$), respectively, as a function of $S = D/d$ ~~[11]~~ [28]. The ranges of S to separate the TE_{011} and the TE_{013} modes simultaneously from the others are S = 1,8 to 2,8, 3,8 to 4,1 and 4,8 to 5,2. The value of $S = D/d = 4$ is recommended because of the ease with which it can be treated.

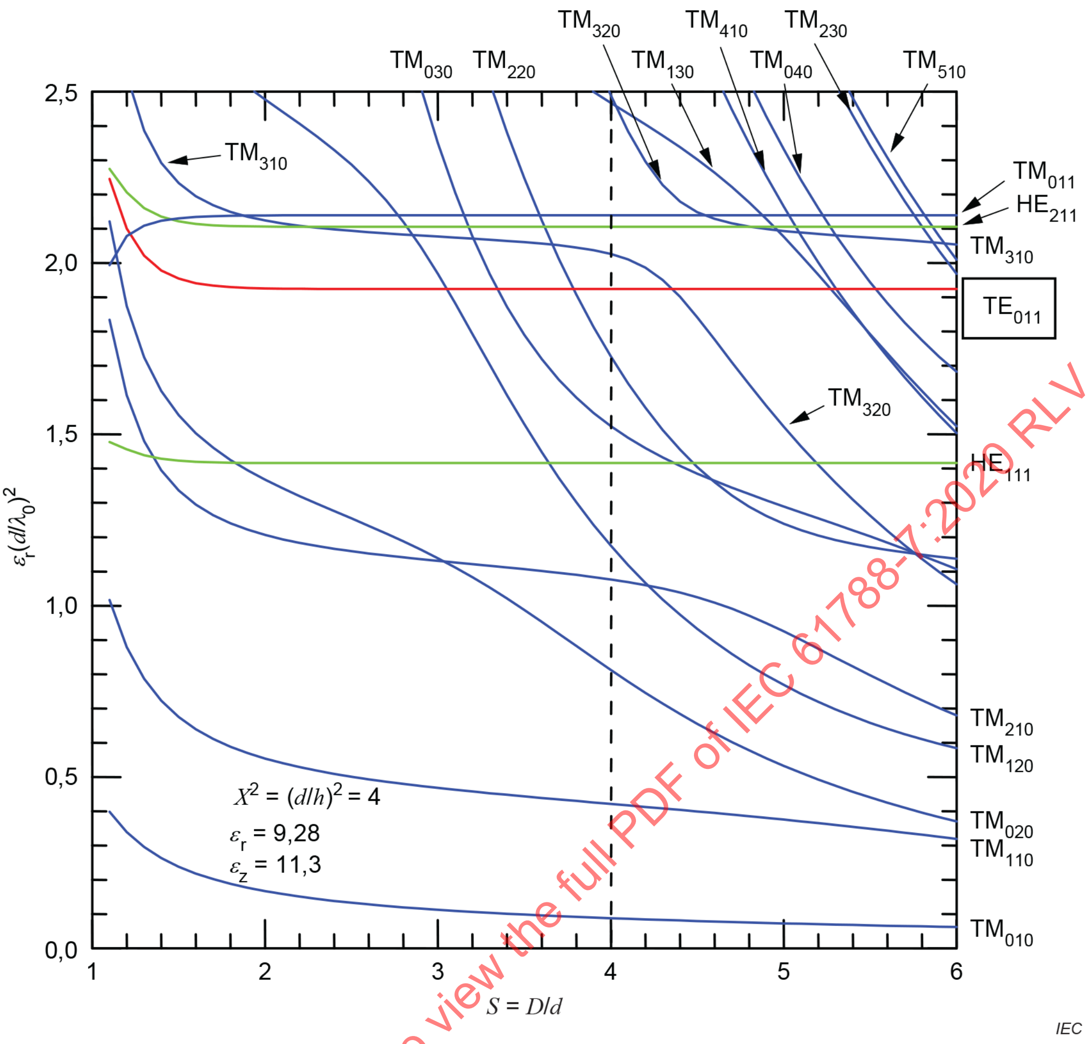

Figure A.8 – Mode chart for TE_{011} closed-type resonator [28]

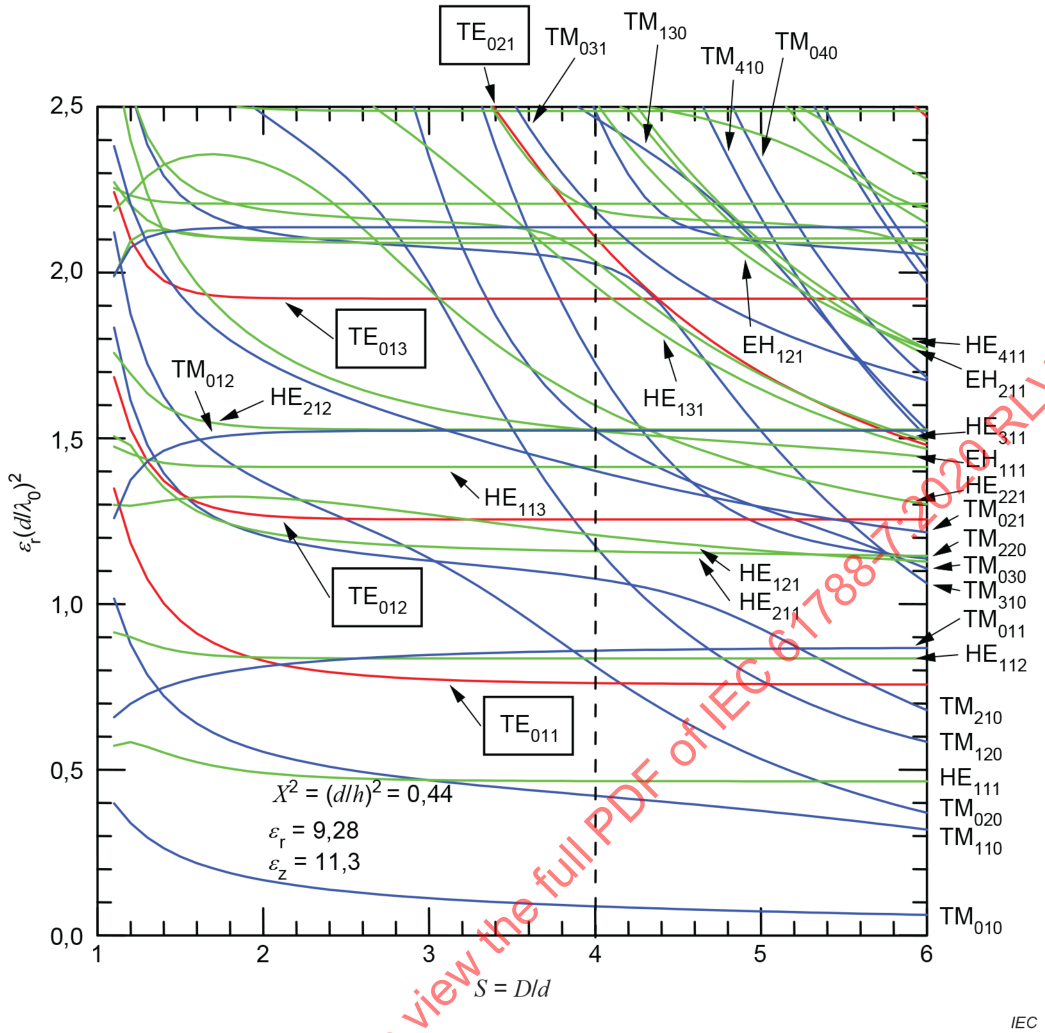

Figure A.9 – Mode chart for TE_{013} closed-type resonator [28]

~~A.7 Precision and accuracy of the test method~~

~~Errors estimation [4][10], sensitivity, accuracy and repeatability for these methods can be obtained by the error analysis concerning R_s as well as by the round robin test.~~

A.7 Sapphire rod reproducibility

Knowing the value of tan δ of the sapphire rod is a difficult problem. One approach based on the single- and triple-height rods involves the selection of a standard rod for each type. The first step is to compare a large number of sapphire rods by measuring them in a single HTS/sapphire resonator. The sapphire rod with the highest unloaded Q-value is the temporary label of standard. This procedure is repeated for a set of triple-height rods. The “standard” single- and triple-height rods are then used as described above to obtain tan δ. The electrical properties, ε' and tan δ, of other rods can then be calibrated by a direct comparison with these standard rods. Using a calibrated single-height rod, it is then possible to extract the R_s values of superconductor films under test.

A.8 Test results

Figure A.10 shows the temperature-dependent R_s of a YBCO film with a thickness of 500 nm and size of 25 mm square. The YBCO film was formed on MgO substrate by a co-evaporation method. The measurement was carried out at 21,8 GHz, which was converted to 10 GHz by the f^2 rule.

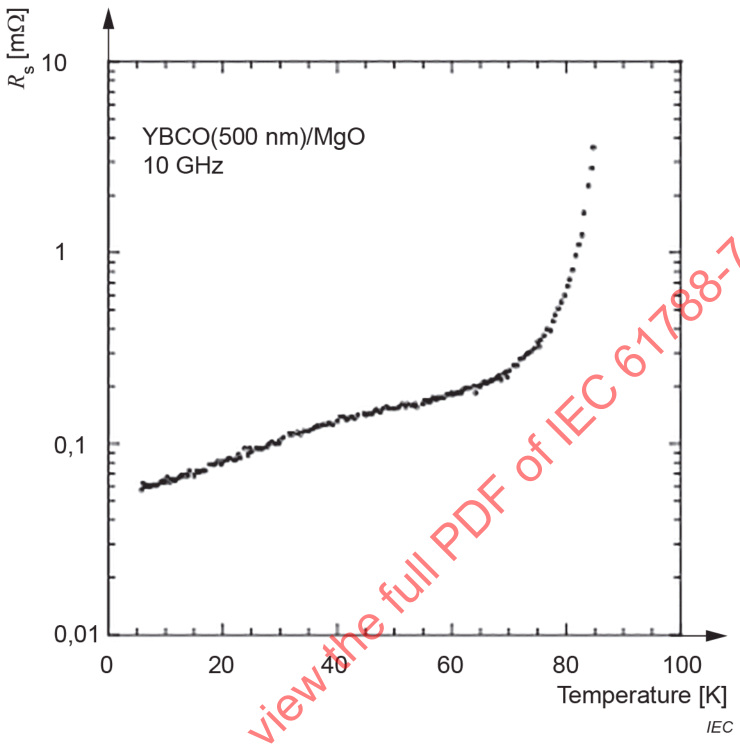

Figure A.10 – Temperature-dependent R_s of YBCO film with a thickness of 500 nm and size of 25 mm square

A.9 Reproducibility of measurement method

In order to evaluate the reproducibility of the surface resistance measurement, R_s of the same sample was measured three times and the variation of R_s was examined. The sample was reset to the measurement cavity each time. Figure A.11 shows the results. Measurement was performed at a frequency of 21,8 GHz and converted to 10 GHz according to the f^2 rule [30]. The variation in R_s was within 10 % in the temperature range of 10 K to 80 K.

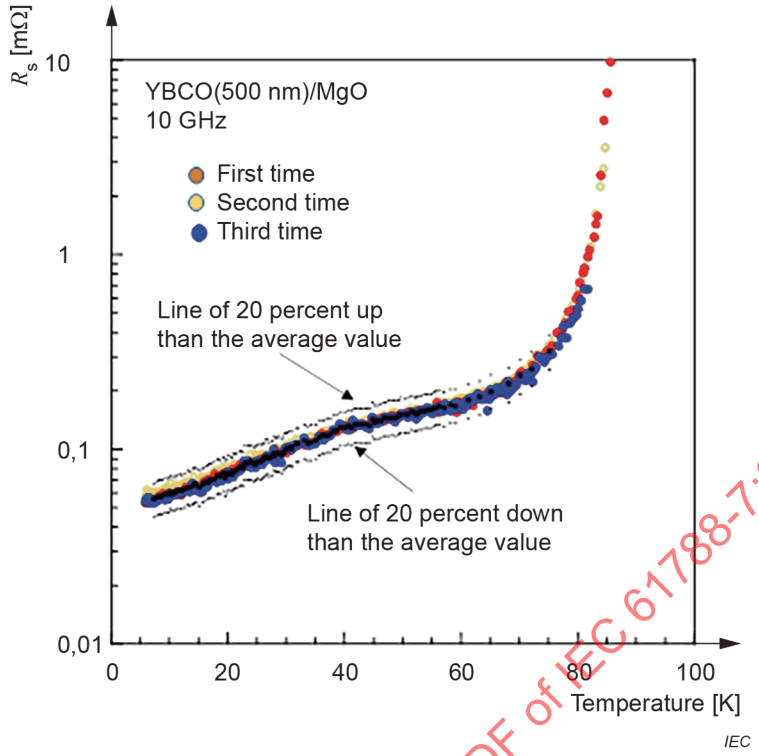

Figure A.11 – Temperature dependent R_s of YBCO film when R_s was measured three times

From the results, the standard deviation of each temperature can be calculated and its values are shown in Table A.1.

Table A.1 – Standard deviation of the surface resistance calculated from the results of Figure A.11

Temperature (K)	20	40	60	80
Standard deviation (%)	0,32	0,23	0,90	6,9

A.10 tan δ deviation effect of sapphire rods on surface resistance

For the two-resonator method, tan δ of the TE_{011} mode and TE_{013} sapphire rods are assumed to be absolutely equal. If tan δ of the two sapphire rods is different, it is not possible to calculate the surface resistance using Equation (6). Therefore, it is necessary to check the effect of tanδ deviation on surface resistance. tan δ of the high-purity sapphire rod used for the standard surface resistance measurement is extremely small, less than 2×10^{-7} [22]. Using such a sapphire rod, uncertainty in the surface resistance is quite small; however, if sapphire rods with a large tan δ are used, uncertainty in the surface resistance increases. tan δ_1 of the sapphire rod for TE_{011} mode is assumed to be 2×10^{-7} and tanδ_3 of the sapphire rod for TE_{013} mode changes according to that value. The difference in tan δ of the two sapphire rods is defined as in Equation (A.12) and the change in surface resistance as in Equation (A.13).

$$x = \frac{\tan\delta_1 - \tan\delta_3}{\tan\delta_1} \times 100 \ [\%] \qquad \text{(A.12)}$$

$$y = \frac{R_S(x) - R_S(0)}{R_S(0)} \quad \text{(A.13)}$$

R_S can be calculated using Equation (A.14) when tan δ_1 and tan δ_3 are different. The relationship between x and y is shown in Table A.2. When the difference in tanδ of the two sapphire rods exceeds ±50 %, the change in surface resistance exceeds ±18 %.

$$R_s = \frac{1}{B_1}\left(\frac{A_1}{Q_{u1}} - \tan\delta_1\right) = \frac{1}{B_3}\left(\frac{A_3}{Q_{u3}} - \tan\delta_3\right) \quad \text{(A.14)}$$

$$A_p = 1 + \frac{W}{\varepsilon'_p} \quad \text{(A.15)}$$

$$B_p = p^2\left(\frac{\lambda_0}{2h_p}\right)^3 \frac{1+W}{30\pi^2\varepsilon'_p}, (p = 1,3) \quad \text{(A.16)}$$

$$W = \frac{J_1^2(u)}{K_1^2(v)} \frac{K_0(v)K_2(v) - K_1^2(v)}{J_1^2(u) - J_0(u)J_2(u)} \quad \text{(A.17)}$$

$$v_0^2 = \left(\frac{\pi d_0}{\lambda_0}\right)^2 \left[\left(\frac{\lambda_0}{2h_0}\right)^2 - 1\right] \quad \text{(A.18)}$$

$$u_0 \frac{J_0(u_0)}{J_1(u_0)} = -v_0 \frac{K_0(v_0)}{K_1(v_0)} \quad \text{(A.19)}$$

Table A.2 – Relationship between x, defined by Equation (A.12), and y, defined by Equation (A.13)

x (%)	−50	−40	−30	−20	−10	0	+10	+20	+30	+40	+50
y (%)	18,0	14,4	10,8	7,2	3,6	0	−3,6	−7,2	−10,8	−14,4	−18,0

~~A.9 Reference documents~~

~~[1] WILKER, C., SHEN, Z.-Y., PANG, P., FACE, DW., HOLSTEIN, WL., MATTHEWS, AL. and LAUBACHER, D.B. 5 GHz high-temperature-superconductor resonators with high Q and low power dependence up to 90 K. *IEEE Trans. Microwave Theory Tech.*, 1991, 39, p.1462.~~

~~[2] TABER, RC. A parallel plate resonator technique for microwave loss measurements on superconductors. *Rev. Sci. Instrum.*, 1990, No. 61, p.2200-2206.~~

~~[3] YOSHITAKE, T. and TSUGE, H. Effects of microstructures on microwave properties in Y-Ba-Cu-O microstrip resonators. *IEEE Trans. Appl. Supercond.*, 1995, 5, p.2571.~~

~~[4] MAZIERSKA, J. Dielectric resonator as a possible standard for characterization of high temperature superconducting films for microwave applications. *J. Supercond.*, 1997, 10, p.73.~~

~~[5] SHEN, Z.-Y., WILKER, C., PANG, P., HOLSTEIN, WL., FACE, DW. and KOUNTZ, DJ. High Tc superconductor-sapphire microwave resonator with extremely high Q-values up to 90 K. *IEEE Trans. Microwave Theory Tech.*, 1992, 40, p.2424.~~

~~[6] KRUPKA, J., KLINGER, M., KUHN, M., BARANYAK, A., STILLER, M., HINKEN, J. and MODELSKI, J. Surface resistance measurements of HTS films by means of sapphire dielectric resonators. *IEEE Trans. Appl. Supercond.*, 1993, 3, p.3043.~~

[7] TELLMANN, N., KLEIN, N., DAHNE, U., SCHOLEN, A., SCHULZ, H. and CHALOUPKA, H. High-Q $LaAlO_3$ dielectric resonators shielded by YBCO-films. *IEEE Trans. Appl. Supercond.*, 1994, 4, p.143.

[8] KOBAYASHI, Y. and KAYANO, H. An improved dielectric resonator method for surface impedance measurement of high-Tc superconductors, *IEEE MTT-S Digest*, 1992, No. IF2 T-3, p.1031.

[9] KOBAYASHI, Y., IMAI, T. and KAYANO, H. Microwave measurement of temperature and current dependences of surface impedance for high-Tc superconductors. *IEEE Trans.Microwave Theory Tech.*, 1991, 39, p.1530.

[10] YOSHIKAWA, H., OKAJIMA, S. and KOBAYASHI, Y. *Comparison between BMT ceramic one-resonator method and sapphire two-resonator method to measure surface resistance of YBCO films*. Proc. Asia-Pacific Microwave Conf., 1998, 2, p.1083.

[11] HASHIMOTO, T and KOBAYASHI, Y. Two-Sapphire-Rod-Resonator method to measure the surface resistance of High-Tc superconductor films. *IEICE Trans. Electron.*, 2004, E87-C, No.5, p. 681.

Annex B
(informative)

Evaluation of relative combined standard uncertainty for surface resistance measurement

B.1 Practical surface resistance measurement

A superconductor shows a significantly increased surface resistance when irradiated by a high frequency current in the microwave range. There are several methods for measuring surface resistance, but the dielectric resonator method can measure surface resistance the most accurately. The method is described in Annex A. Figure B.1 shows these two resonators used to measure the frequency characteristics of TE_{011} and TE_{013} modes.

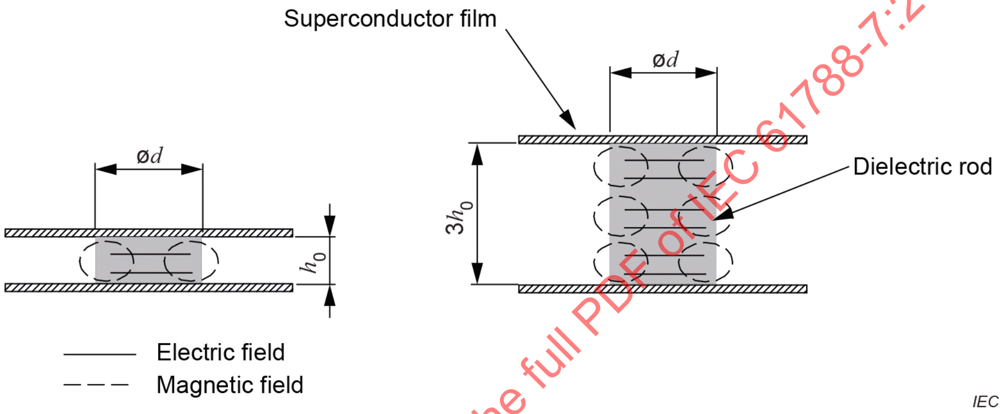

Figure B.1 – Schematic diagram of TE_{011} and TE_{013} mode resonance

Figure B.2 shows the typical frequency characteristics of TE_{011} mode resonance. Q_{L1} is determined using the results of this measurement and Q_{u1} is calculated using Equation (B.2).

$$Q_{L1} = \frac{f_0}{\Delta f} \tag{B.1}$$

$$Q_{u1} = \frac{Q_{L1}}{1 - A_t}, A_t = 10^{-IA[dB]/20} \tag{B.2}$$

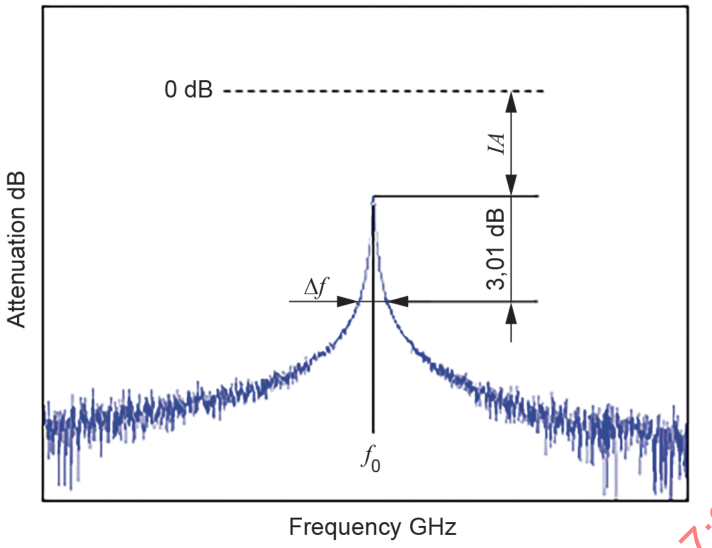

Figure B.2 – Typical frequency characteristics of TE$_{011}$ mode resonance

B.2 Determination of surface resistance of the superconductor

The microwave surface resistance of the superconductor is obtained from Equations (B.3) to (B.8).

$$R_s = \frac{30\pi^2 \times 3}{3-1}\left[\frac{2h_0}{\lambda_0}\right]^3 \frac{\varepsilon' + W}{1+W}\left[\frac{1}{Q_{u1}} - \frac{1}{Q_{u3}}\right] \quad \text{(B.3)}$$

$$\varepsilon' = \left(\frac{\lambda_0}{\pi d}\right)^2 \left(u^2 + v^2\right) + 1 \quad \text{(B.4)}$$

$$W = \frac{J_1^2(u)}{K_1^2(v)} \frac{K_0(v)K_2(v) - K_1^2(v)}{J_1^2(u) - J_0(u)J_2(u)} \quad \text{(B.5)}$$

$$v^2 = \left(\frac{\pi d}{\lambda_0}\right)^2 \left[\left(\frac{3\lambda_0}{2h_0}\right)^2 - 1\right] \quad \text{(B.6)}$$

$$u\frac{J_0(u)}{J_1(u)} = -v\frac{K_0(v)}{K_1(v)} \quad \text{(B.7)}$$

$$\lambda_0 = \frac{c}{f_0} \quad \text{(B.8)}$$

Here, d and h_0 are the diameter and height of the sapphire rod, respectively, ε' is the effective relative permittivity of the sapphire rod, c is the speed of light in vacuum, and f_0 is the resonant frequency of the resonator.

B.3 Combined standard uncertainty

B.3.1 General

By partially differentiating the equation (B.3) with h_0, ε', W, Q_{u1}, *and* Q_{u3}, the equation of uncertainty shown in Equation (B.9) is obtained.

$$\begin{aligned} u_c^2 = \frac{\delta R_s^2}{R_s^2} &= \left(\frac{\partial R_s}{\partial h}\right)^2\left(\frac{\delta h}{R_s}\right)^2 + \left(\frac{\partial R_s}{\partial \varepsilon'}\right)^2\left(\frac{\delta \varepsilon'}{R_s}\right)^2 + \left(\frac{\partial R_s}{\partial W}\right)^2\left(\frac{\delta W}{R_s}\right)^2 \\ &+ \left(\frac{\partial R_s}{\partial Q_{u1}}\right)^2\left(\frac{\delta Q_{u1}}{R_s}\right)^2 + \left(\frac{\partial R_s}{\partial Q_{u3}}\right)^2\left(\frac{\delta Q_{u3}}{R_s}\right)^2 + c_{\text{unknown}}^2 u_{\text{unknown}}^2 \\ &(\delta h = h u_1, \delta\varepsilon' = \varepsilon' u_2, \delta W = W u_3, \delta Q_{u1} = Q_{u1} u_4, \delta Q_{u3} = Q_{u3} u_5) \\ &= \left(\frac{\partial R_s}{\partial h}\right)^2\left(\frac{h}{R_s}\right)^2 u_1^2 + \left(\frac{\partial R_s}{\partial \varepsilon'}\right)^2\left(\frac{\varepsilon'}{R_s}\right)^2 u_2^2 + \left(\frac{\partial R_s}{\partial W}\right)^2\left(\frac{W}{R_s}\right)^2 u_3^2 \\ &+ \left(\frac{\partial R_s}{\partial Q_{u1}}\right)^2\left(\frac{Q_{u1}}{R_s}\right)^2 u_4^2 + \left(\frac{\partial R_s}{\partial Q_{u3}}\right)^2\left(\frac{Q_{u3}}{R_s}\right)^2 u_5^2 + c_{\text{unknown}}^2 u_{\text{unknown}}^2 \\ &= c_1^2 u_1^2 + c_2^2 u_2^2 + c_3^2 u_3^2 + c_4^2 u_4^2 + c_5^2 u_5^2 + c_{\text{unknown}}^2 u_{\text{unknown}}^2 \end{aligned} \quad \text{(B.9)}$$

The variables c_{unknown} and u_{unknown} in Equation (B.9) represent in the uncertainty of unknown factors of measurement system, for example, noise factor. The variables in Equation (B.9) are expressed by Equations (B.10) to (B.14).

$$c_1 = \frac{\partial R_s}{\partial h}\frac{h}{R_s} = \frac{3R_s}{h_0}\frac{h_0}{R_s} = 3 \quad \text{(B.10)}$$

$$c_2 = \frac{\partial R_s}{\partial \varepsilon'}\frac{\varepsilon'}{R_s} = \frac{\varepsilon'}{\varepsilon' + W} \quad \text{(B.11)}$$

$$c_3 = \frac{\partial R_s}{\partial W}\frac{W}{R_s} = \frac{(1-\varepsilon')W}{(1+W)(\varepsilon' + W)} \quad \text{(B.12)}$$

$$c_4 = \frac{\partial R_s}{\partial Q_{u1}}\frac{Q_{u1}}{R_s} = \frac{-Q_{u3}}{Q_{u3} - Q_{u1}} \quad \text{(B.13)}$$

$$c_5 = \frac{\partial R_s}{\partial Q_{u3}}\frac{Q_{u3}}{R_s} = \frac{Q_{u1}}{Q_{u3} - Q_{u1}} \quad \text{(B.14)}$$

B.3.2 Calculation of c_2 to c_5 (12 GHz resonance at 20 K)

When calculating uncertainty using the Equation (B.9), it is necessary to specify the resonant frequency. Here, we will discuss a typical 12 GHz resonator.

12 GHz resonator (f_0 = 12 GHz, d = 11,4 mm, h_0 = 5,7 mm)

Using the above values, we can calculate v^2 and u^2 by Equations (B.6) and (B.7).

$$v^2 = 7{,}815,\ u^2 = 9{,}09 \tag{B.15}$$

ε' and W are determined by Equations (B.4) and (B.5).

$$\varepsilon' = 9{,}22,\ W = 0{,}16 \tag{B.16}$$

Then c_2 and c_3 can be determined using Equations (B.11) and (B.12).

$$c_2 = 0{,}983,\ c_3 = -0{,}122 \tag{B.17}$$

In order to determine c_4 and c_5, we have to know the values of unloaded Q_{u1} and Q_{u3}. Y. Kobayashi reported Q_{u1} and Q_{u3} at 20 K, 12 GHz [28]. Their reported values were Q_{u1} = 2 000 000 (Q_{L1} = 1 800 000) and Q_{u3} = 7 500 000 (Q_{L3} = 6 750 000). Therefore, c_4 and c_{5L} can be calculated.

$$c_4 = 1{,}364,\ c_5 = 0{,}3636 \tag{B.18}$$

B.3.3 Determination of u_1 to u_5

u_1 to u_5, which are derived from the uncertainty of the diameter, height and dielectric constant of sapphire rod and Q_{u1} and Q_{u3} of the cavity, are calculated by the following procedures.

1) u_1

u_1 is determined by the uncertainty of the height of the sapphire rod. The height of the sapphire rod of the 12 GHz resonator is 5,7 mm, and its uncertainty is 50 µm. Therefore, u_1 is as follows.

$$u_1 = \frac{1}{\sqrt{3}}\frac{0{,}05}{5{,}7} = 0{,}005\,07 \tag{B.19}$$

2) u_2

u_2 is determined by the uncertainty in the effective dielectric constant ε'_δ of the sapphire rod and can be calculated using Equation (B.20).

$$u_2 = \frac{1}{\sqrt{3}}\frac{\varepsilon' - \varepsilon'_\delta}{\varepsilon'} \tag{B.20}$$

where ε'_δ is the relative permittivity induced from uncertainty in the shape of the sapphire rod.

$$\varepsilon' = \left(\frac{\lambda_0}{\pi d_0}\right)^2 \left(u_0^2 + v_0^2\right) + 1 \quad (d_0 = 11{,}4\ \text{mm}, h_0 = 5{,}7\ \text{mm}) \tag{B.21}$$

$$\varepsilon'_\delta = \left(\frac{\lambda_0}{\pi d}\right)^2 \left(u_{0\delta}^2 + v_{0\delta}^2\right) + 1 \quad (d_{0\delta} = 11{,}45\ \text{mm}, h_{0\delta} = 5{,}65\ \text{mm}) \tag{B.22}$$

and u_0, v_0, $u_{0\delta}$ and $v_{0\delta}$ are calculated using Equations (B.23) and (B.24).

$$v_0^2 = \left(\frac{\pi d_0}{\lambda_0}\right)^2 \left[\left(\frac{3\lambda_0}{2h_0}\right)^2 - 1\right], v_{0\delta}^2 = \left(\frac{\pi d_{0\delta}}{\lambda_0}\right)^2 \left[\left(\frac{3\lambda_0}{2h_{0\delta}}\right)^2 - 1\right] \tag{B.23}$$

$$u_0 \frac{J_0(u_0)}{J_1(u_0)} = -v_0 \frac{K_0(v_0)}{K_1(v_0)},\ u_{0\delta} \frac{J_0(u_{0\delta})}{J_1(u_{0\delta})} = -v_{0\delta} \frac{K_0(v_{0\delta})}{K_1(v_{0\delta})} \tag{B.24}$$

As a result, we find that ε' = 9,22 and ε'_δ = 9,29.

$$u_2 = 0{,}004\,4 \tag{B.25}$$

3) u_3

u_3 can be determined using Equation (B.26).

$$u_3 = \frac{1}{\sqrt{3}} \frac{W - W_\delta}{W} \tag{B.26}$$

W is determined using Equation (B.5) and W_δ comes from uncertainty in the shape of the sapphire rod and can be determined by using Equation (B.27).

$$W_\delta = \frac{J_1^2(u_\delta)}{K_1^2(v_\delta)} \frac{K_0(v_\delta)K_2(v_\delta) - K_1^2(v_\delta)}{J_1^2(u_\delta) - J_0(u_\delta)J_2(u_\delta)} \tag{B.27}$$

By calculating W and W_δ using u_0, v_0, $u_{0\delta}$, $v_{0\delta}$ in Equations (B.23) and (B.24), u_3 turns out to have the following value.

$$u_3 = 0{,}014\,3 \tag{B.28}$$

4) u_4 and u_5

u_4 and u_5 are determined by measuring the uncertainty in Q_{u1} and Q_{u3}. The measurement of the uncertainty in Q_{u1} and Q_{u3} has the most influence on the dynamic range uncertainty of the vector network analyzer and other factors are negligible. Since the dynamic range uncertainty in the recommended vector network analyzer is ±0,1 dB, u_4 and u_5 are calculated using this value. Regarding the frequency characteristics of the resonator in Figure B.2, the frequency characteristic near the resonant frequency is assumed to be a Lorentz distribution [30].

$$y = \left|\frac{S_{12}(f)}{S_{12}(f_0)}\right| = \frac{1}{\left(1 + Q_L^2 \Delta^2(f)\right)^{1/2}} = \frac{1}{\left(1 + \left(\frac{f - f_0}{f_1}\right)^2\right)^{1/2}},$$

$$\Delta(f) = 1 - \frac{f_0^2}{f^2} = \frac{2(f - f_0)}{f_0} \tag{B.29}$$

The frequency characteristics are shown in Figure B.3 The curve can be approximated by Equation (B.29), where f_0 is the resonant frequency and $2f_1$ is the bandwidth at 3,01 dB. The frequency bandwidth which is 3,01 dB below the resonance peak is defined as Δf and it corresponds to the bandwidth across 0,707 in Figure B.3. The ±0,1 dB of the dynamic range uncertainty corresponds to ±0,008 in Figure B.3. Therefore, Q_{L1}, $Q_{L1\delta}$, Q_{L3}, and $Q_{L3\delta}$

can be calculated. Q_{L1} and Q_{L3} are reported as 1,80 × 10^6 and 6,75 × 10^6, respectively [28]. Using these values, we can calculate $Q_{L1\delta}$ and $Q_{L3\delta}$.

$$Q_{L1} = 1{,}80 \times 10^6, \ Q_{L1\delta} = 1{,}84 \times 10^6, \ Q_{L3} = 6{,}75 \times 10^6, \ Q_{L3\delta} = 6{,}90 \times 10^6$$

Assuming insertion attenuation (IA) = 20dB, Q_{u1}, $Q_{u1\delta}$, Q_{u3}, and $Q_{u3\delta}$ can be calculated.

$$Q_{u1} = 2{,}00 \times 10^6, \ Q_{u1\delta} = 2{,}044 \times 10^6, \ Q_{u3} = 7{,}5 \times 10^6, \ Q_{u3\delta} = 7{,}67 \times 10^6$$

Through these calculations, the values of u_4 and u_5 are obtained.

$$u_4 = \frac{1}{\sqrt{3}} \frac{Q_{u1} - Q_{u1\delta}}{Q_{u1}} = -0{,}012 \quad \text{(B.30)}$$

$$u_5 = \frac{1}{\sqrt{3}} \frac{Q_{u3} - Q_{u3\delta}}{Q_{u3}} = -0{,}013 \quad \text{(B.31)}$$

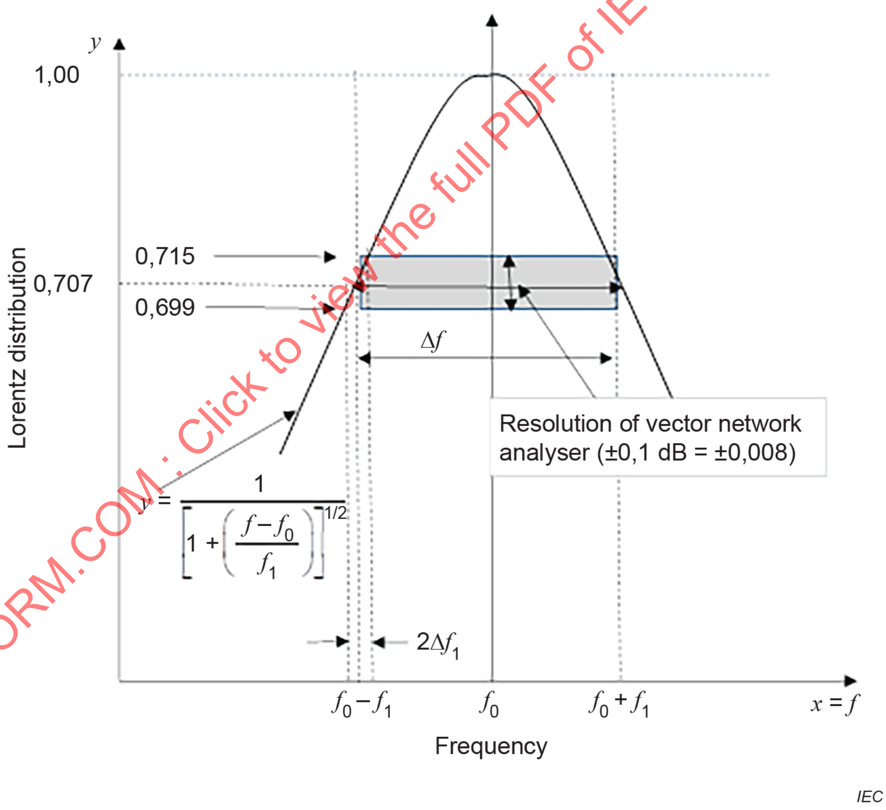

Figure B.3 – Frequency characteristics of a resonator approximated by a Lorentz distribution

B.3.4 Combined relative standard uncertainty

Uncertainties in c_{cavity} and u_{cavity} due to the loss of copper cavity is quite small, however $c_{unknown}$ and $u_{unknown}$ are not small. The combined standard uncertainty at 20 K is calculated as follows.

$$u_c = \sqrt{c_1^2 u_1^2 + c_2^2 u_2^2 + c_3^2 u_3^2 + c_4^2 u_4^2 + c_5^2 u_5^2 + c_{\text{unknown}}^2 u_{\text{unknown}}^2}$$
$$= \sqrt{2{,}31 \times 10^{-4} + 0{,}187 \times 10^{-4} + 0{,}030 \times 10^{-4} + 2{,}68 \times 10^{-4} + 0{,}223 \times 10^{-4} + c_{\text{unknown}}^2 u_{\text{unknown}}^2} \quad \text{(B.32)}$$
$$= \sqrt{5{,}43 \times 10^{-4} + c_{\text{unknown}}^2 u_{\text{unknown}}^2}$$

It is difficult to quantitatively evaluate $c_{\text{unknown}} u_{\text{unknown}}$ in Equation (B.32), but its value can be estimated from the results of surface resistance measurement repeated three times. The variation observed when measuring the surface resistance of the same films repeatedly is believed to be due to the noise and temperature uncertainty of the measurement system. Therefore, from the results in Table A.1, $c_{\text{unknown}} u_{\text{unknown}}$ can be estimated as about 0,32 % for 20 K, about 0,9 % for 60 K, and about 6,9 % for 80 K ($c_{\text{unknown}} u_{\text{unknown}}$ increases as the measurement temperature increases). From the above results, the combined relative standard uncertainty of Equation (B.32) was about 2,4 % at 20 K and about 7,3 % at 80 K. The value is smaller than the target combined relative standard uncertainty.

When the measured temperature exceeds 70 K, large noise is superimposed on the resonance peak, and the uncertainty in R_s increases. In that case, it is difficult express the resonance peak with Lorentz distribution. Therefore, the deviation of u_4 and u_5 have to be reviewed. However, as is clear from the results in Figure A.11 and Table A.1, the uncertainty of R_s measured by the standard dielectric resonator method is less than 10 % below 80 K.

Bibliography

[1] ZHANG, D., LIANG, G-C., SHIH, CF., LU, ZH. and JOHANSSON, ME. A 19-pole cellular bandpass filters using 75-mm diameter high temperature superconducting thin films. *IEEE Microwave and Guided Wave Letters*, 1995, 5, p.405.

[2] ONO, RH., BOOTH, JC., STORK, F. and WILKER, C. *Developing standards for the emerging technology of high temperature superconducting electronics*. Adv. in Superconductivity X, Tokyo: Springer, 1998, p.1407.

[3] KINDER, H., BERBERICH, P., UTZ, B. and PRUSSEIT, W. Double sided YBCO films on 4" substrates by thermal reactive evaporation. *IEEE Trans. Appl. Supercond.*, 1995, 5, p.1575.

[4] FACE, DW., WILKER, C., SHEN, Z-Y., PANG, P. and SMALL, R.J. Large area YBa2Cu3O7 films for high power microwave applications. *IEEE Trans. Appl. Supercond.*, 1995, 5, p.1581.

[5] KOBAYASHI, Y., IMAI, T. and KAYANO, H. Microwave measurement of temperature and current dependences of surface impedance for high-Tc superconductors. *IEEE Trans. Microwave Theory Tech.*, 1991, 39, p.1530.

[6] WILKER, C., SHEN, Z.-Y., NGUYEN, VX., and BRENNER, MS. A sapphire resonator for microwave characterization of superconducting thin films. *IEEE Trans. Appl. Supercond.*, 1993, 3, p.1457.

[7] MAZIERSKA, J. Dielectric resonator as a possible standard for characterization of high temperature superconducting films for microwave applications. *J. Supercond.*, 1997, 10, p.73.

[8] LLOPIS, O. and GRAFFEUIL, J. Microwave characterization of high Tc superconductors with a dielectric resonator. *J. Less-Common Met.*, 1990, 164, p.1248.

[9] MAZIERSKA, J. and WILKER, C. Accuracy issues in surface resistance measurements of high temperature superconductors using dielectric resonators (corrected). *IEEE Trans. Appl. Supercond.*, 2001, 11, p.4140.

[1] ZHANG, D., LIANG, G-C., SHIH, CF., LU, ZH. and JOHANSSON, ME. A 19-pole cellular bandpass filter using 75-mm diameter high-temperature superconducting thin films. *IEEE Microwave and Guided Wave Letters*, 1995, 5, p.405

[2] SIMON, RW., HAMMOND, RB., BERKOWITZ, SJ. and WILLEMSEN, BA. Supercoducting microwave filter systems for cellular telephone base station. *Proc. IEEE*, 2004, 92, p.1585

[3] PETERSON, GE., WTAWAXKI, R.P. and ALFORD, N.McN. Helical resonators containing high Tc ceramic superconductors. *Appl. Phys. Lett.*, 1989, 55, p.1798

[4] TSUZUKI, G., SUZUKI, M. and SAKAKIBARA, N. Superconducting Filter for IMT-2000 Band. *IEEE Trans. Microwave Theory Tech.*, 2000, 48, p.2519

[5] ITOH, K., ISHII, O., NAGAI, Y., SUZUKI, N., KIMACHI, Y. and MICHIKAMI, O. High Tc superconducting small antenna. *IEEE Trans. Appl. Supercond.*, 1993, 3, p.2836

[6] HOHENWATER, GK., TRACK, EK., DRAKE, RE. and PATT, R. Forty five nanosecond superconducting delay line. *IEEE Trans. Magn.,* 1993, 3, p.2804

[7] KINDER, H., BERBERICH, P., UTZ, B. and PRUSSEIT, W. Double sided YBCO films on 4" substrates by thermal reactive evaporation. *IEEE Trans. Appl. Supercond.*, 1995, 5, p.1575

[8] FACE, DW., WILKER, C., SHEN, Z-Y., PANG, P. and SMALL, R.J. Large area $YBa_2Cu_3O_7$ films for high power microwave applications. *IEEE Trans. Appl. Supercond.*, 1995, 5, p.1581

[9] NAKAGAWA, K., HONMA, T., TAKEDA, K., ONO, S., KAI, H., SAITO, A., MUKAIDA, M., NAKAJIMA, K. and OHSHIMA, S., Intrinsic Surface Resistance of YBCO Thin Films Under DC Magnetic Field, *IEEE Trans. Appl. Supercond.*, 2011, 21, p.587

[10] GUREVICH, A., Theory of RF superconductivity for resonant cavities, *Supercond. Sci. Technol.*, 2017, 30, 034004

[11] WILKER, C., SHEN, Z.-Y., NGUYEN, VX. and BRENNER, MS. A sapphire resonator for microwave characterization of superconducting thin films. *IEEE Trans. Appl. Supercond.*, 1993, 3, p.1457

[12] LLOPIS, O. and GRAFFEUIL, J. Microwave characterization of high Tc superconductors with a dielectric resonator. *J. Less-Common Met.*, 1990, 164, p.1248

[13] MAZIERSKA, J. and WILKER, C. Accuracy issues in surface resistance measurements of high temperature superconductors using dielectric resonators (corrected). *IEEE Trans. Appl. Supercond.*, 2001, 11, p.4140

[14] POMPEO, N., TOROKHTII, K. and SILVA, E. Dielectric Resonators for Measurements of the Surface Impedance of Superconducting Films. *Meas. Sci. Rev.* 2014, 14, p.164

[15] OBARA, H. and KOSAKA, S. Microwave power dependence measurement of surface resistance of superconducting films using a dielectric resonator method with circle fit and two-mode techniques. *IEICE Trans. Electron.*, 2006, E89C, 2, p.125

[16] LEONG, K. and MAZIERSKA, J. Accurate measurement of surface resistance of HTS films using a noble transmission mode Q-factor technique. *J. Superconductivity*, 2001, 14, p.93

[17] PALMIERI, V., ROSSI, AA., STARK, SY. and VAGLIO, R., Evidence for boundary resistance effect on superconducting radiofrequency cavity performances. *Supercond. Sci. Technol.*, 2014, 27, 085004

[18] TABER, RC. A parallel plate resonator technique for microwave loss measurements on superconductors. *Rev. Sci. Instrum.*, 1990, 61, p.2200

[19] FLETCHER, R. and COOK, J. Measurement of surface impedance versus temperature using a generalized sapphire resonator technique, *Rev. Sci, Instrum.,* 1994, 65, p. 2658.

[20] YOSHITAKE, T. and TSUGE, H. Effects of microstructures on microwave properties in Y-Ba-Cu-O microstrip resonators. *IEEE Trans. Appl. Supercond.*, 1995, 5, p.2571

[21] OKAI, D., KUSUNOKI, M., MUKAIDA, M. and OHSHIMA, S. New surface resistance measurement technique of high-temperature superconductors using a probe coupling microstrip line resonator, *IEEE Trans. Appl. Supercond.,* 2001, 11 p. 3078

[22] MAZIERSKA, J. Dielectric resonator as a possible standard for characterization of high temperature superconducting films for microwave applications. *J. Supercond.*, 1997, 10, p.73

[23] SHEN, Z.-Y., WILKER, C., PANG, P., HOLSTEIN, WL., FACE, DW. and KOUNTZ, DJ. High Tc superconductor-sapphire microwave resonator with extremely high Q-values up to 90 K. *IEEE Trans. Microwave Theory Tech.*, 1992, 40, p.2424

[24] KOBAYASHI, Y., IMAI, T. and KAYANO, H. Microwave measurement of temperature and current dependences of surface impedance for high-Tc superconductors. *IEEE Trans. Microwave Theory Tech.*, 1991, 39, p.1530

[25] SATO, K., SATO, S., ICHIKAWA, K., WATANABE, M., HONMA, T., TANAKA, Y., OIKAWA, S., SAITO, A. and OHSHIMA, S. Dependence of microwave surface resistance of HTS thin films on applied dc magnetic fields parallel and normal to the substrate. *J. Phys*. 2014, 507, 012045

[26] ZENG, C., LUO, ZX., BU, SR., YANG, K. and ZHANG, QS. A novel method for the measurement of frequency-character of surface resistance of HTS thin film. *Chinese Science Bulletin*, 2010, 55, p.1088

[27] ZENG, C., CHEN, L., BU, SR., NING, JS. MENG, B. and ZHANG, QS. An efficient and accurate method for HTS surface resistance measurement. *J. Supercond. Nov. Magn.*, 2015, 28, p. 3179

[28] HASHIMOTO, T. and KOBAYASHI, Y. Two-Sapphire-Rod-Resonator method to measure the surface resistance of High-Tc superconductor films. *IEICE Trans. Electron.*, 2004, E87-C, No.5, p. 681

[29] LEE, JH., KIM, MS., HAN, HK., JUNG, HS., YANG, WI., LEE, SY., PARK, B. and LEE, SG., Improved Measurement Accuracy for Thickness of $YBa_2Cu_3O_y$ Films by Using a Single Two-resonance-mode Sapphire Resonator, *J. Korean Phys. Soc.* 2012, 60, p.1072

[30] LANCASTER, MJ. *Passive microwave device applications of high-temperature superconductors*, Cambridge University Press, 1997, p.138

IEC 61788-7

Edition 3.0 2020-03

INTERNATIONAL STANDARD

NORME INTERNATIONALE

colour inside

Superconductivity –
Part 7: Electronic characteristic measurements – Surface resistance of high-temperature superconductors at microwave frequencies

Supraconductivité –
Partie 7: Mesurages des caractéristiques électronique – Résistance de surface des supraconducteurs haute température critique aux hyperfréquences

IEC 61788-7:2020-03(en-fr)

CONTENTS

INTERNATIONAL ELECTROTECHNICAL COMMISSION

____

SUPERCONDUCTIVITY –

Part 7: Electronic characteristic measurements – Surface resistance of high-temperature superconductors at microwave frequencies

FOREWORD

1) The International Electrotechnical Commission (IEC) is a worldwide organization for standardization comprising all national electrotechnical committees (IEC National Committees). The object of IEC is to promote international co-operation on all questions concerning standardization in the electrical and electronic fields. To this end and in addition to other activities, IEC publishes International Standards, Technical Specifications, Technical Reports, Publicly Available Specifications (PAS) and Guides (hereafter referred to as "IEC Publication(s)"). Their preparation is entrusted to technical committees; any IEC National Committee interested in the subject dealt with may participate in this preparatory work. International, governmental and non-governmental organizations liaising with the IEC also participate in this preparation. IEC collaborates closely with the International Organization for Standardization (ISO) in accordance with conditions determined by agreement between the two organizations.
2) The formal decisions or agreements of IEC on technical matters express, as nearly as possible, an international consensus of opinion on the relevant subjects since each technical committee has representation from all interested IEC National Committees.
3) IEC Publications have the form of recommendations for international use and are accepted by IEC National Committees in that sense. While all reasonable efforts are made to ensure that the technical content of IEC Publications is accurate, IEC cannot be held responsible for the way in which they are used or for any misinterpretation by any end user.
4) In order to promote international uniformity, IEC National Committees undertake to apply IEC Publications transparently to the maximum extent possible in their national and regional publications. Any divergence between any IEC Publication and the corresponding national or regional publication shall be clearly indicated in the latter.
5) IEC itself does not provide any attestation of conformity. Independent certification bodies provide conformity assessment services and, in some areas access to IEC marks of conformity. IEC is not responsible for any services carried out by independent certification bodies.
6) All users should ensure that they have the latest edition of this publication.
7) No liability shall attach to IEC or its directors, employees, servants or agents including individual experts and members of its technical committees and IEC National Committees for any personal injury, property damage or other damage of any nature whatsoever, whether direct or indirect, or for costs (including legal fees) and expenses arising out of the publication, use of, or reliance upon, this IEC Publication or any other IEC Publications.
8) Attention is drawn to the normative references cited in this publication. Use of the referenced publications is indispensable for the correct application of this publication.
9) Attention is drawn to the possibility that some of the elements of this IEC Publication may be the subject of patent rights. IEC shall not be held responsible for identifying any or all such patent rights.

International Standard IEC 61788-7 has been prepared by IEC technical committee 90: Superconductivity.

This third edition cancels and replaces the second edition, published in 2006. This edition constitutes a technical revision.

This edition includes the following significant technical changes with respect to the previous edition:

a) informative Annex B, relative combined standard uncertainty for surface resistance measurement has been added;
b) precision and accuracy statements have been converted to uncertainty;
c) reproducibility in surface resistant measurement has been added.

The text of this International Standard is based on the following documents:

FDIS	Report on voting
90/447/FDIS	90/452/RVD

Full information on the voting for the approval of this International Standard can be found in the report on voting indicated in the above table.

This document has been drafted in accordance with the ISO/IEC Directives, Part 2.

A list of all parts of the IEC 61788 series, published under the general title *Superconductivity*, can be found on the IEC website.

The committee has decided that the contents of this document will remain unchanged until the maintenance result date indicated on the IEC web site under "http://webstore.iec.ch" in the data related to the specific publication. At this date, the document will be

- reconfirmed;
- withdrawn;
- replaced by a revised edition, or
- amended.

IMPORTANT – The 'colour inside' logo on the cover page of this publication indicates that it contains colours which are considered to be useful for the correct understanding of its contents. Users should therefore print this document using a colour printer.

INTRODUCTION

Since the discovery of some Perovskite-type Cu-containing oxides, extensive research and development (R & D) work on high-temperature superconductors (HTS) has been, and is being, done worldwide, and its application to high-field magnet machines, low-loss power transmission, electronics and many other technologies is in progress.

In various fields of electronics, especially in telecommunication fields, microwave passive devices such as filters using HTS are being developed and are undergoing on-site testing [1][1] [2].

Superconductor materials for microwave resonators [3], filters [4], antennas [5] and delay lines [6] have the advantage of very low loss characteristics. The parameters of superconductor materials needed for the design of microwave low loss components are the surface resistance, (R_s) and the temperature dependence of the R_s. Knowledge of this parameter is of primary importance for the development of new materials on the supplier side and for the design of superconductor microwave components on the customer side.

R_s of high quality HTS films is generally several orders of magnitude lower than that of normal metals [7] [8] [9] [10], which has increased the need for a reliable characterization technique to measure this property. Traditionally, the R_s of niobium or any other low-temperature superconducting material was measured by first fabricating an entire three-dimensional resonant cavity and then measuring its Q-value [11]. The R_s could be calculated by solving the electro-magnetic field (EM) distribution inside the cavity. Another technique involves placing a small sample inside a larger cavity. This technique has many forms but usually involves the uncertainty introduced by extracting the loss contribution due to the HTS films from the experimentally measured total loss of the cavity.

The best HTS samples are epitaxial films grown on flat crystalline substrates and no high-quality films have been grown on any curved surface so far. What is needed is a technique that: can use these small flat samples; requires no sample preparation; does not damage or change the film; is highly repeatable; has great sensitivity (down to 1/1 000 the R_s of copper); has great dynamic range (up to the R_s of copper); can reach high internal powers with only modest input powers; and has broad temperature coverage (4,2 K to 150 K).

The dielectric resonator method is selected among several methods to determine the surface resistance at microwave frequencies because it is considered to be the most popular and practical at present. Especially, the sapphire resonator is an excellent tool for measuring the R_s of HTS materials [12] [13] [14]

The test method given in this document can also be applied to other superconductor bulk plates including low T_c materials.

This document is intended to provide an appropriate and agreeable technical base for the time being to engineers working in the fields of electronics and superconductivity technology.

The test method covered in this document is based on the VAMAS (Versailles Project on Advanced Materials and Standards) pre-standardization work on the thin film properties of superconductors.

1 Numbers in square brackets refer to the bibliography.

SUPERCONDUCTIVITY –

Part 7: Electronic characteristic measurements – Surface resistance of high-temperature superconductors at microwave frequencies

1 Scope

This part of IEC 61788 describes measurement of the surface resistance (R_s) of superconductors at microwave frequencies by the standard two-resonator method. The object of measurement is the temperature dependence of R_s at the resonant frequency.

The applicable measurement range of R_s for this method is as follows:

– Frequency: 8 GHz < f < 30 GHz

– Measurement resolution: 0,01 mΩ at 10 GHz

The R_s data at the measured frequency, and that scaled to 10 GHz, assuming the f^2 rule for comparison, is reported.

2 Normative references

The following documents are referred to in the text in such a way that some or all of their content constitutes requirements of this document. For dated references, only the edition cited applies. For undated references, the latest edition of the referenced document (including any amendments) applies.

IEC 60050-815, *International Electrotechnical Vocabulary (IEV) – Part 815: Superconductivity*

3 Terms and definitions

For the purposes of this document, the terms and definitions given in IEC 60050-815 apply.

ISO and IEC maintain terminological databases for use in standardization at the following addresses:

- IEC Electropedia: available at http://www.electropedia.org/
- ISO Online browsing platform: available at http://www.iso.org/obp

4 Requirements

The R_s of a superconductor film shall be measured by applying a microwave signal to a dielectric resonator with the superconductor film specimen and then measuring the attenuation of the resonator at each frequency. The frequency shall be swept around the resonant frequency as the centre, and the attenuation–frequency characteristics shall be recorded to obtain the Q- value, which corresponds to the loss.

The target relative combined standard uncertainty of this method is less than 20 % for the measurement temperature range from 20 K to 80 K.

It is the responsibility of the user of this document to establish appropriate safety and health practices and to determine the applicability of regulatory limitations prior to use.

Hazards exist in this type of measurement. The use of a cryogenic system is essential to cool the superconductors to allow transition into the superconducting state. Direct contact of skin with cold apparatus components can cause immediate freezing, as can direct contact with a spilled cryogen. The use of an RF generator is also essential to measure high-frequency properties of materials. If its power is too high, direct contact to human bodies can cause an immediate burn.

5 Apparatus

5.1 Measurement system

Figure 1 shows a schematic diagram of the system required for the microwave measurement. The system consists of a network analyzer system for transmission measurement, a measurement apparatus, and a thermometer for monitoring the measuring temperature.

An incident power generated from a suitable microwave source such as a synthesized sweeper is applied to the dielectric resonator fixed in the measurement apparatus. The transmission characteristics are shown on the display of the network analyzer. The measurement apparatus is fixed in a temperature-controlled cryocooler.

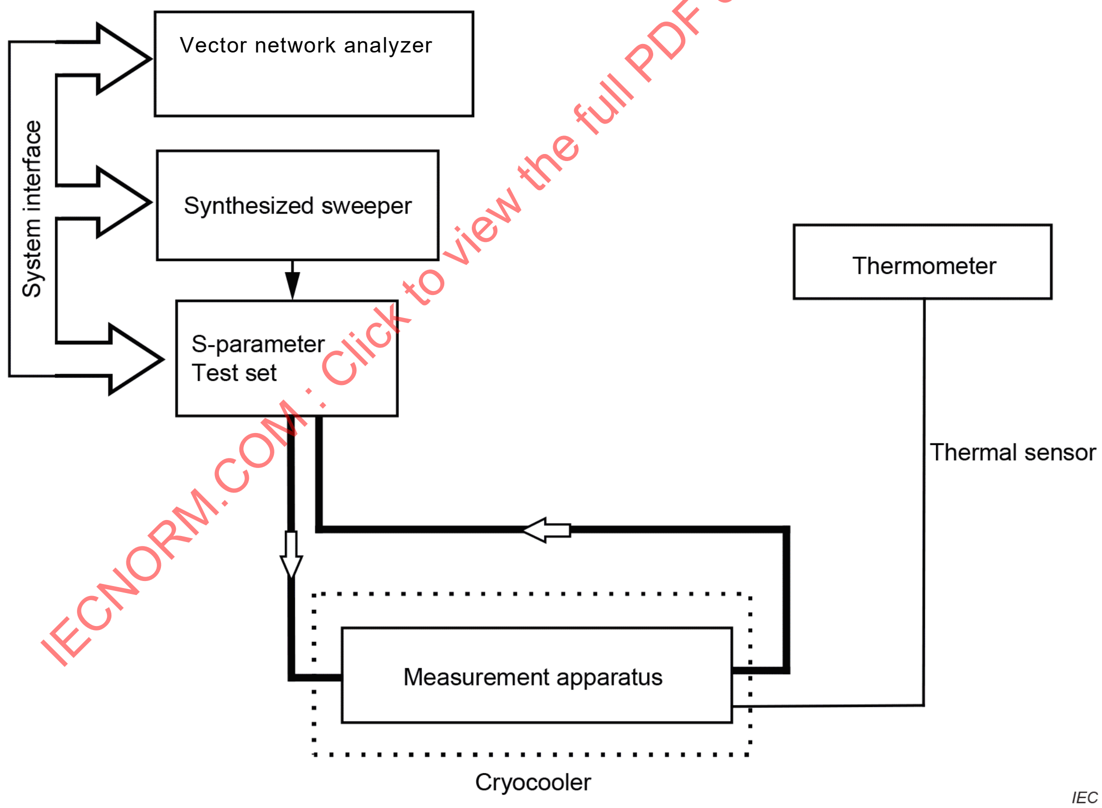

Figure 1 – Schematic diagram of measurement system for temperature dependence of R_s using a cryocooler

For the measurement of R_s for superconductor films, a vector network analyzer is recommended. A vector network analyzer has better measurement accuracy than a scalar network analyser due to its wide dynamic range. The performance requirements of the vector network analyzer are specified in 7.1.

5.2 Measurement apparatus for R_s

Figure 2 shows a schematic of a typical measurement apparatus (closed type resonator) for the R_s of HTS films deposited on a substrate with a flat surface. The upper HTS film is pressed down by a spring, which is made of phosphor bronze. The plate type spring should be used for the improvement of measurement uncertainty. This type of spring reduces the friction between the spring and the other part of the apparatus, and allows the smooth movement of superconductor films due to the thermal expansion of the dielectric rod. In order to minimize the measurement uncertainty, the sapphire rod and the copper ring shall be arranged coaxially.

Two semi-rigid cables for measuring transmission characteristics of the resonator shall be attached on both sides of the resonator in an axial symmetrical position (ϕ = 0 and π, where ϕ is the rotational angle around the central axis of the sapphire rod). Each of the two semi-rigid cables shall have a small loop at the ends. The plane of the loop shall be set parallel to that of the superconductor films in order to suppress the unwanted Transverse Magnetic Wave Modes (TM_{mn0} modes). The coupling loops shall be carefully checked for cracks in the spot weld joint that may have developed upon repeated thermal cycling. These cables can move right and left to adjust the insertion attenuation (IA). In this adjustment, coupling of unwanted cavity modes to the interested dielectric resonance mode shall be suppressed. Unwanted, parasitic coupling to the other modes reduces the high Q-value of the Transverse Electro-Magnetic Mode (TE mode) resonator. For suppressing the parasitic coupling, special attention shall be paid to designing high-Q resonators. Two other types of resonators along with the closed type shown in Figure 2 can be used. They are explained in A.4.

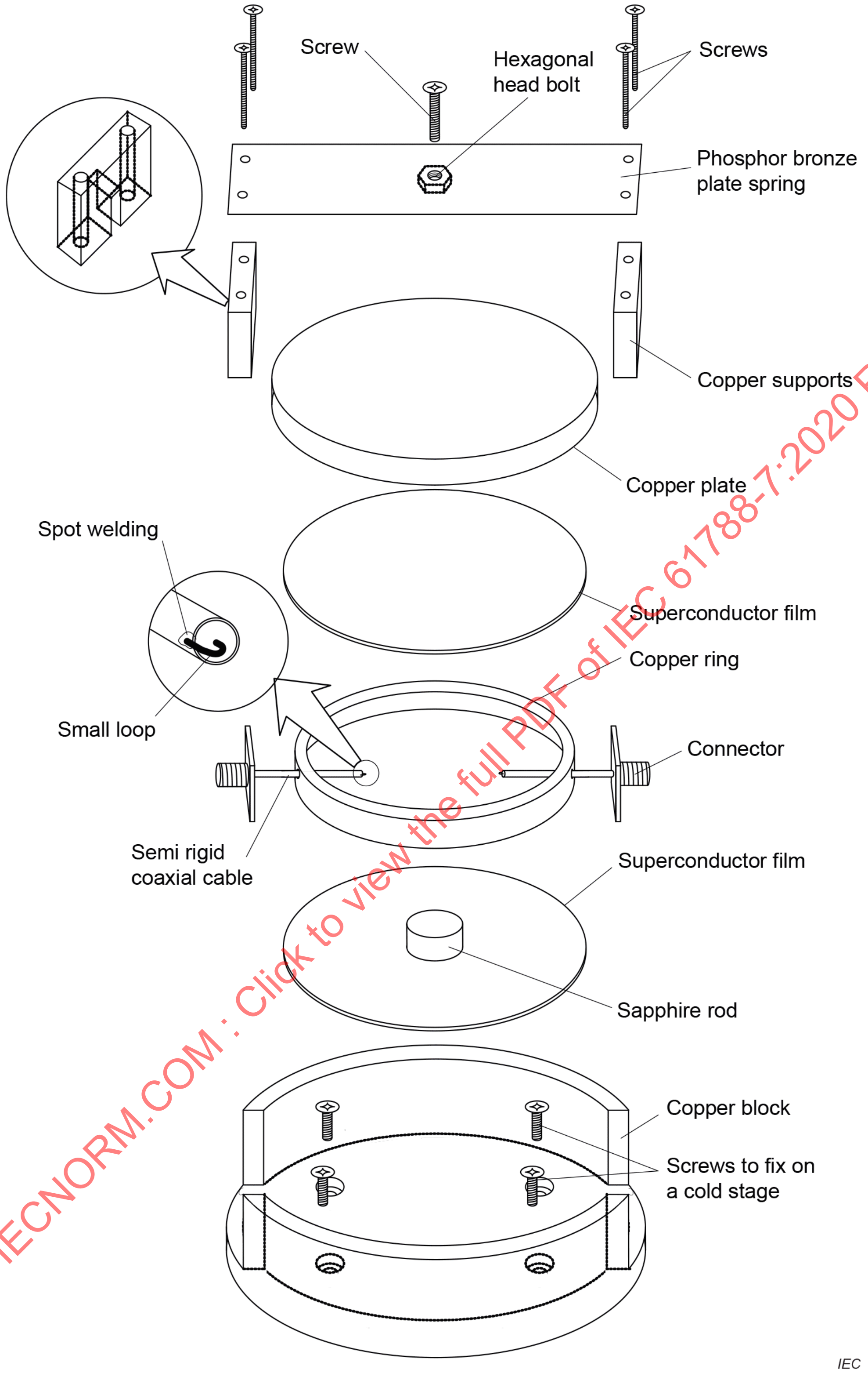

Figure 2 – Typical measurement apparatus for R_s

A reference line made of a semi-rigid cable shall be used to measure the full transmission power level, i.e. the reference level. This cable has a length equal to the sum of the two cables of the measurement apparatus. Semi-rigid cable with an outer diameter of 1,20 mm is recommended.

In order to minimize the measurement uncertainty, two superconductor films shall be set to be parallel to each other. To ensure that the two superconductor films remain in tight contact with the ends of the sapphire rod, without any air gap, both of the surfaces of the films and the ends of the rod shall be cleaned carefully.

5.3 Dielectric rods

Two dielectric rods with the same relative permittivity, ε', and loss factor, tan δ, preferably cut from one cylindrical dielectric rod, are required. These two rods, standard dielectric rods, shall have the same diameter but different heights: one shall have height three times longer than the other.

It is preferable to use dielectric rods with low tan δ to achieve the requisite measurement uncertainty on R_s. Recommended dielectric rods are single-crystal sapphire rods with tan δ less than 2×10^{-7} at 77 K. Specifications on the sapphire rods are described in 7.1. In order to minimize the measurement error in R_s of the superconductor films, both ends of the sapphire rods shall be polished parallel to each other and perpendicular to the axis. Specifications for the sapphire rods are given in Clause 7.

The diameter and the heights of the standard sapphire rods shall be carefully designed so that the TE_{011} and TE_{013} modes do not couple to other TM, HE and EH modes, since the coupling between TE mode and other modes causes the degradation of unloaded Q. A design guideline for the standard sapphire rods is described in Clause A.5. Table 1 shows typical examples of dimensions of the standard sapphire rods for 12 GHz, 18 GHz, and 22 GHz resonance. In the R_s measurement at 22 GHz, the required film diameter can be set to 20 mm, and the measured Q_L is small, therefore the effect of the dielectric loss of sapphire rod can be reduced.

Table 1 – Typical dimensions of pairs of single-crystal sapphire rods for 12 GHz, 18 GHz and 22 GHz

Frequency GHz		Diameter, d mm	Height, h mm
12	Short rod (TE_{011} resonator)	11,40 ± 0,05	5,70 ± 0,05
	Long rod (TE_{013} resonator)	11,40 ± 0,05	17,10 ± 0,05
18	Short rod (TE_{011} resonator)	7,60 ± 0,05	3,80 ± 0,05
	Long rod (TE_{013} resonator)	7,60 ± 0,05	11,40 ± 0,05
22	Short rod (TE_{011} resonator)	6,20 ± 0,05	3,10 ± 0,05
	Long rod (TE_{013} resonator)	6,20 ± 0,05	9,30 ± 0,05

6 Measurement procedure

6.1 Specimen preparation

From uncertainty estimation, the film diameter shall be about three times larger than that of the sapphire rods. In this configuration, the increase in uncertainty of R_s due to the different radiation losses between TE_{011} and TE_{013} mode can be considered negligible, given the target relative combined standard uncertainty of 20 %. The film thickness shall be about two times larger than the magnetic-field penetration depth value at the maximum temperature in the measurement temperature range. If the film thickness is much less than two times the magnetic-field penetration depth, the measured R_s should mean the effective surface resistance.

Table 2 shows dimensions of the superconductor films recommended for the standard sapphire rods of 12 GHz, 18 GHz, and 22 GHz.

Table 2 – Dimensions of superconductor film for 12 GHz, 18 GHz, and 22 GHz

c-cut single-crystal sapphire rod		Superconductor film	
Frequency GHz	**Diameter**, d mm	**Diameter**, d' mm	**Thickness** µm
12	11,40 ± 0,05	> 35	≅ 0,5
18	7,60 ± 0,05	> 25	≅ 0,5
22	6,20 ± 0,05	> 20	≅ 0,5

In case of using closed type resonators, the dimensions of the superconductor films shall also be designed taking into account the dimension of the copper cylinder between the superconductor films. A design guideline for the dimension of the copper cylinder of the closed type resonator is described in Clause A.6.

6.2 Set-up

Set up the measurement equipment as shown in Figure 1. All of the measurement apparatus, standard sapphire rods, and superconductor films shall be kept in a clean and dry state as high humidity may degrade the unloaded Q-value. The specimen and the measurement apparatus shall be fixed in a temperature-controlled cryocooler. The specimen chamber shall be totally evacuated. The temperatures of the superconductor films and standard sapphire rods shall be measured by a diode thermometer, or a thermocouple. The temperatures of the upper and lower superconductor films and standard sapphire rods shall not differ by more than 0,5 K. This can be achieved by covering the measurement apparatus with aluminium foil or filling the specimen chamber with helium gas.

6.3 Measurement of reference level

The level of full transmission power (reference level) shall be measured first. Fix the output power of the synthesized sweeper below 10 mW because the measurement uncertainty depends on the measuring signal level. Connect the reference line of semi-rigid cable between the input and output connectors. Then, measure the transmission power level over the entire measurement frequency and temperature range. The reference level can change several decibels when temperature of the apparatus is changed from room temperature to the lowest measurement temperature. Therefore, the temperature dependence of the reference level must be taken into account.

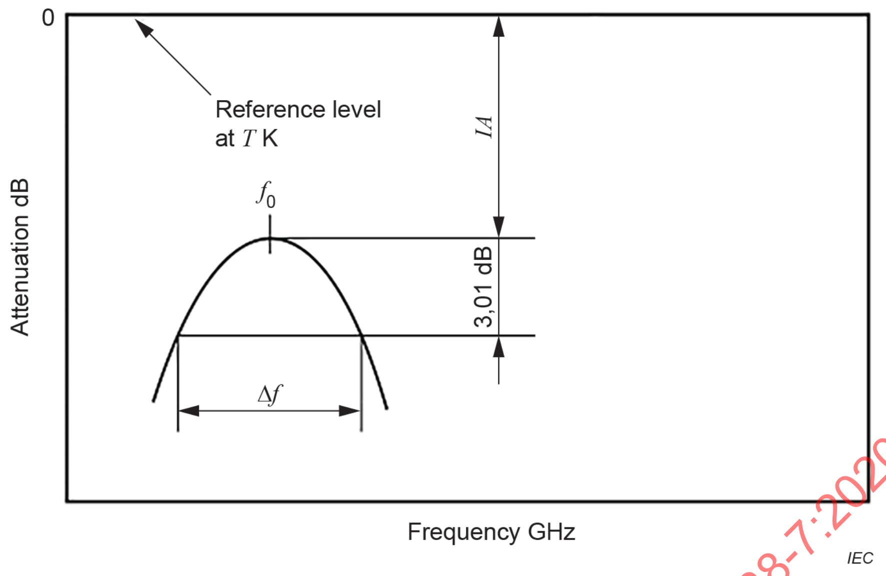

Figure 3 – Insertion attenuation, IA, resonant frequency, f_0, and half power bandwidth, Δf, measured at T kelvin

6.4 Measurement of the frequency response of resonators

The temperature dependence of the R_s can be obtained through the measurements of resonant frequency, f_0, and unloaded quality factor, Q_u, for TE_{011} and TE_{013} resonators, which shall be measured as follows.

a) Connect the measurement apparatus between the input and output connectors (Figure 1). Insert the standard short sapphire rod near the centre of the lower superconductor film and fix the distance between the rod and each of the loops of the semi-rigid cables to be equal to each other, so that this transmission-type resonator can be under-coupled equally to both loops. Put down the upper superconductor film gently to touch the top face of the rod. Be careful not to damage the surface of the superconductor films by excessive pressure. Evacuate and cool down the specimen chamber below the critical temperature.

b) Find the TE_{011} mode resonance peak of this resonator at a frequency nearly equal to the designed value of f_0.

c) Narrow the frequency span on the display so that only the resonance peak of TE_{011} mode can be shown (Figure 3). Confirm that the insertion attenuation, IA, of this mode is larger than 20 dB from the reference level, which depends strongly on the temperature.

d) Measure the temperature dependence of f_0 and the half power band width Δf. The loaded Q-value, Q_L, of the TE_{011} resonator is given by

$$Q_L = \frac{f_0}{\Delta f} \quad (1)$$

e) The unloaded Q-value, Q_u, shall be extracted from the Q_L by at least one of the two following techniques.

1) One technique for extracting the unloaded Q-value involves measuring the insertion attenuation IA. Q_u is given by

$$Q_u = \frac{Q_L}{1 - A_t}, \; A_t = 10^{-IA[\text{dB}]/20} \quad (2)$$

The IA of each temperature is determined as follows. In the R_s measurement system shown in Figure 2, a semi-rigid cable is connected instead of the measurement apparatus, and the measurement system is short-circuited to determine the reference level. Measure the reference level at each temperature and use it to determine IA at each temperature.

This technique of using insertion attenuation assumes that the coupling on both sides of the resonator is identical. The coupling loops are difficult to fabricate, the orientation of the loop is difficult to control, and any movement of the sapphire rod during measurement is not known. These assembly-dependent effects are also temperature dependent. This potential asymmetry in coupling can result in large errors in calculating the coupling factor if the coupling is strong (IA <~ 10 dB). If the coupling is weak enough (IA > 20 dB), asymmetry in the coupling becomes less important.

2) Another technique for extracting the unloaded Q-value involves measuring the reflection scattering parameters at the resonant frequency of both sides of the resonator.

$$Q_u = Q_L(1+\beta_1+\beta_2) \tag{3}$$

$$\beta_1 = \frac{1-|S_{11}|}{|S_{11}|+|S_{22}|} \tag{4}$$

$$\beta_2 = \frac{1-|S_{22}|}{|S_{11}|+|S_{22}|} \tag{5}$$

In Equations (4) and (5), S_{11} and S_{22} are the reflection scattering parameters as shown in Figure 4, and are measured in linear units of power, not relative dB. β_1 and β_2 are the coupling coefficients.

This technique of using the reflection scattering parameters has two advantages. It does not require the additional step of calibration of the reference level and it gives a measurement of the coupling values for both sides of the resonator. This also has two disadvantages. It only works for a narrow band resonance (which is fortunately the case) and is limited by the dynamic range of the network analyzer in measuring the reflection coefficients [15] [16].

A combination of the two techniques is useful for a "double" check.

f) The f_0 and Q_u measured for this short rod are denoted as f_{01} and Q_{u1} for TE_{011} mode resonance. By slowly changing the temperature of the cryocooler the temperature dependence of f_{01} and Q_{u1} shall be measured.

g) After the temperature dependence measurement of f_{01} and Q_{u1} is finished, the measurement apparatus shall be heated up to room temperature.

h) Then, replace the TE_{011} resonator in the apparatus with the TE_{013} resonator at room temperature, cool down the apparatus to a temperature lower than the critical temperature, and measure the temperature dependence of f_0 and Q_u of its TE_{013} resonance mode, denoted as f_{03} and Q_{u3}, in a similar way to the TE_{011} resonator case. When the length of the sapphire rod of the TE_{013} resonator is precisely three times longer than that of the TE_{011} resonator, the f_{03} of the TE_{013} resonator must coincide with f_{01} of the TE_{011} resonator. If carefully designed, the difference between f_{01} and f_{03} is usually very small (<~ 0,25 %). We can consider that the f_0 in equation (9) can be replaced by f_{01} or f_{03}.

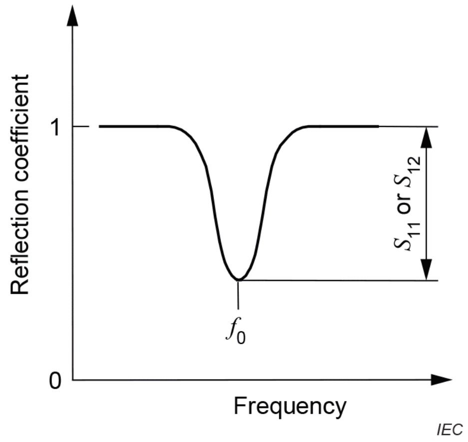

Figure 4 – Reflection scattering parameters (S_{11} and S_{22})

6.5 Determination of surface resistance of the superconductor and ε' and tan δ of the standard sapphire rods

Calculate the temperature dependence of the R_s of the superconductor films, and ε' and tan δ of the standard sapphire rods using the temperature dependence of Q_{u1} and Q_{u3}. Q_{u1} and Q_{u3} can be calculated using equations (1) and (2). If the measured temperatures for Q_{u3} appear to be slightly different from those for Q_{u1}, interpolation can be used for preparing adjusted temperature values for the former at the same temperatures for the later. Equations (6) to (12) are established in the open type cavity, but when the superconductor film size is three times larger than sapphire rod diameter, these equations can be used for closed type cavity.

$$R_s = \frac{30\pi^2 \times 3}{(3-1)}\left(\frac{2h_0}{\lambda 0}\right)^3 \frac{\varepsilon' + W}{1+W}\left(\frac{1}{Q_{u1}} - \frac{1}{Q_{u3}}\right) \tag{6}$$

$$\varepsilon' = \left(\frac{\lambda 0}{\pi d}\right)^2 \left(u^2 + v^2\right) + 1 \tag{7}$$

$$\tan\delta = \frac{1+\dfrac{W}{\varepsilon'}}{(3-1)}\left(\frac{3}{Q_{u3}} - \frac{1}{Q_{u1}}\right) \tag{8}$$

where

$$\lambda_0 = \frac{c}{f_0} \tag{9}$$

$$W = \frac{J_1^2(u)}{K_1^2(v)} \frac{K_0(v)K_2(v) - K_1^2(v)}{J_1^2(u) - J_0(u)J_2(u)} \tag{10}$$

$$v^2 = \left(\frac{\pi d}{\lambda_0}\right)^2 \left[\left(\frac{3\lambda_0}{2h_0}\right)^2 - 1\right] \tag{11}$$

$$u\frac{J_0(u)}{J_1(u)} = -v\frac{K_0(v)}{K_1(v)} \tag{12}$$

In the equations, λ_0 is the free space resonant wavelength, c is the speed of light in vacuum (c = 2,997 9 × 10^8 m/s), h_0 is the height of the short standard dielectric rod. The value u^2 is given by the transcendental Equation (12) using the value of v^2, where $J_n(u)$ is the Bessel function of the first kind, and $K_n(v)$ is the modified Bessel function of the second kind. The derivations of the equations are described in Clause A.3.

Generally the thermal expansion coefficient of the rods must be known to determine the temperature dependence of their sizes. However, the thermal expansion effect of the sapphire rods can be neglected for the target relative standard uncertainty of R_s (20 %).

It is noted that the measured R_s means the effective surface resistance if the film thickness is less than two times the temperature-dependent penetration depth.

7 Uncertainty of the test method

7.1 Surface resistance

The surface resistance (R_s) shall be determined from the Q-value measured with a dielectric resonator technique.

A vector network analyser as specified in Table 3 shall be used to record the frequency dependence of attenuation. The resulting record shall allow the determination of Q to a relative uncertainty of 10^{-2}.

Table 3 – Specifications for vector network analyzer

Dynamic range of S_{21}	above 60 dB
Frequency resolution	below 1 Hz
Attenuation uncertainty	below 0,1 dB
Input power limitation	below 10 dBm

The dielectric resonators shall be provided with two dielectric rods with low tan δ of less than 2 × 10^{-7} at 77 K and a radius less than 1/3 of the superconducting specimen's radius. The best candidate for the rods is sapphire as specified in Table 4. Term definitions in Table 4 are shown in Figure 5.

Table 4 – Specifications for sapphire rods

Diameter	±0,05 mm
Height	±0,05 mm
Flatness	below 0,005 mm
Surface roughness	top and bottom surface: below 10 nm RMS cylindrical surface: below 0,001 mm RMS
Perpendicularity	within 0,1 degree
Axis	parallel to *c*-axis within 0,3°

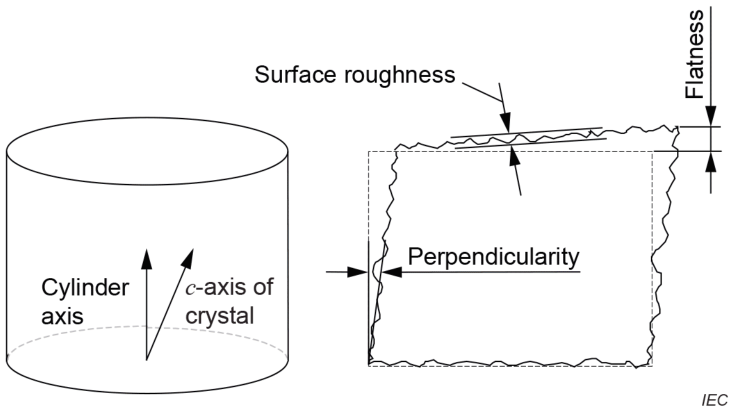

Figure 5 – Term definitions in Table 4

The technique as described assumes that single- and triple-height sapphire rods can be fabricated with the same tan δ. However, the variation of the tan δ between nominally identical rods, cut from the same boule and polished by the same technique, may be as large as two orders of magnitude. To date, the smallest variation in tan δ between nominally identical sapphire rods has been a factor of four. Therefore, the uncertainty in the measured tan δ is large. The variation of tan δ of the present sapphire rod causes an additional uncertainty up to at least 10 % in the surface resistance measurement. This limits the target uncertainty of the present technique at 5 %. If reproducibility of sapphire rods is improved, or a selection method for standard sapphire rods is established, a target uncertainty can be improved.

7.2 Temperature

The measurement apparatus is cooled down to the specified temperature by any means during testing. An easy choice would be to immerse the apparatus into a liquid cryogen. This technique is quick and simple and yields a known and stable temperature. Unfortunately, most HTS materials are damaged by the condensation of moisture that occurs when removing the sample from the cryogen. In addition, uncertainties generated by the presence of a gas/liquid mixture within the cavity, and the inability to measure R_s as a function of temperature support the use of other cooling methods. These limitations can be circumvented by the immersion of a vacuum can into a liquid cryogen. If the vacuum can is backfilled with gas, then rapid cooling and uniform temperatures occur. If heaters are attached to the apparatus, then the temperature dependence of the HTS material can be measured. A third and equally good choice is the use of a cryocooler. In this case, the resonator is under vacuum and cooled by conduction through the metallic package. Temperature gradients with the apparatus shall be avoided.

A cryostat shall be provided with the necessary environment for measuring R_s and the specimen shall be measured while in a stable and isothermal state. The specimen temperature is assumed to be the same as the sample holder temperature. The holder temperature shall be reported to an accuracy of ±0,5 K, measured by means of an appropriate temperature sensor.

The difference between the specimen temperature and the holder temperature shall be minimized by using shields with good thermal conductivity.

7.3 Specimen and holder support structure

The support structure shall provide adequate support for the specimen. The two films shall be parallel and mechanically stable throughout the measurement, especially in a cryocooler and over a wide temperature range. The parallelism of the two films can be achieved by using a sapphire rod satisfying the specifications described in Table 4.

7.4 Specimen protection

Condensation of moisture and scratching of the film deteriorate superconducting properties. Some protection measures should be provided for the specimens. Polytetrafluoroethylene (PTFE) or polymethylmethacrylate (PMMA) coating does not affect the measurements, thus they can be used for protection. A coating material thickness of less than several micrometers is recommended.

7.5 Uncertainty of surface resistance measured by standard two-resonator method

For the dielectric resonance method, tan δ of the TE_{011} mode and TE_{013} mode sapphire rods are assumed to be absolutely equal. If tan δ of two sapphire rods is different, it is not possible to calculate the surface resistance using Equation (6). The effect of tan δ deviation on surface resistance was checked (see Annex B). Uncertainty in the microwave surface resistance of superconductors by dielectric resonator method depends on size, dielectric constant, tan δ of sapphire rods and uncertainty in measured Q of the resonator. The relative combined standard uncertainty is less than 20 % (see Annex B)

8 Test report

8.1 Identification of test specimen

The test specimen shall be identified, if possible, by the following:

a) name of the manufacturer of the specimen;
b) classification and/or symbol;
c) lot number;
d) chemical composition of the thin film and the substrate;
e) thickness and roughness of the thin film;
f) manufacturing process technique.

8.2 Report of R_s values

The R_s values at the measured frequency, and that scaled to 10 GHz, together with their corresponding f_{01}, f_{03}, Q_{u1}, Q_{u3}, IA and/or (β_1, β_2), ε' and tan δ values, and their temperature dependence shall be reported.

8.3 Report of test conditions

The following test conditions shall be reported:

a) test frequency and resolution of frequency;
b) test maximum RF power;
c) test temperature, accuracy of temperature and temperature difference in two plates;
d) sample history with temperature variation.

Annex A
(informative)

Additional information relating to Clauses 1 to 8

A.1 Scope

A.1.1 General

The establishment of the standard measurement method is needed to evaluate film quality of HTS films having low surface resistance, R_s, values such as 0,1 mΩ at 10 GHz. Several resonance methods as shown in Figure A.1 have been proposed so far to measure them in microwave and millimetre wave range. These resonator structures are grouped into six types (see A.1.2 to A.1.7).

A.1.2 Cylindrical cavity method [10] [17]

Figure A.1 a) shows a cavity structure using the TE_{011} mode, which is constructed from a copper cylinder and two HTS films. In the microwave range below 30 GHz, the R_s measurement precision of this method is rather low, because the R_s value of the copper cylinder is 100 times higher than that of HTS films. This method is suitable in the millimetre wave region, because the R_s values increase with f^2 of HTS films and $f^{½}$ for copper.

A.1.3 Parallel-plates resonator method [18] [19]

Figure A.1 b) shows a structure of a parallel-plates resonator using the TM_{nm0} mode, which is constructed by inserting a thin low loss dielectric spacer between two rectangular HTS films. This method offers the possibility of measuring extremely small R_s values, but from the viewpoint of the absolute estimation of R_s there are some problems, such as low measurement precision of thickness and tan δ of the dielectric spacer, uncertain estimations of radiation loss and an air-gap effect between the plates and the spacer, and critical excitation technique of the resonance modes.

A.1.4 Microstrip-line resonance method [20] [21]

Figure A.1 c) shows a structure of a microstrip-line resonator using the TE_{0mp} mode, which is fabricated by a pattern fabrication process and is close to the real microwave passive devices. However, this method is not suitable for the HTS film estimation because it includes an uncertain influence of the pattern fabrication process.

A.1.5 Dielectric resonator method [22] [23] [24] [25]

Figure A.1 d) shows a structure of a dielectric resonator using a TE_{011} mode, where a low loss sapphire rod is placed between two parallel HTS films. For the TE_{0mp} mode, we can eliminate the air-gap effects, because the normal component of electric field does not exist on the HTS films. In this method the R_s values of the HTS films have been measured by ignoring the effect of tan δ on the assumption of tan $\delta < 1 \times 10^{-8}$ for single-crystal sapphire [24]. However, the tan δ values measured for sapphire at 10 GHz and near 50 K, as is well known, take values between 10^{-6} to 10^{-8} due to quantity of lattice defect. Therefore, preparation of very-low-loss sapphire rods with tan $\delta < 2 \times 10^{-7}$ (at 80 K and at 10 GHz) is essential for this method.

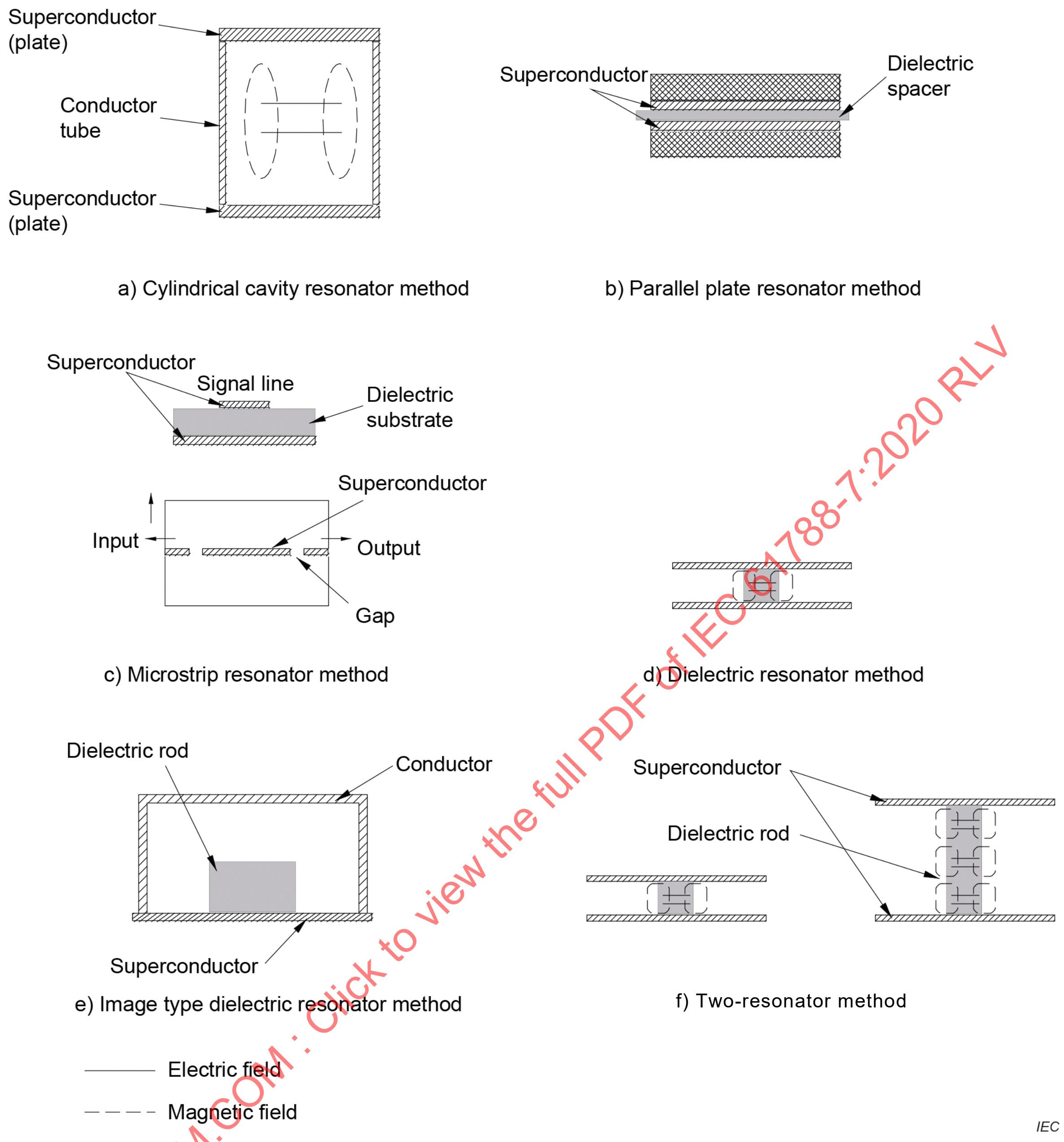

Figure A.1 – Schematic configuration of several measurement methods for the surface resistance

A.1.6 Image-type dielectric resonator method [26] [27]

Figure A.1 e) shows a structure of an image-type dielectric resonator using the $TE_{01\delta}$ mode. This structure is available to measure only one HTS film. However, preparation of very-low-loss sapphire rods is essential also for this method, because the R_s is measured by ignoring the effect of tan δ.

In an improved image-type sapphire rod resonator method, R_s can be obtained with simple calibration process. In this method, the exact R_s of a single HTS film can be obtained by one measurement under the 20 % limitation of variation coefficient.

A.1.7 Two-resonator method [28] [29]

In this method, two sapphire rod resonators with the same tan δ values are used; one is a TE_{011} mode resonator and the other is a TE_{013} mode resonator, as shown in Figure A.1 f). Similarly to the dielectric resonator method, the air-gap effects can be eliminated in this method. The tan δ value of the sapphire rods and the R_s value of the HTS films can be determined separately from the resonant frequencies and unloaded Q-values measured for these resonators by using simple formulas derived from the rigorous analysis based on the mode matching method. Thus this method can eliminate the ambiguity of the tan δ affected to the R_s measurements. Actually, the results of R_s measured for six YBCO films with R_s = 0,1 mΩ at 12 GHz have verified that the measurement uncertainty of 20 % is realized by this method [22]. However, if there is a difference between two tan δ values (Δtan δ), the uncertainty in R_s due to Δtan δ must be taken into account. This effect can be estimated from results of the inter-laboratory round robin test of the same HTS films by this method. Recently, the R_s of YBCO film was measured three times and its deviation was less than 20 % (see Figure A.11).

As a result of comparisons among the six methods described above, the two-resonator method is recommended as the standard measurement method of R_s of HTS films, due to the following two advantages:

– absolute measurement of R_s is possible;

– the numerical treatment is simple and easy.

A.2 Requirements

Higher measurement frequencies are desirable for determination of lower R_s because R_s of superconductor films increases with the frequency according to the f^2 rule. The size of the resonators also can be made smaller by using higher measurement frequencies. However, it becomes difficult to set up a microwave measurement system as the measurement frequency becomes higher.

For the measurement temperatures of below 10 K or above 80 K, this test method is sufficiently applicable, where some new cooling techniques may be required.

A.3 Theory and calculation equations

Figure A.2 shows the configuration of the TE_{0mn} mode resonator, which is used to eliminate the air-gap effects. A cylindrical dielectric rod with diameter, d, and height, h, is short-circuited at both ends by surfaces of two parallel superconductor films deposited on dielectric substrates with diameter, d', thus constituting a resonator. These superconductor films are required to have the same value of R_s. The value of R_s is calculated from the measured resonant frequency f_0 and unloaded quality factor Q_u for the TE_{0mn} resonance mode. When the two superconductor films have different values of R_s, the measured R_s value corresponds to the average value of these two films.

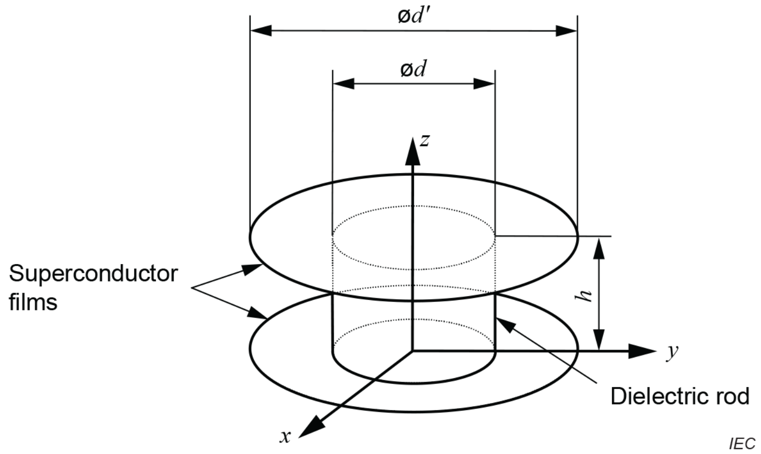

Figure A.2 – Configuration of a cylindrical dielectric rod resonator short-circuited at both ends by two parallel superconductor films deposited on dielectric substrates

The value of R_s is given by [25]

$$R_s = \frac{1}{B}\left(\frac{A}{Q_u} - \tan\delta\right) \tag{A.1}$$

where

$$A = 1 + \frac{W}{\varepsilon'} \tag{A.2}$$

$$B = p^2\left(\frac{\lambda_0}{2h}\right)^3 \frac{1+W}{30\pi^2\varepsilon'}, p = 1,2,\ldots, \tag{A.3}$$

$$\lambda_0 = \frac{c}{f_0} \tag{A.4}$$

$$W = \frac{J_1^2(u)}{K_1^2(v)} \frac{K_0(v)K_2(v) - K_1^2(v)}{J_1^2(u) - J_0(u)J_2(u)} \tag{A.5}$$

$$v^2 = \left(\frac{\pi d}{\lambda_0}\right)^2\left[\left(\frac{3\lambda_0}{2h}\right)^2 - 1\right] \tag{A.6}$$

$$u\frac{J_0(u)}{J_1(u)} = -v\frac{K_0(v)}{K_1(v)} \tag{A.7}$$

In Equations (A.1) and (A.2), ε' and tan δ are the relative permittivity and the loss factor of the dielectric rod, respectively. In Equations (A.3) and (A.4), λ_0 is the free space resonant wavelength, and c is the speed of light in vacuum (c = 2,9979 × 10^8 m/s). The function W/ε' equals the ratio of electric-field energy stored outside to that stored inside the dielectric rod. If all of the electric field is concentrated inside the dielectric rod, the value W equals zero.

The value u^2 is given by the transcendental Equation (A.7) using the value of v^2, where $J_n(u)$ is the Bessel function of the first kind and $K_n(v)$ is the modified Bessel function of the second kind. For any value of v, the m-th solution u exists between u_{0m} and u_{1m}, where $J_0(u_{0m})$ = 0 and $J_1(u_{1m})$ = 0. The first solution (m = 1), which is used for easy mode identification, is shown in Figure A.3 by curve (A). The computed result of the W-v relation for m = 1 of TE_{0mp} resonance mode is shown in Figure A.3 by curve (B).

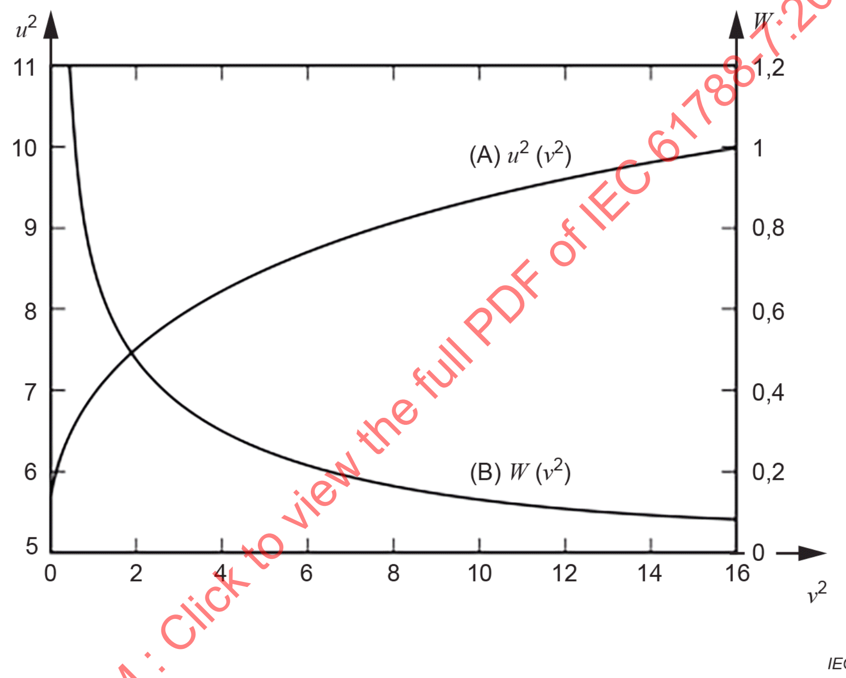

Figure A.3 – Computed results of the u-v and W-v relations for TE_{01p} mode

The value of ε' is given by

$$\varepsilon' = \left(\frac{\lambda_0}{\pi d}\right)^2 \left(u^2 + v^2\right) + 1 \quad \text{(A.8)}$$

using the value of v^2 and u^2.

In the two-resonator method, a pair of dielectric rods, which are called "standard dielectric rods", are used. These two rods have the same diameter but have different heights. The rod heights are such that one rod is p times the height of the other; p is commonly set equal to three. They are required to have the same values of ε' and tan δ.

Figure A.4 shows the configuration of the standard dielectric rods in the case of p = 3. To avoid confusion, the height of the short standard dielectric rod is denoted by h_0. Each resonator is called "TE_{011} resonator" and "TE_{013} resonator", respectively. The same superconductor films are used in these resonators. The values of f_0 and Q_u for the TE_{011} mode are measured using the TE_{011} resonator, and those for the TE_{01p} mode are measured using the TE_{01p} resonator. We denote the f_0 and Q_u for each resonator by using the subscripts 1 and p, respectively: f_{01} and Q_{u1} for TE_{011} resonator, and f_{0p} and Q_{up} for TE_{01p} resonator.

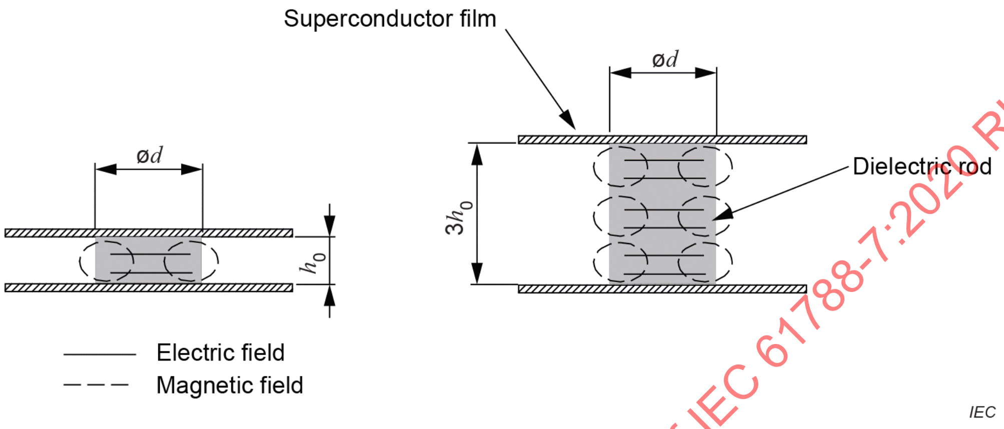

Figure A.4 – Configuration of standard dielectric rods for measurement of R_s and tan δ

The value of tan δ is given from the measured values of Q_u. When the TE_{01p} resonator is precisely p times longer than the TE_{011} resonator, f_{0p} coincides with f_{01}. However, Q_{up} is higher than Q_{u1} according to the different magnitude of the electric field energy stored in the two resonators. Because both dielectric rods are short-circuited at both ends by the same superconductor films, Equation (A.1) yields

$$\tan\delta = \frac{A}{(3-1)}\left(\frac{3}{Q_{up}} - \frac{1}{Q_{u1}}\right) \tag{A.9}$$

As an alternative method, the value of R_s of superconductor films can be directly measured by

$$R_s = \frac{30\pi^2 \times 3}{(3-1)}\left(\frac{2h_0}{\lambda 0}\right)^3 \frac{\varepsilon' + W}{1+W}\left(\frac{1}{Q_{u1}} - \frac{1}{Q_{up}}\right) \tag{A.10}$$

where Equation (A.10) is derived by substituting Equation (A.9) into Equation (A.1).

A.4 Apparatus

Unwanted parasitic coupling to the other mode reduces the high Q-value of the TE mode resonator. For suppressing the parasitic coupling, special attention is paid to design high Q-value resonators. Three types of resonators are proposed and shown in Figure A.5.

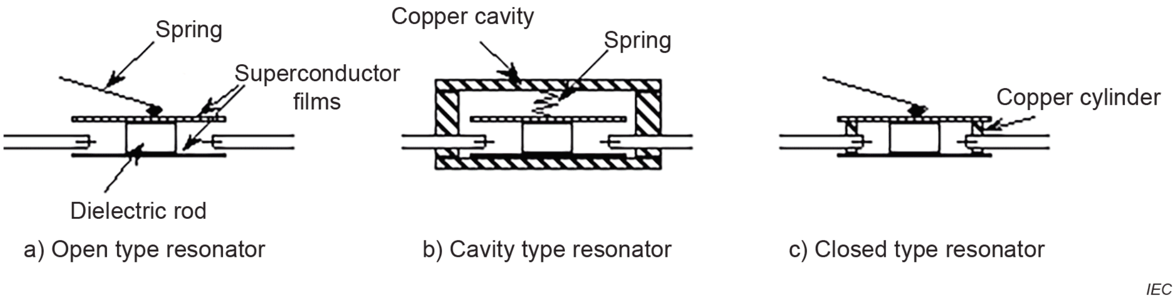

a) Open type resonator b) Cavity type resonator c) Closed type resonator

Figure A.5 – Three types of dielectric resonators

a) Open type resonator: a low loss dielectric rod is placed between two parallel superconductor films. Two semi-rigid cables for the RF input and output magnetic dipole coupling are attached on both sides of the resonator. In this configuration, the vertical position of the coupling cables should be carefully designed so as to prevent the radiation loss propagating along the coupling cables, which degrades the high Q-value of the TE_{0mp} mode and causes the increase in error for the R_s measurements. The coupling cables should be set as close as possible to the lower superconductor film.

b) Cavity type resonator: the open type resonator shown in a) is placed in a conductor (copper) cavity.

c) Closed type resonator: conductor (copper) cylinder is put between the superconductor films. In this configuration, the radiation loss along the coupling cable is strongly blocked by the copper cylinder. The vertical position of the coupling cables (z) at the highest z-axis magnetic field component (H_z), i.e. $z = h/2$, is recommended.

The measuring apparatus on the cryocooler is protected from mechanical and thermal disturbances, and installed in an X-Y and/or Z-axial manipulator for adjusting sample positions in the range of approximately ±1 mm.

A loop length of the antenna is designed on the basis of the quarter-wavelength rule for achieving the maximum measuring sensitivity.

A.5 Dimensions of the standard sapphire rods

Figure A.6 and Figure A.7 show the mode charts for designing the TE_{011} and TE_{013} mode resonators, respectively, short-circuited at both ends by parallel superconductor films, in which a uniaxial-anisotropic characteristic of the relative permittivity of the sapphire rod is taken into consideration [28]. ε_z is the relative permittivity in the direction of the c-axis, ε_r is that in the plane perpendicular to the c-axis, d is the diameter of the sapphire rod, h is the height of the sapphire rod, and λ_0 is the free space resonant wavelength. As shown in Figure A.6 and Figure A.7, TE_{013} resonance mode is apt to be affected by TM or HE mode in comparison with TE_{011} resonance mode. Since the coupling between TE mode and other modes causes the degradation of unloaded Q, the (d/h) of the sapphire rods shall be selected so as to avoid the unwanted couplings.

As shown in Figure A.7, the value $(d/h)^2$ for the TE_{013} resonator is selected from 0,24 to 0,46 in order that the TE_{013} resonance mode is not affected by the other modes. This value $(d/h)^2$ = 0,24 to 0,46 leads to a value of $(d/h)^2$ = 2,2 to 4,1 for the TE_{011} resonator. The TE_{011} resonance mode does not also couple with other modes when the value $(d/h)^2$ is in the region of 2,2 to 4,1 as shown in Figure A.6.

As the resonant frequency of TE mode is a function of relative permittivity and dimensions of the sapphire rod, its diameter and height are selected so that the desired f_0 is obtained.

From the curve of TE_{011} mode in Figure A.6, the value of $\varepsilon_r (d/\lambda_0)^2$ can be determined for each $(d/h)^2$ value. When the value $(d/h)^2$ equals 4,0, for example, the value of $\varepsilon_r (d/\lambda_0)^2$ equals 1,92. Thus, the resonant frequency of TE_{011} mode for the sapphire rod with dimension of $(d/h)^2$ = 4,0 is calculated from Equation (A.11) by specifying d and ε_r of the sapphire rod:

$$\varepsilon_r (d / \lambda_0)^2 = \varepsilon_r (d \times f_0 / c)^2 = 1{,}92 \quad \text{(A.11)}$$

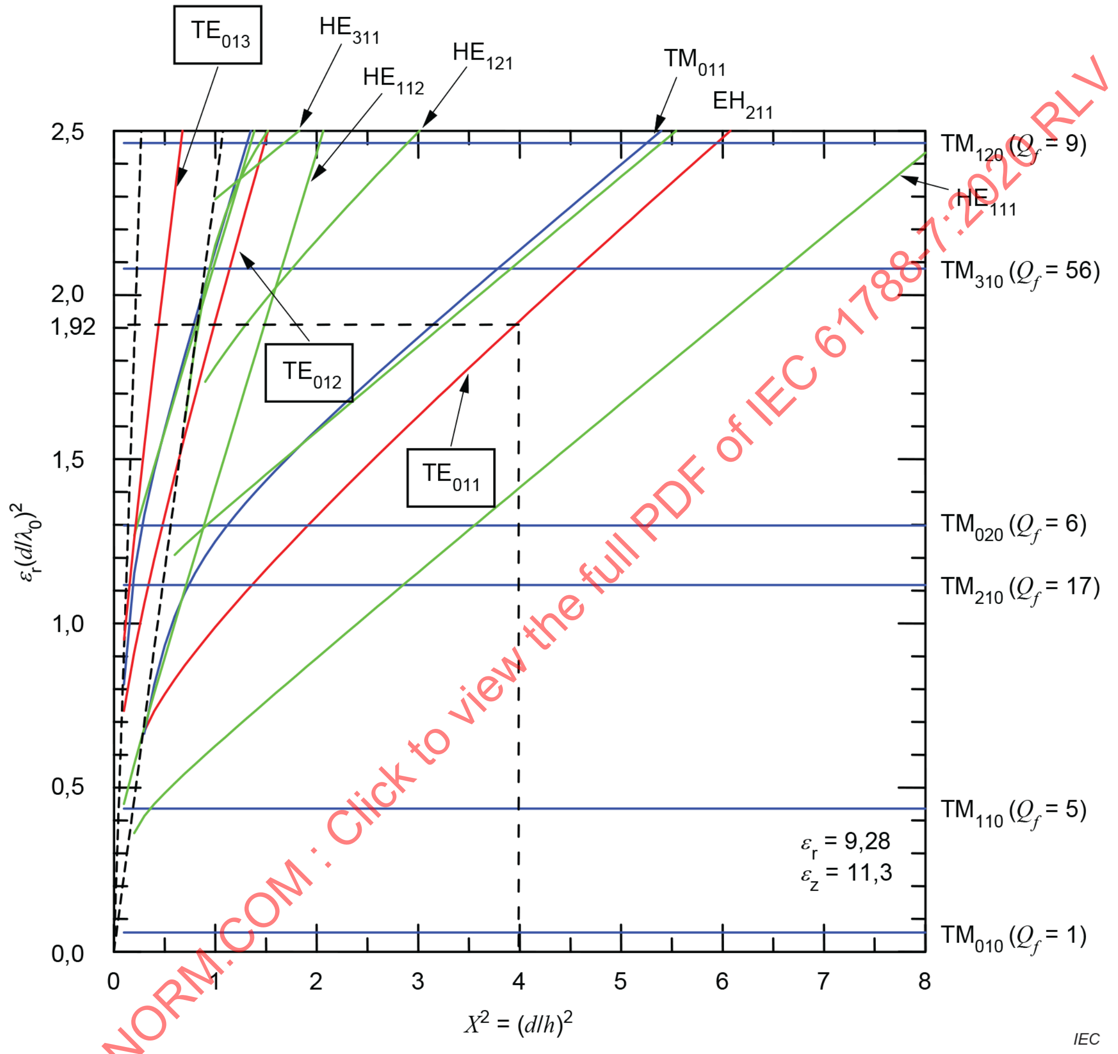

Figure A.6 – Mode chart to design TE_{011} resonator short-circuited at both ends by parallel superconductor films [28]

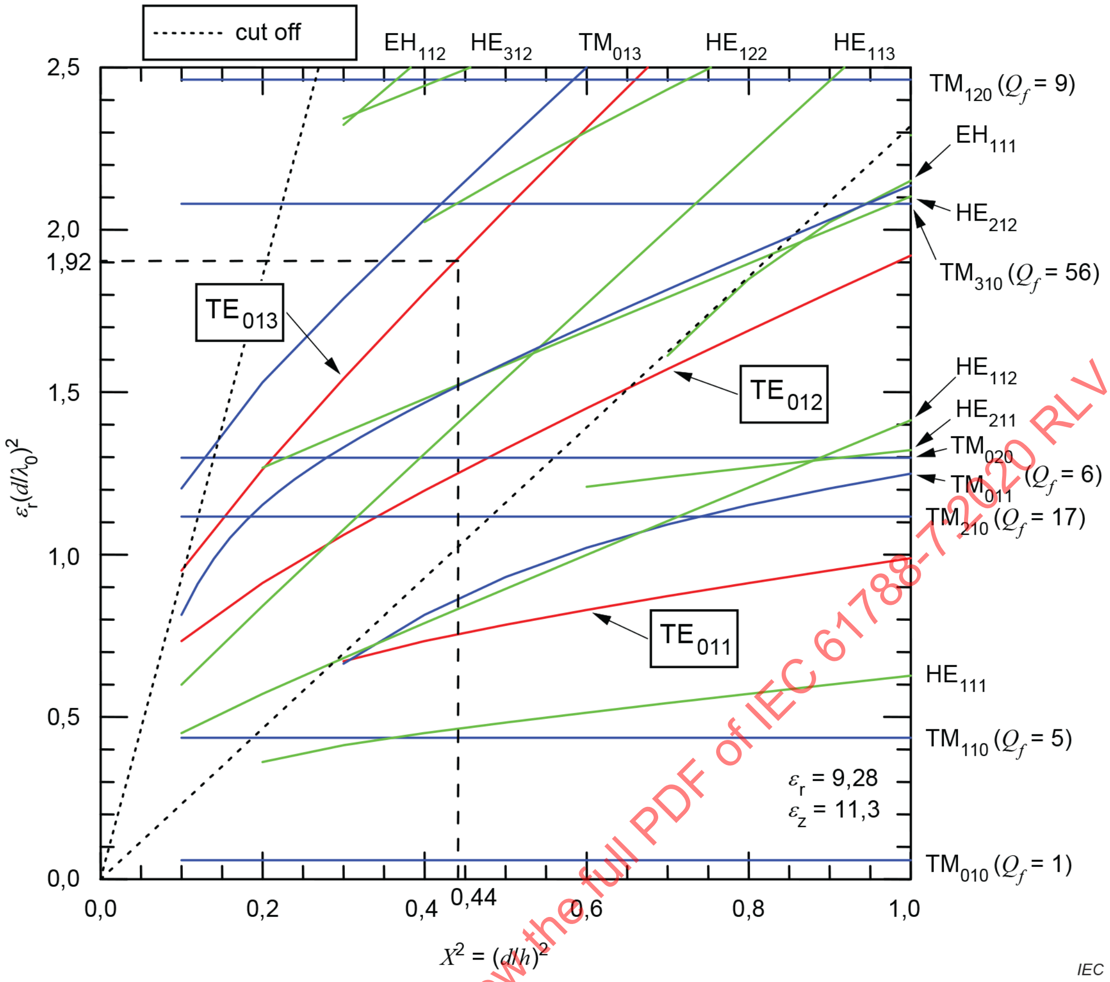

Figure A.7 – Mode chart to design TE_{013} resonator short-circuited at both ends by parallel superconductor films [28]

A.6 Dimension of the closed type resonator

In the closed type resonator, a copper cylinder is put between the superconductor films and a sapphire rod is placed in the center of the copper cylinder (Figure A.5 c)). The resonant frequency of each mode changes with the inner diameter of the copper cylinder, D. Therefore, D shall be selected so as to avoid the unwanted coupling with the other modes. In Figure A.8 and Figure A.9, mode charts of the closed type resonators are shown for the short sapphire rod ($(d/h)^2$ = 4) and the long sapphire rod ($(d/h)^2$ = 0,44), respectively, as a function of $S = D/d$ [28]. The ranges of S to separate the TE_{011} and the TE_{013} modes simultaneously from the others are S = 1,8 to 2,8, 3,8 to 4,1 and 4,8 to 5,2. The value of $S = D/d$ = 4 is recommended because of the ease with which it can be treated.

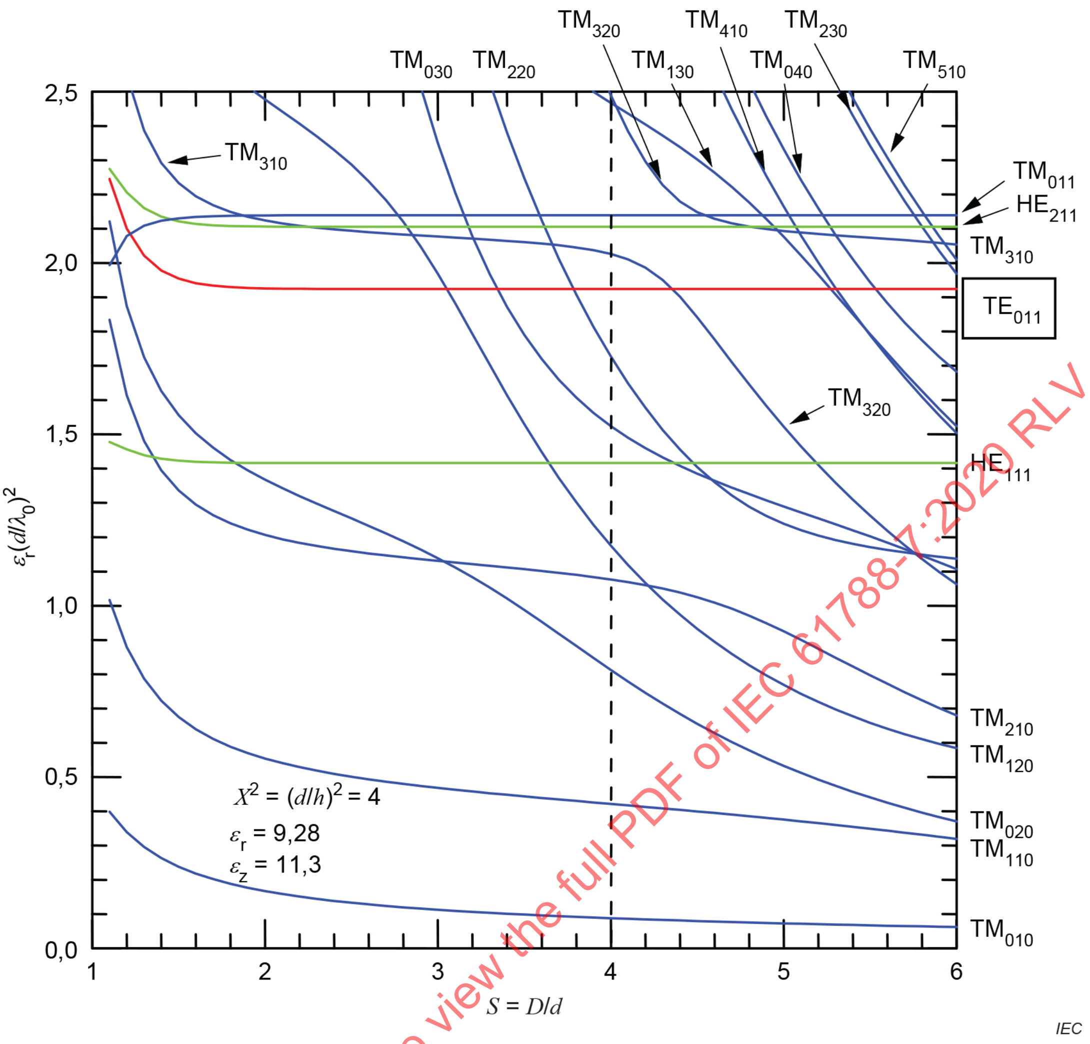

Figure A.8 – Mode chart for TE_{011} closed-type resonator [28]

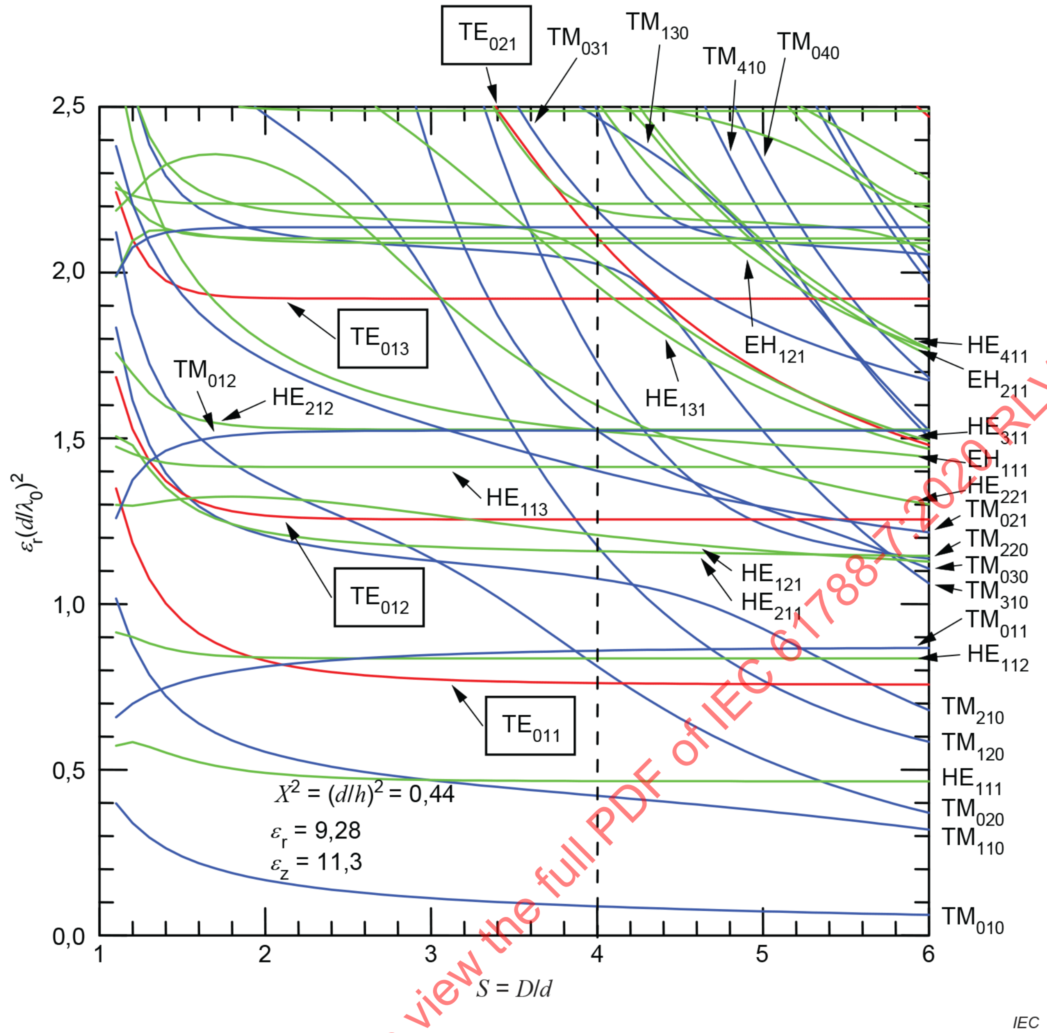

Figure A.9 – Mode chart for TE$_{013}$ closed-type resonator [28]

A.7 Sapphire rod reproducibility

Knowing the value of tan δ of the sapphire rod is a difficult problem. One approach based on the single- and triple-height rods involves the selection of a standard rod for each type. The first step is to compare a large number of sapphire rods by measuring them in a single HTS/sapphire resonator. The sapphire rod with the highest unloaded Q-value is the temporary label of standard. This procedure is repeated for a set of triple-height rods. The “standard” single- and triple-height rods are then used as described above to obtain tan δ. The electrical properties, ε' and tan δ, of other rods can then be calibrated by a direct comparison with these standard rods. Using a calibrated single-height rod, it is then possible to extract the R_s values of superconductor films under test.

A.8 Test results

Figure A.10 shows the temperature-dependent R_s of a YBCO film with a thickness of 500 nm and size of 25 mm square. The YBCO film was formed on MgO substrate by a co-evaporation method. The measurement was carried out at 21,8 GHz, which was converted to 10 GHz by the f^2 rule.

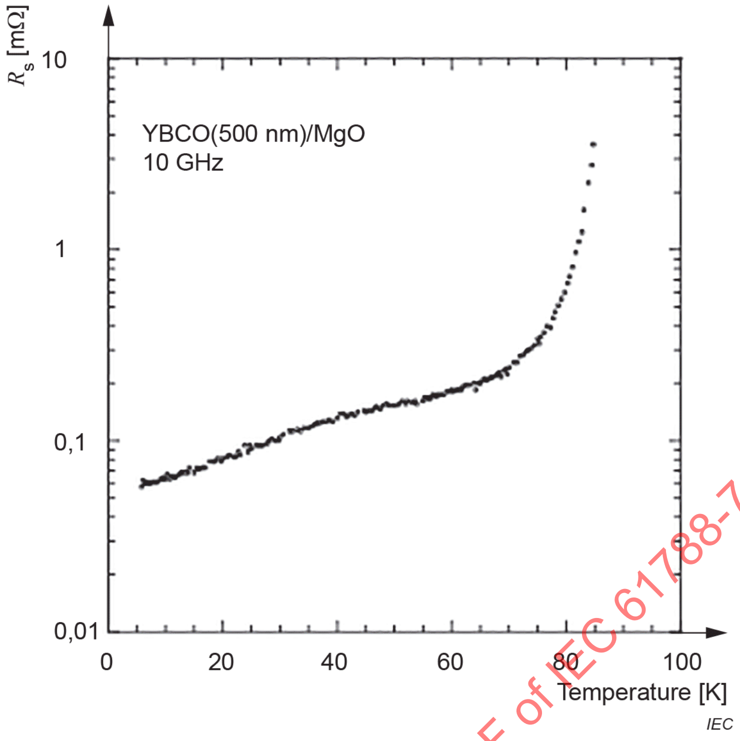

Figure A.10 – Temperature-dependent R_s of YBCO film with a thickness of 500 nm and size of 25 mm square

A.9 Reproducibility of measurement method

In order to evaluate the reproducibility of the surface resistance measurement, R_s of the same sample was measured three times and the variation of R_s was examined. The sample was reset to the measurement cavity each time. Figure A.11 shows the results. Measurement was performed at a frequency of 21,8 GHz and converted to 10 GHz according to the f^2 rule [30]. The variation in R_s was within 10 % in the temperature range of 10 K to 80 K.

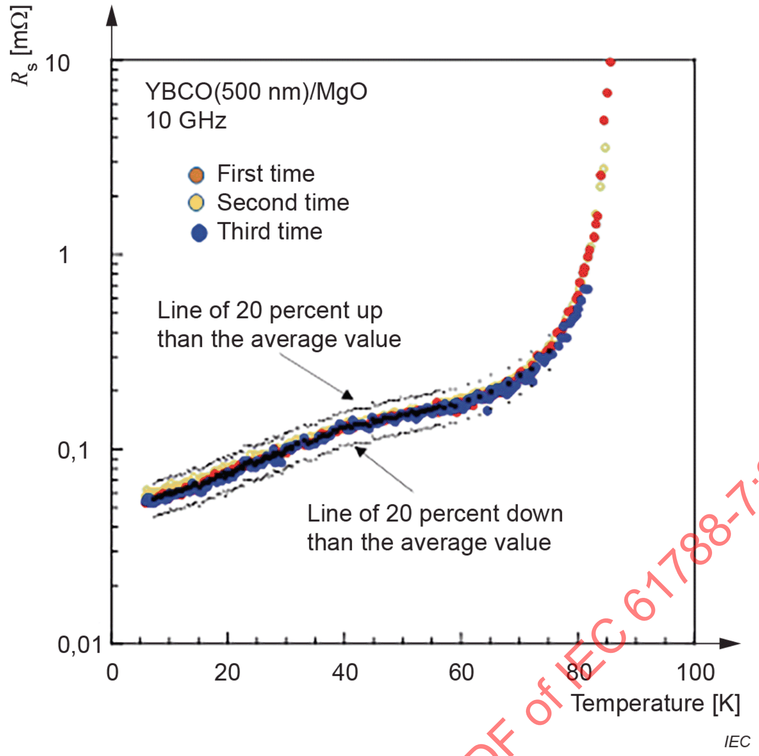

Figure A.11 – Temperature dependent R_s of YBCO film when R_s was measured three times

From the results, the standard deviation of each temperature can be calculated and its values are shown in Table A.1.

Table A.1 – Standard deviation of the surface resistance calculated from the results of Figure A.11

Temperature (K)	20	40	60	80
Standard deviation (%)	0,32	0,23	0,90	6,9

A.10 tan δ deviation effect of sapphire rods on surface resistance

For the two-resonator method, tan δ of the TE_{011} mode and TE_{013} sapphire rods are assumed to be absolutely equal. If tan δ of the two sapphire rods is different, it is not possible to calculate the surface resistance using Equation (6). Therefore, it is necessary to check the effect of tanδ deviation on surface resistance. tan δ of the high-purity sapphire rod used for the standard surface resistance measurement is extremely small, less than 2 × 10^{-7} [22]. Using such a sapphire rod, uncertainty in the surface resistance is quite small; however, if sapphire rods with a large tan δ are used, uncertainty in the surface resistance increases. tan δ_1 of the sapphire rod for TE_{011} mode is assumed to be 2 × 10^{-7} and tanδ_3 of the sapphire rod for TE_{013} mode changes according to that value. The difference in tan δ of the two sapphire rods is defined as in Equation (A.12) and the change in surface resistance as in Equation (A.13).

$$x = \frac{\tan\delta_1 - \tan\delta_3}{\tan\delta_1} \times 100\ [\%] \quad \text{(A.12)}$$

$$y = \frac{R_s(x) - R_s(0)}{R_s(0)} \quad \text{(A.13)}$$

R_s can be calculated using Equation (A.14) when tan δ_1 and tan δ_3 are different. The relationship between x and y is shown in Table A.2. When the difference in tanδ of the two sapphire rods exceeds ±50 %, the change in surface resistance exceeds ±18 %.

$$R_s = \frac{1}{B_1}\left(\frac{A_1}{Q_{u1}} - \tan\delta_1\right) = \frac{1}{B_3}\left(\frac{A_3}{Q_{u3}} - \tan\delta_3\right) \quad \text{(A.14)}$$

$$A_p = 1 + \frac{W}{\varepsilon'_p} \quad \text{(A.15)}$$

$$B_p = p^2 \left(\frac{\lambda_0}{2h_p}\right)^3 \frac{1+W}{30\pi^2 \varepsilon'_p}, (p = 1, 3) \quad \text{(A.16)}$$

$$W = \frac{J_1^2(u)}{K_1^2(v)} \frac{K_0(v)K_2(v) - K_1^2(v)}{J_1^2(u) - J_0(u)J_2(u)} \quad \text{(A.17)}$$

$$v_0^2 = \left(\frac{\pi d_0}{\lambda_0}\right)^2 \left[\left(\frac{\lambda_0}{2h_0}\right)^2 - 1\right] \quad \text{(A.18)}$$

$$u_0 \frac{J_0(u_0)}{J_1(u_0)} = -v_0 \frac{K_0(v_0)}{K_1(v_0)} \quad \text{(A.19)}$$

Table A.2 – Relationship between x, defined by Equation (A.12), and y, defined by Equation (A.13)

x (%)	−50	−40	−30	−20	−10	0	+10	+20	+30	+40	+50
y (%)	18,0	14,4	10,8	7,2	3,6	0	−3,6	−7,2	−10,8	−14,4	−18,0

Annex B
(informative)

Evaluation of relative combined standard uncertainty for surface resistance measurement

B.1 Practical surface resistance measurement

A superconductor shows a significantly increased surface resistance when irradiated by a high frequency current in the microwave range. There are several methods for measuring surface resistance, but the dielectric resonator method can measure surface resistance the most accurately. The method is described in Annex A. Figure B.1 shows these two resonators used to measure the frequency characteristics of TE_{011} and TE_{013} modes.

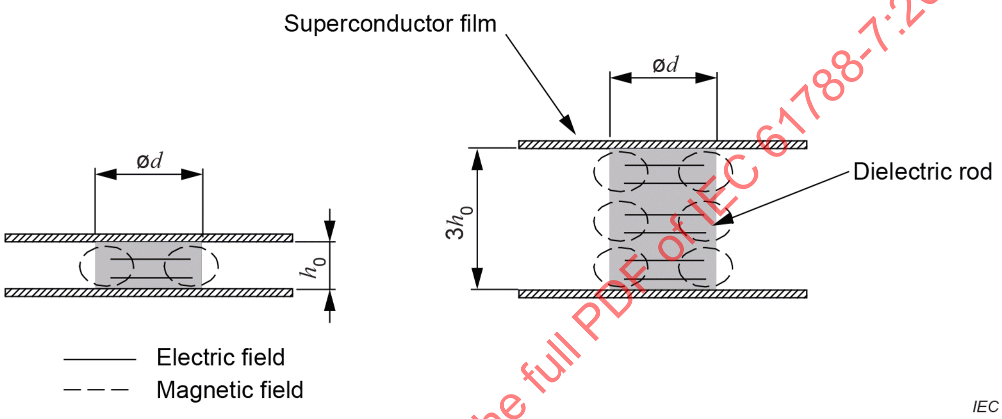

Figure B.1 – Schematic diagram of TE_{011} and TE_{013} mode resonance

Figure B.2 shows the typical frequency characteristics of TE_{011} mode resonance. Q_{L1} is determined using the results of this measurement and Q_{u1} is calculated using Equation (B.2).

$$Q_{L1} = \frac{f_0}{\Delta f} \tag{B.1}$$

$$Q_{u1} = \frac{Q_{L1}}{1 - A_t}, A_t = 10^{-IA[\text{dB}]/20} \tag{B.2}$$

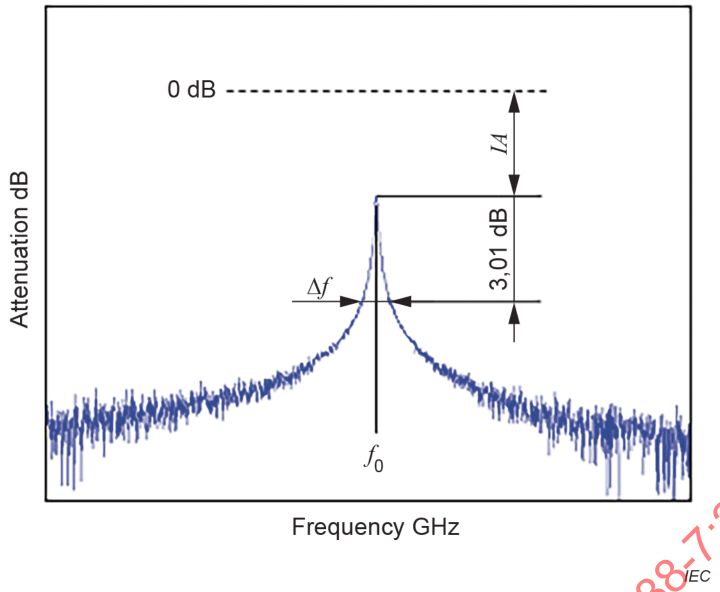

Figure B.2 – Typical frequency characteristics of TE_{011} mode resonance

B.2 Determination of surface resistance of the superconductor

The microwave surface resistance of the superconductor is obtained from Equations (B.3) to (B.8).

$$R_s = \frac{30\pi^2 \times 3}{3-1}\left[\frac{2h_0}{\lambda_0}\right]^3 \frac{\varepsilon' + W}{1+W}\left[\frac{1}{Q_{u1}} - \frac{1}{Q_{u3}}\right] \tag{B.3}$$

$$\varepsilon' = \left(\frac{\lambda_0}{\pi d}\right)^2 \left(u^2 + v^2\right) + 1 \tag{B.4}$$

$$W = \frac{J_1^2(u)}{K_1^2(v)} \frac{K_0(v)K_2(v) - K_1^2(v)}{J_1^2(u) - J_0(u)J_2(u)} \tag{B.5}$$

$$v^2 = \left(\frac{\pi d}{\lambda_0}\right)^2 \left[\left(\frac{3\lambda_0}{2h_0}\right)^2 - 1\right] \tag{B.6}$$

$$u\frac{J_0(u)}{J_1(u)} = -v\frac{K_0(v)}{K_1(v)} \tag{B.7}$$

$$\lambda_0 = \frac{c}{f_0} \tag{B.8}$$

Here, d and h_0 are the diameter and height of the sapphire rod, respectively, ε' is the effective relative permittivity of the sapphire rod, c is the speed of light in vacuum, and f_0 is the resonant frequency of the resonator.

B.3 Combined standard uncertainty

B.3.1 General

By partially differentiating the equation (B.3) with h_0, ε', W, Q_{u1}, *and* Q_{u3}, the equation of uncertainty shown in Equation (B.9) is obtained.

$$\begin{aligned} u_c^2 = \frac{\delta R_s^2}{R_s^2} &= \left(\frac{\partial R_s}{\partial h}\right)^2\left(\frac{\delta h}{R_s}\right)^2 + \left(\frac{\partial R_s}{\partial \varepsilon'}\right)^2\left(\frac{\delta \varepsilon'}{R_s}\right)^2 + \left(\frac{\partial R_s}{\partial W}\right)^2\left(\frac{\delta W}{R_s}\right)^2 \\ &+ \left(\frac{\partial R_s}{\partial Q_{u1}}\right)^2\left(\frac{\delta Q_{u1}}{R_s}\right)^2 + \left(\frac{\partial R_s}{\partial Q_{u3}}\right)^2\left(\frac{\delta Q_{u3}}{R_s}\right)^2 + c_{\text{unknown}}^2 u_{\text{unknown}}^2 \\ &(\delta h = h u_1, \delta\varepsilon' = \varepsilon' u_2, \delta W = W u_3, \delta Q_{u1} = Q_{u1} u_4, \delta Q_{u3} = Q_{u3} u_5) \\ &= \left(\frac{\partial R_s}{\partial h}\right)^2\left(\frac{h}{R_s}\right)^2 u_1^2 + \left(\frac{\partial R_s}{\partial \varepsilon'}\right)^2\left(\frac{\varepsilon'}{R_s}\right)^2 u_2^2 + \left(\frac{\partial R_s}{\partial W}\right)^2\left(\frac{W}{R_s}\right)^2 u_3^2 \\ &+ \left(\frac{\partial R_s}{\partial Q_{u1}}\right)^2\left(\frac{Q_{u1}}{R_s}\right)^2 u_4^2 + \left(\frac{\partial R_s}{\partial Q_{u3}}\right)^2\left(\frac{Q_{u3}}{R_s}\right)^2 u_5^2 + c_{\text{unknown}}^2 u_{\text{unknown}}^2 \\ &= c_1^2 u_1^2 + c_2^2 u_2^2 + c_3^2 u_3^2 + c_4^2 u_4^2 + c_5^2 u_5^2 + c_{\text{unknown}}^2 u_{\text{unknown}}^2 \end{aligned} \quad \text{(B.9)}$$

The variables c_{unknown} and u_{unknown} in Equation (B.9) represent in the uncertainty of unknown factors of measurement system, for example, noise factor. The variables in Equation (B.9) are expressed by Equations (B.10) to (B.14).

$$c_1 = \frac{\partial R_s}{\partial h}\frac{h}{R_s} = \frac{3R_s}{h_0}\frac{h_0}{R_s} = 3 \quad \text{(B.10)}$$

$$c_2 = \frac{\partial R_s}{\partial \varepsilon'}\frac{\varepsilon'}{R_s} = \frac{\varepsilon'}{\varepsilon' + W} \quad \text{(B.11)}$$

$$c_3 = \frac{\partial R_s}{\partial W}\frac{W}{R_s} = \frac{(1-\varepsilon')W}{(1+W)(\varepsilon'+W)} \quad \text{(B.12)}$$

$$c_4 = \frac{\partial R_s}{\partial Q_{u1}}\frac{Q_{u1}}{R_s} = \frac{-Q_{u3}}{Q_{u3} - Q_{u1}} \quad \text{(B.13)}$$

$$c_5 = \frac{\partial R_s}{\partial Q_{u3}}\frac{Q_{u3}}{R_s} = \frac{Q_{u1}}{Q_{u3} - Q_{u1}} \quad \text{(B.14)}$$

B.3.2 Calculation of c_2 to c_5 (12 GHz resonance at 20 K)

When calculating uncertainty using the Equation (B.9), it is necessary to specify the resonant frequency. Here, we will discuss a typical 12 GHz resonator.

12 GHz resonator (f_0 = 12 GHz, d = 11,4 mm, h_0 = 5,7 mm)

Using the above values, we can calculate v^2 and u^2 by Equations (B.6) and (B.7).

$$v^2 = 7{,}815,\ u^2 = 9{,}09 \tag{B.15}$$

ε' and W are determined by Equations (B.4) and (B.5).

$$\varepsilon' = 9{,}22,\ W = 0{,}16 \tag{B.16}$$

Then c_2 and c_3 can be determined using Equations (B.11) and (B.12).

$$c_2 = 0{,}983,\ c_3 = -0{,}122 \tag{B.17}$$

In order to determine c_4 and c_5, we have to know the values of unloaded Q_{u1} and Q_{u3}. Y. Kobayashi reported Q_{u1} and Q_{u3} at 20 K, 12 GHz [28]. Their reported values were Q_{u1} = 2 000 000 (Q_{L1} = 1 800 000) and Q_{u3} = 7 500 000 (Q_{L3} = 6 750 000). Therefore, c_4 and c_{5L} can be calculated.

$$c_4 = 1{,}364,\ c_5 = 0{,}3636 \tag{B.18}$$

B.3.3 Determination of u_1 to u_5

u_1 to u_5, which are derived from the uncertainty of the diameter, height and dielectric constant of sapphire rod and Q_{u1} and Q_{u3} of the cavity, are calculated by the following procedures.

1) u_1

u_1 is determined by the uncertainty of the height of the sapphire rod. The height of the sapphire rod of the 12 GHz resonator is 5,7 mm, and its uncertainty is 50 μm. Therefore, u_1 is as follows.

$$u_1 = \frac{1}{\sqrt{3}}\frac{0{,}05}{5{,}7} = 0{,}005\,07 \tag{B.19}$$

2) u_2

u_2 is determined by the uncertainty in the effective dielectric constant ε'_δ of the sapphire rod and can be calculated using Equation (B.20).

$$u_2 = \frac{1}{\sqrt{3}}\frac{\varepsilon' - \varepsilon'_\delta}{\varepsilon'} \tag{B.20}$$

where ε'_δ is the relative permittivity induced from uncertainty in the shape of the sapphire rod.

$$\varepsilon' = \left(\frac{\lambda_0}{\pi d_0}\right)^2 \left(u_0^2 + v_0^2\right) + 1 \quad (d_0 = 11{,}4\ \text{mm}, h_0 = 5{,}7\ \text{mm}) \tag{B.21}$$

$$\varepsilon'_\delta = \left(\frac{\lambda_0}{\pi d}\right)^2 \left(u_{0\delta}^2 + v_{0\delta}^2\right) + 1 \quad (d_{0\delta} = 11{,}45\ \text{mm}, h_{0\delta} = 5{,}65\ \text{mm}) \tag{B.22}$$

and u_0, v_0, $u_{0\delta}$ and $v_{0\delta}$ are calculated using Equations (B.23) and (B.24).

$$v_0^2 = \left(\frac{\pi d_0}{\lambda_0}\right)^2 \left[\left(\frac{3\lambda_0}{2h_0}\right)^2 - 1\right], v_{0\delta}^2 = \left(\frac{\pi d_{0\delta}}{\lambda_0}\right)^2 \left[\left(\frac{3\lambda_0}{2h_{0\delta}}\right)^2 - 1\right] \tag{B.23}$$

$$u_0 \frac{J_0(u_0)}{J_1(u_0)} = -v_0 \frac{K_0(v_0)}{K_1(v_0)}, \; u_{0\delta} \frac{J_0(u_{0\delta})}{J_1(u_{0\delta})} = -v_{0\delta} \frac{K_0(v_{0\delta})}{K_1(v_{0\delta})} \tag{B.24}$$

As a result, we find that ε' = 9,22 and ε'_δ = 9,29.

$$u_2 = 0{,}004\,4 \tag{B.25}$$

3) u_3

u_3 can be determined using Equation (B.26).

$$u_3 = \frac{1}{\sqrt{3}} \frac{W - W_\delta}{W} \tag{B.26}$$

W is determined using Equation (B.5) and W_δ comes from uncertainty in the shape of the sapphire rod and can be determined by using Equation (B.27).

$$W_\delta = \frac{J_1^2(u_\delta)}{K_1^2(v_\delta)} \frac{K_0(v_\delta)K_2(v_\delta) - K_1^2(v_\delta)}{J_1^2(u_\delta) - J_0(u_\delta)J_2(u_\delta)} \tag{B.27}$$

By calculating W and W_δ using u_0, v_0, $u_{0\delta}$, $v_{0\delta}$ in Equations (B.23) and (B.24), u_3 turns out to have the following value.

$$u_3 = 0{,}014\,3 \tag{B.28}$$

4) u_4 and u_5

u_4 and u_5 are determined by measuring the uncertainty in Q_{u1} and Q_{u3}. The measurement of the uncertainty in Q_{u1} and Q_{u3} has the most influence on the dynamic range uncertainty of the vector network analyzer and other factors are negligible. Since the dynamic range uncertainty in the recommended vector network analyzer is ±0,1 dB, u_4 and u_5 are calculated using this value. Regarding the frequency characteristics of the resonator in Figure B.2, the frequency characteristic near the resonant frequency is assumed to be a Lorentz distribution [30].

$$y = \left|\frac{S_{12}(f)}{S_{12}(f_0)}\right| = \frac{1}{\left(1 + Q_L^2 \Delta^2(f)\right)^{1/2}} = \frac{1}{\left(1 + \left(\frac{f - f_0}{f_1}\right)^2\right)^{1/2}},$$

$$\Delta(f) = 1 - \frac{f_0^2}{f^2} = \frac{2(f - f_0)}{f_0} \tag{B.29}$$

The frequency characteristics are shown in Figure B.3 The curve can be approximated by Equation (B.29), where f_0 is the resonant frequency and $2f_1$ is the bandwidth at 3,01 dB. The frequency bandwidth which is 3,01 dB below the resonance peak is defined as Δf and it corresponds to the bandwidth across 0,707 in Figure B.3. The ±0,1 dB of the dynamic range uncertainty corresponds to ±0,008 in Figure B.3. Therefore, Q_{L1}, $Q_{L1\delta}$, Q_{L3}, and $Q_{L3\delta}$

can be calculated. Q_{L1} and Q_{L3} are reported as 1,80 × 10[6] and 6,75 × 10[6], respectively [28]. Using these values, we can calculate $Q_{L1\delta}$ and $Q_{L3\delta}$.

$$Q_{L1} = 1{,}80\times10^6,\ \ Q_{L1\delta} = 1{,}84\times10^6,\ \ Q_{L3} = 6{,}75\times10^6,\ \ Q_{L3\delta} = 6{,}90\times10^6$$

Assuming insertion attenuation (IA) = 20dB, Q_{u1}, $Q_{u1\delta}$, Q_{u3}, and $Q_{u3\delta}$ can be calculated.

$$Q_{u1} = 2{,}00\times10^6,\ \ Q_{u1\delta} = 2{,}044\times10^6,\ \ Q_{u3} = 7{,}5\times10^6,\ \ Q_{u3\delta} = 7{,}67\times10^6$$

Through these calculations, the values of u_4 and u_5 are obtained.

$$u_4 = \frac{1}{\sqrt{3}}\frac{Q_{u1} - Q_{u1\delta}}{Q_{u1}} = -0{,}012 \qquad \text{(B.30)}$$

$$u_5 = \frac{1}{\sqrt{3}}\frac{Q_{u3} - Q_{u3\delta}}{Q_{u3}} = -0{,}013 \qquad \text{(B.31)}$$

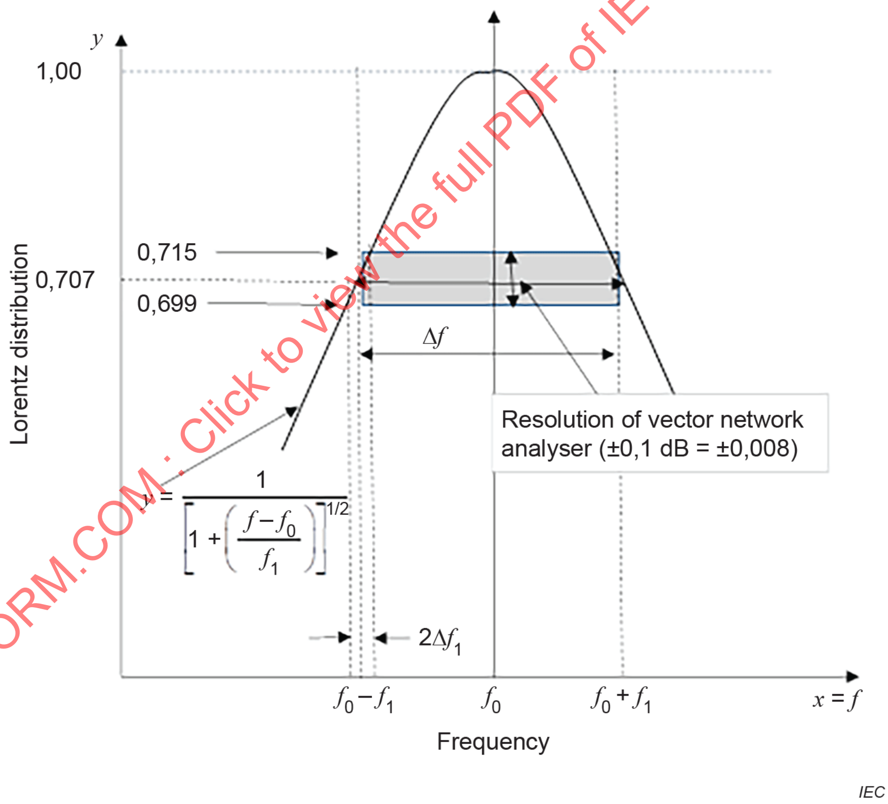

Figure B.3 – Frequency characteristics of a resonator approximated by a Lorentz distribution

B.3.4 Combined relative standard uncertainty

Uncertainties in c_{cavity} and u_{cavity} due to the loss of copper cavity is quite small, however c_{unknown} and u_{unknown} are not small. The combined standard uncertainty at 20 K is calculated as follows.

$$
\begin{aligned}
u_c &= \sqrt{c_1^2 u_1^2 + c_2^2 u_2^2 + c_3^2 u_3^2 + c_4^2 u_4^2 + c_5^2 u_5^2 + c_{\text{unknown}}^2 u_{\text{unknown}}^2} \\
&= \sqrt{2{,}31 \times 10^{-4} + 0{,}187 \times 10^{-4} + 0{,}030 \times 10^{-4} + 2{,}68 \times 10^{-4} + 0{,}223 \times 10^{-4} + c_{\text{unknown}}^2 u_{\text{unknown}}^2} \\
&= \sqrt{5{,}43 \times 10^{-4} + c_{\text{unknown}}^2 u_{\text{unknown}}^2}
\end{aligned}
\qquad \text{(B.32)}
$$

It is difficult to quantitatively evaluate $c_{\text{unknown}} u_{\text{unknown}}$ in Equation (B.32), but its value can be estimated from the results of surface resistance measurement repeated three times. The variation observed when measuring the surface resistance of the same films repeatedly is believed to be due to the noise and temperature uncertainty of the measurement system. Therefore, from the results in Table A.1, $c_{\text{unknown}} u_{\text{unknown}}$ can be estimated as about 0,32 % for 20 K, about 0,9 % for 60 K, and about 6,9 % for 80 K ($c_{\text{unknown}} u_{\text{unknown}}$ increases as the measurement temperature increases). From the above results, the combined relative standard uncertainty of Equation (B.32) was about 2,4 % at 20 K and about 7,3 % at 80 K. The value is smaller than the target combined relative standard uncertainty.

When the measured temperature exceeds 70 K, large noise is superimposed on the resonance peak, and the uncertainty in R_s increases. In that case, it is difficult express the resonance peak with Lorentz distribution. Therefore, the deviation of u_4 and u_5 have to be reviewed. However, as is clear from the results in Figure A.11 and Table A.1, the uncertainty of R_s measured by the standard dielectric resonator method is less than 10 % below 80 K.

Bibliography

[1] ZHANG, D., LIANG, G-C., SHIH, CF., LU, ZH. and JOHANSSON, ME. A 19-pole cellular bandpass filter using 75-mm diameter high-temperature superconducting thin films. *IEEE Microwave and Guided Wave Letters*, 1995, 5, p.405

[2] SIMON, RW., HAMMOND, RB., BERKOWITZ, SJ. and WILLEMSEN, BA. Supercoducting microwave filter systems for cellular telephone base station. *Proc. IEEE*, 2004, 92, p.1585

[3] PETERSON, GE., WTAWAXKI, R.P. and ALFORD, N.McN. Helical resonators containing high Tc ceramic superconductors. *Appl. Phys. Lett.*, 1989, 55, p.1798

[4] TSUZUKI, G., SUZUKI, M. and SAKAKIBARA, N. Superconducting Filter for IMT-2000 Band. *IEEE Trans. Microwave Theory Tech.*, 2000, 48, p.2519

[5] ITOH, K., ISHII, O., NAGAI, Y., SUZUKI, N., KIMACHI, Y. and MICHIKAMI, O. High Tc superconducting small antenna. *IEEE Trans. Appl. Supercond.*, 1993, 3, p.2836

[6] HOHENWATER, GK., TRACK, EK., DRAKE, RE. and PATT, R. Forty five nanosecond superconducting delay line. *IEEE Trans. Magn.,* 1993, 3, p.2804

[7] KINDER, H., BERBERICH, P., UTZ, B. and PRUSSEIT, W. Double sided YBCO films on 4" substrates by thermal reactive evaporation. *IEEE Trans. Appl. Supercond.*, 1995, 5, p.1575

[8] FACE, DW., WILKER, C., SHEN, Z-Y., PANG, P. and SMALL, R.J. Large area $YBa_2Cu_3O_7$ films for high power microwave applications. *IEEE Trans. Appl. Supercond.*, 1995, 5, p.1581

[9] NAKAGAWA, K., HONMA, T., TAKEDA, K., ONO, S., KAI, H., SAITO, A., MUKAIDA, M., NAKAJIMA, K. and OHSHIMA, S., Intrinsic Surface Resistance of YBCO Thin Films Under DC Magnetic Field, *IEEE Trans. Appl. Supercond.*, 2011, 21, p.587

[10] GUREVICH, A., Theory of RF superconductivity for resonant cavities, *Supercond. Sci. Technol.*, 2017, 30, 034004

[11] WILKER, C., SHEN, Z.-Y., NGUYEN, VX. and BRENNER, MS. A sapphire resonator for microwave characterization of superconducting thin films. *IEEE Trans. Appl. Supercond.*, 1993, 3, p.1457

[12] LLOPIS, O. and GRAFFEUIL, J. Microwave characterization of high Tc superconductors with a dielectric resonator. *J. Less-Common Met.*, 1990, 164, p.1248

[13] MAZIERSKA, J. and WILKER, C. Accuracy issues in surface resistance measurements of high temperature superconductors using dielectric resonators (corrected). *IEEE Trans. Appl. Supercond.*, 2001, 11, p.4140

[14] POMPEO, N., TOROKHTII, K. and SILVA, E. Dielectric Resonators for Measurements of the Surface Impedance of Superconducting Films. *Meas. Sci. Rev.* 2014, 14, p.164

[15] OBARA, H. and KOSAKA, S. Microwave power dependence measurement of surface resistance of superconducting films using a dielectric resonator method with circle fit and two-mode techniques. *IEICE Trans. Electron.*, 2006, E89C, 2, p.125

[16] LEONG, K. and MAZIERSKA, J. Accurate measurement of surface resistance of HTS films using a noble transmission mode Q-factor technique. *J. Superconductivity*, 2001, 14, p.93

[17] PALMIERI, V., ROSSI, AA., STARK, SY. and VAGLIO, R., Evidence for boundary resistance effect on superconducting radiofrequency cavity performances. *Supercond. Sci. Technol.*, 2014, 27, 085004

[18] TABER, RC. A parallel plate resonator technique for microwave loss measurements on superconductors. *Rev. Sci. Instrum.*, 1990, 61, p.2200

[19] FLETCHER, R. and COOK, J. Measurement of surface impedance versus temperature using a generalized sapphire resonator technique, *Rev. Sci, Instrum.,* 1994, 65, p. 2658.

[20] YOSHITAKE, T. and TSUGE, H. Effects of microstructures on microwave properties in Y-Ba-Cu-O microstrip resonators. *IEEE Trans. Appl. Supercond.*, 1995, 5, p.2571

[21] OKAI, D., KUSUNOKI, M., MUKAIDA, M. and OHSHIMA, S. New surface resistance measurement technique of high-temperature superconductors using a probe coupling microstrip line resonator, *IEEE Trans. Appl. Supercond.,* 2001, 11 p. 3078

[22] MAZIERSKA, J. Dielectric resonator as a possible standard for characterization of high temperature superconducting films for microwave applications. *J. Supercond.*, 1997, 10, p.73

[23] SHEN, Z.-Y., WILKER, C., PANG, P., HOLSTEIN, WL., FACE, DW. and KOUNTZ, DJ. High Tc superconductor-sapphire microwave resonator with extremely high Q-values up to 90 K. *IEEE Trans. Microwave Theory Tech.*, 1992, 40, p.2424

[24] KOBAYASHI, Y., IMAI, T. and KAYANO, H. Microwave measurement of temperature and current dependences of surface impedance for high-Tc superconductors. *IEEE Trans. Microwave Theory Tech.*, 1991, 39, p.1530

[25] SATO, K., SATO, S., ICHIKAWA, K., WATANABE, M., HONMA, T., TANAKA, Y., OIKAWA, S., SAITO, A. and OHSHIMA, S. Dependence of microwave surface resistance of HTS thin films on applied dc magnetic fields parallel and normal to the substrate. *J. Phys*. 2014, 507, 012045

[26] ZENG, C., LUO, ZX., BU, SR., YANG, K. and ZHANG, QS. A novel method for the measurement of frequency-character of surface resistance of HTS thin film. *Chinese Science Bulletin*, 2010, 55, p.1088

[27] ZENG, C., CHEN, L., BU, SR., NING, JS. MENG, B. and ZHANG, QS. An efficient and accurate method for HTS surface resistance measurement. *J. Supercond. Nov. Magn.*, 2015, 28, p. 3179

[28] HASHIMOTO, T. and KOBAYASHI, Y. Two-Sapphire-Rod-Resonator method to measure the surface resistance of High-Tc superconductor films. *IEICE Trans. Electron.*, 2004, E87-C, No.5, p. 681

[29] LEE, JH., KIM, MS., HAN, HK., JUNG, HS., YANG, WI., LEE, SY., PARK, B. and LEE, SG., Improved Measurement Accuracy for Thickness of $YBa_2Cu_3O_y$ Films by Using a Single Two-resonance-mode Sapphire Resonator, *J. Korean Phys. Soc.* 2012, 60, p.1072

[30] LANCASTER, MJ. *Passive microwave device applications of high-temperature superconductors*, Cambridge University Press, 1997, p.138

____

SOMMAIRE

COMMISSION ÉLECTROTECHNIQUE INTERNATIONALE

____

SUPRACONDUCTIVITÉ –

Partie 7: Mesurages des caractéristiques électronique – Résistance de surface des supraconducteurs haute température critique aux hyperfréquences

AVANT-PROPOS

1) La Commission Électrotechnique Internationale (IEC) est une organisation mondiale de normalisation composée de l'ensemble des comités électrotechniques nationaux (Comités nationaux de l'IEC). L'IEC a pour objet de favoriser la coopération internationale pour toutes les questions de normalisation dans les domaines de l'électricité et de l'électronique. À cet effet, l'IEC – entre autres activités – publie des Normes internationales, des Spécifications techniques, des Rapports techniques, des Spécifications accessibles au public (PAS) et des Guides (ci-après dénommés «Publication(s) de l'IEC»). Leur élaboration est confiée à des comités d'études, aux travaux desquels tout Comité national intéressé par le sujet traité peut participer. Les organisations internationales, gouvernementales et non gouvernementales, en liaison avec l'IEC, participent également aux travaux. L'IEC collabore étroitement avec l'Organisation Internationale de Normalisation (ISO), selon des conditions fixées par accord entre les deux organisations.
2) Les décisions ou accords officiels de l'IEC concernant les questions techniques représentent, dans la mesure du possible, un accord international sur les sujets étudiés, étant donné que les Comités nationaux de l'IEC intéressés sont représentés dans chaque comité d'études.
3) Les Publications de l'IEC se présentent sous la forme de recommandations internationales et sont agréées comme telles par les Comités nationaux de l'IEC. Tous les efforts raisonnables sont entrepris afin que l'IEC s'assure de l'exactitude du contenu technique de ses publications; l'IEC ne peut pas être tenue responsable de l'éventuelle mauvaise utilisation ou interprétation qui en est faite par un quelconque utilisateur final.
4) Dans le but d'encourager l'uniformité internationale, les Comités nationaux de l'IEC s'engagent, dans toute la mesure possible, à appliquer de façon transparente les Publications de l'IEC dans leurs publications nationales et régionales. Toutes divergences entre toutes Publications de l'IEC et toutes publications nationales ou régionales correspondantes doivent être indiquées en termes clairs dans ces dernières.
5) L'IEC elle-même ne fournit aucune attestation de conformité. Des organismes de certification indépendants fournissent un service d'évaluation de conformité et, dans certains secteurs, accèdent aux marques de conformité de l'IEC. L'IEC n'est responsable d'aucun des services effectués par les organismes de certification indépendants.
6) Tous les utilisateurs doivent s'assurer qu'ils sont en possession de la dernière édition de cette publication.
7) Aucune responsabilité ne doit être imputée à l'IEC, à ses administrateurs, employés, auxiliaires ou mandataires, y compris ses experts particuliers et les membres de ses comités d'études et des Comités nationaux de l'IEC, pour tout préjudice causé en cas de dommages corporels et matériels, ou de tout autre dommage de quelque nature que ce soit, directe ou indirecte, ou pour supporter les coûts (y compris les frais de justice) et les dépenses découlant de la publication ou de l'utilisation de cette Publication de l'IEC ou de toute autre Publication de l'IEC, ou au crédit qui lui est accordé.
8) L'attention est attirée sur les références normatives citées dans cette publication. L'utilisation de publications référencées est obligatoire pour une application correcte de la présente publication.
9) L'attention est attirée sur le fait que certains des éléments de la présente Publication de l'IEC peuvent faire l'objet de droits de brevet. L'IEC ne saurait être tenue pour responsable de ne pas avoir identifié de tels droits de brevets et de ne pas avoir signalé leur existence.

La Norme internationale IEC 61788-7 a été établie par le comité d'études 90 de l'IEC: Supraconductivité.

Cette troisième édition annule et remplace la deuxième édition parue en 2006. Cette édition constitue une révision technique.

Cette édition inclut les modifications techniques majeures suivantes par rapport à l'édition précédente:

a) l'ajout de l'Annexe B informative, incertitude type composée relative pour le mesurage de la résistance de surface;
b) les déclarations de fidélité et d'exactitude ont été converties en incertitude;

c) l'ajout de la reproductibilité du mesurage de résistance de surface.

Le texte de cette Norme internationale est issu des documents suivants:

FDIS	Rapport de vote
90/447/FDIS	90/452/RVD

Le rapport de vote indiqué dans le tableau ci-dessus donne toute information sur le vote ayant abouti à l'approbation de cette Norme internationale.

Ce document a été rédigé selon les Directives ISO/IEC, Partie 2.

Une liste de toutes les parties de la série IEC 61788, publiées sous le titre général *Supraconductivité*, peut être consultée sur le site web de l'IEC.

Le comité a décidé que le contenu de ce document ne sera pas modifié avant la date de stabilité indiquée sur le site web de l'IEC sous «http://webstore.iec.ch» dans les données relatives à la publication recherchée. À cette date, le document sera

- reconduit,
- supprimé,
- remplacée par une édition révisée, ou
- amendé.

IMPORTANT – Le logo "*colour inside*" qui se trouve sur la page de couverture de cette publication indique qu'elle contient des couleurs qui sont considérées comme utiles à une bonne compréhension de son contenu. Les utilisateurs devraient, par conséquent, imprimer cette publication en utilisant une imprimante couleur.

INTRODUCTION

Depuis la découverte de certains oxydes de cuivre de type Perovskite, un travail approfondi de recherche et développement (R et D) sur les supraconducteurs haute température (HTS – *high-temperature superconductors*) a été, et est toujours, réalisé dans le monde entier, et son application aux machines à aimant à effet de champ, à la transmission à faible perte de puissance, aux composants électroniques et à d'autres technologies est en cours.

Dans différents domaines de l'électronique, et plus particulièrement dans ceux des télécommunications, les dispositifs hyperfréquences passifs (des filtres utilisant des HTS, par exemple) ont été développés et font actuellement l'objet d'essais sur site [1][1] [2].

Les matériaux supraconducteurs destinés aux résonateurs à hyperfréquences [3], aux filtres [4], aux antennes [5] et aux lignes à retard [6] ont l'avantage de présenter des caractéristiques à très faible perte. Les paramètres des matériaux supraconducteurs nécessaires à la conception des composants hyperfréquences à faible perte sont la résistance de surface (R_s) et la dépendance de R_s vis-à-vis de la température. La connaissance de ce paramètre est d'une importance essentielle pour le développement de nouveaux matériaux côté fournisseur et pour la conception de composants hyperfréquences supraconducteurs côté client.

L'amplitude de la résistance de Surface R_s des films HTS de grande qualité est en général inférieure de plusieurs ordres à celle des métaux normaux [7] [8] [9] [10], ce qui a renforcé la nécessité d'une technique de caractérisation fiable pour mesurer cette propriété. Traditionnellement, la résistance de surface R_s du niobium (Nb) ou de tout autre matériau supraconducteur basse température est mesurée en fabriquant d'abord une cavité (optique) résonante à trois dimensions, puis en mesurant sa valeur Q [11]. La résistance de surface R_s peut être calculée en résolvant la distribution de champ électromagnétique (CEM) à l'intérieur de la cavité. Une autre technique consiste à placer un petit échantillon à l'intérieur d'une cavité plus grande. Cette technique prend de nombreuses formes, mais implique souvent l'incertitude introduite par le retrait de la contribution de la perte due aux films supraconducteurs à haute température de la perte totale mesurée de manière expérimentale de la cavité.

Les meilleurs échantillons HTS sont des films épitaxiaux formés sur des substrats cristallins plats, en effet aucun film de grande qualité n'a été jusqu'ici formé sur une surface arrondie. Il est donc nécessaire de disposer d'une technique qui peut utiliser ces petits échantillons plats, qui n'exige aucune préparation des échantillons, qui n'endommage ni n'altère le film, qui est hautement répétable, qui présente une grande sensibilité (jusqu'à 1/1 000e de la résistance de surface R_s du cuivre), qui présente une large plage dynamique (jusqu'à la résistance de surface R_s du cuivre), qui peut atteindre des puissances internes élevées avec de faibles puissances d'entrée et qui présente une large couverture de températures (4,2 K à 150 K).

La méthode du résonateur diélectrique a été choisie parmi plusieurs méthodes de détermination de la résistance de surface aux hyperfréquences, car elle s'est avérée la plus populaire et la plus pratique actuellement. Plus particulièrement, le résonateur saphir est un excellent outil de mesure de la résistance de surface R_s des matériaux supraconducteurs à haute température [12] [13] [14].

La méthode d'essai spécifiée dans le présent document peut également être appliquée à d'autres éléments supraconducteurs, y compris les matériaux à faible T_c.

Le présent document est destiné à fournir une base technique appropriée et convenable pour le moment aux ingénieurs qui travaillent dans le domaine de l'électronique et des technologies liées à la supraconductivité.

[1] Les chiffres entre crochets se réfèrent à la bibliographie.

La méthode d'essai couverte par le présent document repose sur le travail de normalisation préalable réalisé dans le cadre du Programme de Versailles sur les matériaux de pointe et les normes (VAMAS – Versailles Project on Advanced Materials and Standards) sur les propriétés des films fins supraconducteurs.

SUPRACONDUCTIVITÉ –

Partie 7: Mesurages des caractéristiques électronique – Résistance de surface des supraconducteurs haute température critique aux hyperfréquences

1 Domaine d'application

La présente partie de l'IEC 61788 décrit le mesurage de la résistance de surface (R_s) des supraconducteurs aux hyperfréquences par la méthode normalisée à deux résonateurs. L'objet du mesurage est la dépendance de la résistance de surface R_s vis-à-vis de la température à la fréquence de résonance.

La plage de mesures applicable des résistances de surface R_s pour cette méthode est la suivante:

– Fréquence: 8 GHz < f < 30 GHz
– Résolution de mesure: 0,01 mΩ à 10 GHz

Les données de R_s à la fréquence mesurée, et celles mises à l'échelle à 10 GHz, en prenant pour hypothèse la règle de comparaison f^2, doivent être consignées.

2 Références normatives

Les documents suivants cités dans le texte constituent, pour tout ou partie de leur contenu, des exigences du présent document. Pour les références datées, seule l'édition citée s'applique. Pour les références non datées, la dernière édition du document de référence s'applique (y compris les éventuels amendements).

IEC 60050-815, *Vocabulaire Électrotechnique International (IEV) – Partie 815: Supraconductivité*

3 Termes et définitions

Pour les besoins du présent document, les termes et définitions de l'IEC 60050-815 s'appliquent.

L'ISO et l'IEC tiennent à jour des bases de données terminologiques destinées à être utilisées en normalisation, consultables aux adresses suivantes:

- IEC Electropedia: disponible à l'adresse http://www.electropedia.org/
- ISO Online browsing platform: disponible à l'adresse http://www.iso.org/obp

4 Exigences

La résistance de surface R_s d'un film supraconducteur doit être mesurée en appliquant un signal hyperfréquences à un résonateur diélectrique avec l'éprouvette de film supraconducteur, puis en mesurant l'affaiblissement du résonateur à chaque fréquence. La fréquence doit être balayée autour de la fréquence de résonance au centre, et les caractéristiques de fréquence d'affaiblissement doivent être consignées afin d'obtenir une valeur Q correspondant à la perte.

L'incertitude type composée relative cible de cette méthode est inférieure à 20 % pour la plage de températures de mesure comprise entre 20 K et 80 K.

Il incombe à l'utilisateur du présent document d'établir, avant de l'utiliser, des pratiques d'hygiène et de sécurité appropriées et de déterminer l'applicabilité des restrictions réglementaires.

Ce type de mesure présente certains dangers. Il est essentiel d'utiliser un système cryogénique pour refroidir les supraconducteurs et permettre leur passage à l'état supraconducteur. Un contact direct de la peau avec des composants froids de l'appareillage peut provoquer une congélation immédiate, comme le peut un contact direct avec un produit cryogène qui s'est déversé. L'utilisation d'un générateur de radiofréquences est également essentielle au mesurage des propriétés haute fréquence des matériaux. Si sa puissance est trop élevée, un contact direct avec des personnes peut provoquer des brûlures immédiates.

5 Appareillage

5.1 Système de mesure

La Figure 1 présente un schéma du système exigé pour le mesurage aux hyperfréquences. Ce système est composé d'un système d'analyseurs de réseau pour la mesure de transmission, d'un appareil de mesure et d'un thermomètre pour surveiller la température de mesure.

Une puissance incidente générée par une source hyperfréquence adaptée (un analyseur synthétisé, par exemple) est appliquée au résonateur diélectrique fixé dans l'appareil de mesure. Les caractéristiques de transmission sont présentées sur l'écran de l'analyseur de réseau. L'appareil de mesure est placé dans un cryoréfrigérateur à régulation de température.

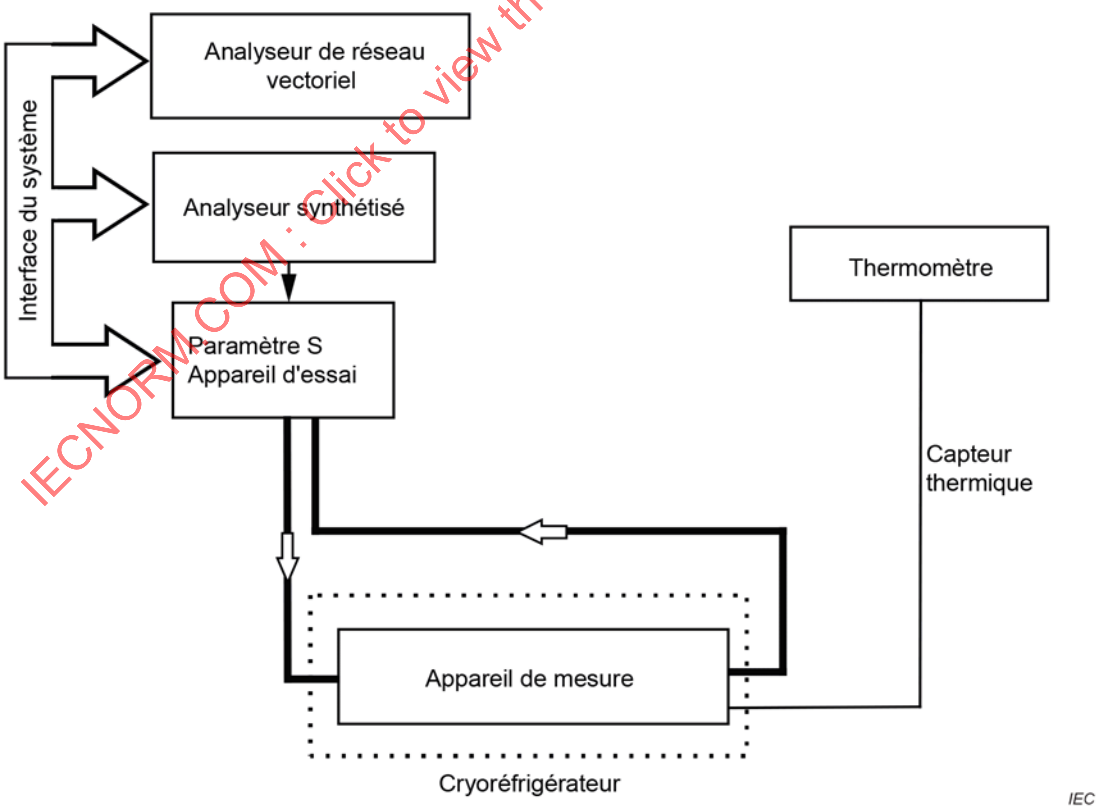

Figure 1 – Schéma du système de mesure de la dépendance de la résistance de surface R_s vis-à-vis de la température à l'aide d'un cryoréfrigérateur

Pour le mesurage de la résistance de surface R_s des films supraconducteurs, un analyseur de réseau vectoriel est recommandé. Un analyseur de réseau vectoriel présente une meilleure fidélité de mesure qu'un analyseur de réseau scalaire, en raison de sa large plage dynamique. Les exigences de performances de l'analyseur de réseau vectoriel sont présentées en 7.1.

5.2 Appareil de mesure de R_s

La Figure 2 présente le schéma d'un appareil de mesure classique (résonateur fermé) de la résistance de surface R_s des films HTS déposés sur un substrat avec une surface plane. Le film HTS supérieur est comprimé à l'aide d'un ressort en bronze phosphoreux. Il convient d'utiliser le ressort à plaque pour améliorer l'incertitude de mesure. Ce type de ressort permet de réduire le frottement entre le ressort et l'autre partie de l'appareil, et d'assurer la fluidité de mouvement des films supraconducteurs en raison de la dilatation thermique de la tige diélectrique. Pour réduire le plus possible l'incertitude de mesure, la tige de saphir et l'anneau en cuivre doivent être coaxiaux.

Deux câbles semi-rigides de mesure des caractéristiques de transmission du résonateur doivent être fixés des deux côtés du résonateur dans une position axiale symétrique (ϕ = 0 et π, où ϕ est l'angle de rotation autour de l'axe central de la tige de saphir). L'extrémité de chacun des deux câbles semi-rigides doit comporter une petite boucle. Le plan de la boucle doit être parallèle à celui des films supraconducteurs afin de supprimer les modes d'ondes magnétiques transverses (TM_{mn0}) non souhaités. Les boucles de couplage doivent être soigneusement vérifiées pour détecter des fissures dans le joint soudé par points qui peuvent s'être développées lors de cycles thermiques répétés. Ces câbles peuvent se déplacer vers la droite et la gauche pour ajuster l'affaiblissement d'insertion (IA). Lors de cet ajustement, le couplage des modes de cavité non souhaités au mode de résonance diélectrique concerné doit être supprimé. Le couplage parasite non souhaité aux autres modes permet de réduire la valeur Q élevée du résonateur de mode électromagnétique transverse TE. Pour supprimer le couplage parasite, la conception des résonateurs Q élevés doit faire l'objet d'une attention particulière. Deux autres types de résonateurs, avec celui de type fermé représenté à la Figure 2, peuvent être utilisés. Ils sont expliqués en A.4.

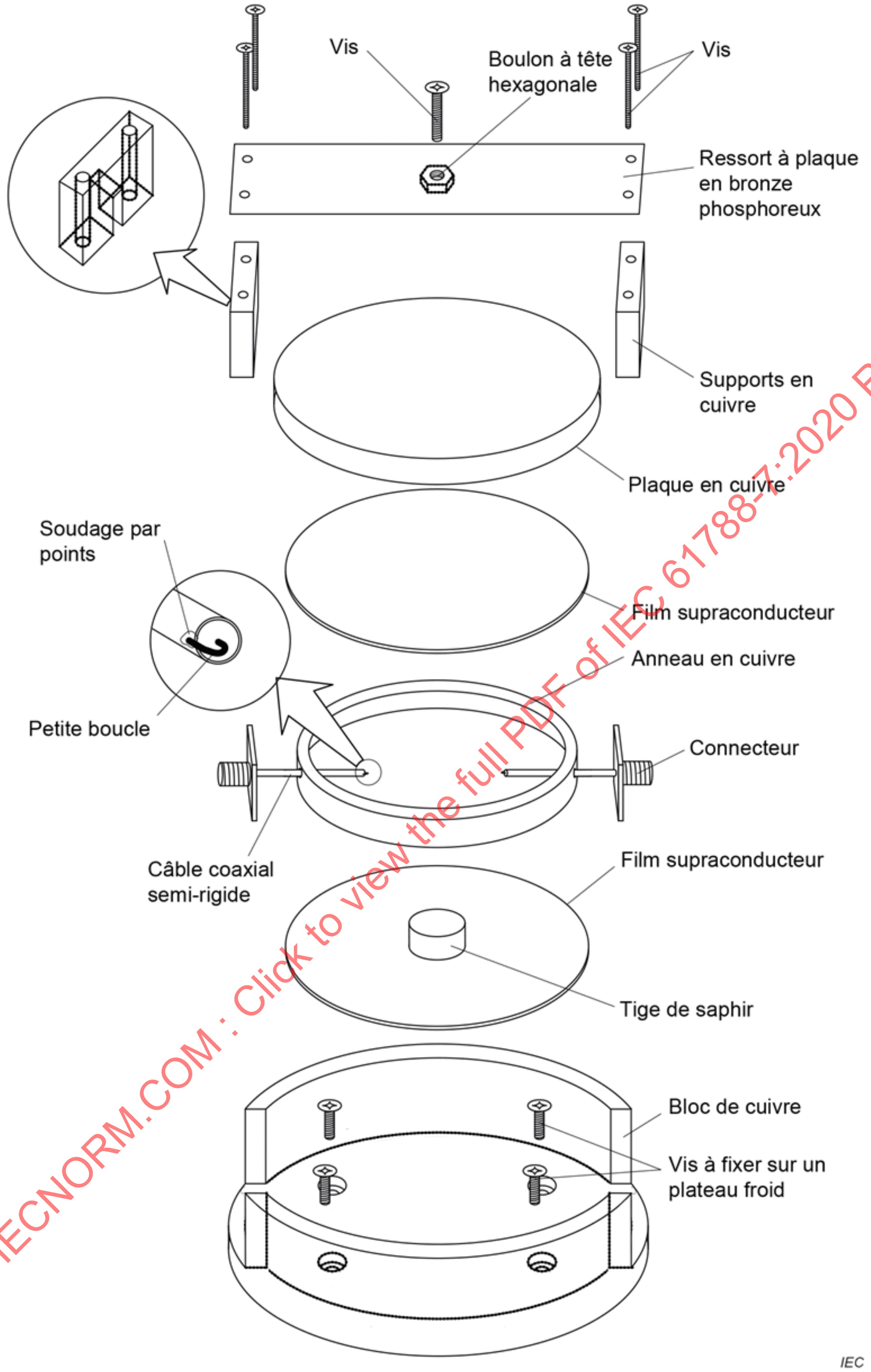

Figure 2 – Appareil de mesure classique de R_s

Une ligne de référence composée d'un câble semi-rigide doit être utilisée pour mesurer le niveau de puissance de transmission totale, c'est-à-dire le niveau de référence. La longueur de ce câble est égale à la somme des deux câbles de l'appareil de mesure. Le câble semi-rigide de diamètre extérieur de 1,20 mm est recommandé.

Pour réduire le plus possible l'incertitude de mesure, deux films supraconducteurs doivent être placés en parallèle. Pour veiller à ce que les deux films supraconducteurs restent en contact étroit avec les extrémités de la tige de saphir, sans entrefer, les deux surfaces des films et les extrémités de la tige doivent être soigneusement nettoyées.

5.3 Tiges diélectriques

Deux tiges diélectriques présentant une permittivité relative identique, ε', et un facteur de perte, tan δ, de préférence prélevés sur une tige diélectrique cylindrique, sont exigées. Ces deux tiges (tiges diélectriques normalisées) doivent présenter le même diamètre, mais des hauteurs différentes: l'une doit être trois fois supérieure à celle de l'autre.

Il est préférable d'utiliser des tiges diélectriques dont la valeur tan δ est faible afin d'obtenir l'incertitude de mesure exigée sur R_s. Les tiges diélectriques recommandées sont les tiges de saphir monocristallin dont tan δ est inférieur à 2 × 10^{-7} à 77 K. Les spécifications relatives aux tiges de saphir sont présentées en 7.1. Pour réduire le plus possible les erreurs de mesure de la résistance de surface R_s des films supraconducteurs, les deux extrémités des tiges de saphir doivent être polies parallèles l'une à l'autre et perpendiculaires à l'axe. Des spécifications relatives aux tiges de saphir sont données à l'Article 7.

Le diamètre et les hauteurs des tiges de saphir normalisées doivent être soigneusement conçus de manière à ne pas coupler les modes TE_{011} et TE_{013} à d'autres modes TM, HE et EH, étant donné que le couplage entre le mode TE et les autres modes provoque la dégradation de Q à vide. Des lignes directrices de conception pour les tiges de saphir normalisées sont données à l'Article A.5. Le Tableau 1 donne des exemples classiques de tiges de saphir normalisées pour une résonance de 12 GHz, de 18 GHz et de 22 GHz. Pour le mesurage de R_s à 22 GHz, le diamètre de film exigé peut être de 20 mm, et la valeur Q_L mesurée est faible, les effets de la perte diélectrique de la tige de saphir pouvant donc être réduits.

Tableau 1 – Dimensions classiques de paires de tiges de saphir monocristallin pour 12 GHz, 18 GHz et 22 GHz

Fréquence GHz		Diamètre, d mm	Hauteur, h mm
12	Tige courte (résonateur TE_{011})	11,40 ± 0,05	5,70 ± 0,05
	Tige longue (résonateur TE_{013})	11,40 ± 0,05	17,10 ± 0,05
18	Tige courte (résonateur TE_{011})	7,60 ± 0,05	3,80 ± 0,05
	Tige longue (résonateur TE_{013})	7,60 ± 0,05	11,40 ± 0,05
22	Tige courte (résonateur TE_{011})	6,20 ± 0,05	3,10 ± 0,05
	Tige longue (résonateur TE_{013})	6,20 ± 0,05	9,30 ± 0,05

6 Procédure de mesure

6.1 Préparation de l'éprouvette

Pour l'estimation de l'incertitude, le diamètre du film doit être environ trois fois plus grand que celui des tiges de saphir. Dans cette configuration, l'augmentation de l'incertitude de R_s en raison des différentes pertes par rayonnement entre le mode TE_{011} et le mode TE_{013} peut être considérée comme étant négligeable, compte tenu de l'incertitude type composée relative cible de 20 %. L'épaisseur de film doit être environ deux fois plus grande que la valeur de profondeur de pénétration du champ magnétique à la température maximale dans la plage de températures de mesure. Si l'épaisseur de film est bien inférieure à deux fois la profondeur de pénétration du champ magnétique, il convient que la R_s mesurée soit la résistance de surface efficace.

Le Tableau 2 donne les dimensions des films supraconducteurs des tiges de saphir normalisées de 12 GHz, 18 GHz et 22 GHz.

Tableau 2 – Dimensions du film supraconducteur pour 12 GHz, 18 GHz et 22 GHz

Tige de saphir à découpe en *c*		Film supraconducteur	
Fréquence GHz	**Diamètre**, d mm	**Diamètre**, d' mm	**Épaisseur** µm
12	11,40 ± 0,05	> 35	≅ 0,5
18	7,60 ± 0,05	> 25	≅ 0,5
22	6,20 ± 0,05	> 20	≅ 0,5

Dans le cas des résonateurs fermés, les dimensions des films supraconducteurs doivent également être prévues en tenant compte de la dimension du cylindre en cuivre entre les films supraconducteurs. Des lignes directrices de conception pour la dimension du cylindre en cuivre du résonateur fermé sont présentées à l'Article A.6.

6.2 Montage

Monter le matériel de mesure comme représenté à la Figure 1. Tous les appareils de mesure, tiges de saphir normalisées et films supraconducteurs doivent rester propres et secs, une humidité importante pouvant dégrader la valeur Q à vide. L'éprouvette et l'appareil de mesure doivent être placés dans un cryoréfrigérateur à régulation de température. La chambre de l'éprouvette doit être complètement sous vide. Les températures des films supraconducteurs et des tiges de saphir normalisées doivent être mesurées par un thermomètre à diode ou un couple thermoélectrique. Les températures des films supraconducteurs supérieur et inférieur et les tiges de saphir normalisées ne doivent pas différer de plus de 0,5 K. Pour ce faire, couvrir l'appareil de mesure d'une feuille d'aluminium ou remplir la chambre de l'éprouvette avec de l'hélium.

6.3 Mesurage du niveau de référence

Le niveau de puissance de transmission totale (niveau de référence) doit être mesuré en premier. Fixer la puissance de sortie de l'analyseur synthétisé sous 10 mW, l'incertitude de mesure dépendant du niveau du signal de mesure. Connecter la ligne de référence du câble semi-rigide entre les connecteurs d'entrée et de sortie. Ensuite, mesurer le niveau de puissance de transmission sur l'ensemble de la fréquence de mesure et de la plage de températures. Le niveau de référence peut varier de plusieurs décibels si la température de l'appareil passe de la température ambiante à la température de mesure la plus basse. Par conséquent, la dépendance du niveau de référence vis-à-vis de la température doit être prise en considération.

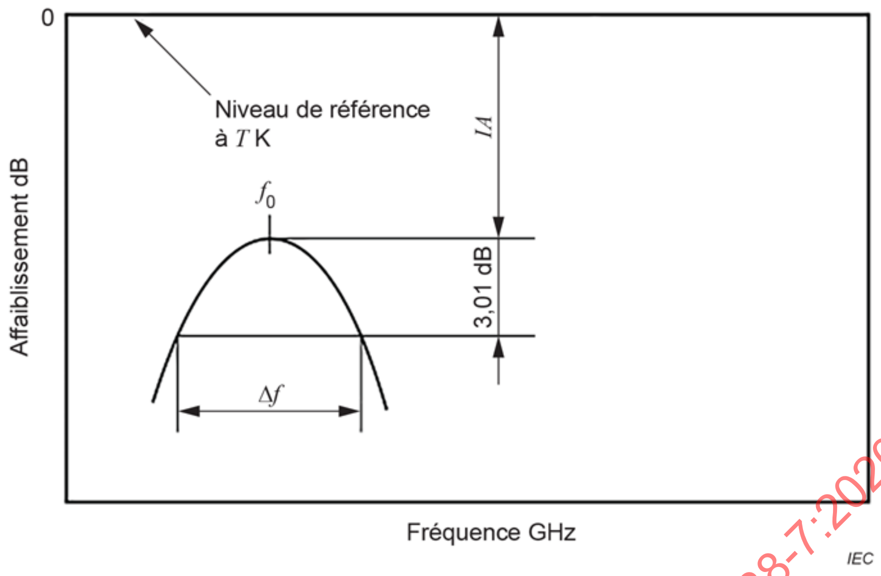

Figure 3 – Affaiblissement d'insertion IA, fréquence de résonance f_0 et bande passante à mi-puissance Δf, mesurés à T kelvin

6.4 Mesurage de la réponse en fréquence des résonateurs

La dépendance de la résistance de surface R_s vis-à-vis de la température peut être obtenue en mesurant la fréquence de résonance f_0 et le facteur de qualité à vide Q_u pour les résonateurs TE_{011} et TE_{013}, qui doivent être mesurés comme suit.

a) Connecter l'appareil de mesure entre les connecteurs d'entrée et de sortie (Figure 1). Insérer la courte tige de saphir normalisée à proximité du centre du film supraconducteur inférieur, et placer la tige et chacune des boucles des câbles semi-rigides à égale distance, de sorte que ce résonateur à transmission puisse être sous-couplé de manière égale aux autres boucles. Déposer doucement le film supraconducteur pour le faire entrer en contact avec la face supérieure de la tige. Veiller à ne pas appuyer trop fort pour ne pas endommager la surface du film supraconducteur. Faire le vide dans la chambre de l'éprouvette et la refroidir sous la température critique.

b) Déterminer le pic de résonance du mode TE_{011} de ce résonateur à une fréquence pratiquement égale à la valeur de conception de f_0.

c) Réduire l'intervalle de fréquence sur l'affichage de manière à ne pouvoir afficher que le pic de résonance du mode TE_{011} (Figure 3). Confirmer que l'affaiblissement d'insertion IA de ce mode est supérieur à 20 dB par rapport au niveau de référence, qui dépend fortement de la température.

d) Mesurer la dépendance de f_0 vis-à-vis de la température et la bande passante à mi-puissance Δf. La valeur Q à vide, Q_L, du résonateur TE_{011} est donnée par

$$Q_L = \frac{f_0}{\Delta f} \tag{1}$$

e) La valeur Q à vide, Q_u, doit être extraite de Q_L selon au moins l'une des deux techniques décrites ci-dessous.

   1) Une technique d'extraction de la valeur Q à vide implique de mesurer l'affaiblissement d'insertion IA. Q_u est donné par

$$Q_u = \frac{Q_L}{1 - A_t}, A_t = 10^{-IA[\text{dB}]/20} \tag{2}$$

L'affaiblissement d'insertion IA de chaque température est déterminé comme suit. Dans le système de mesure R_s représenté à la Figure 2, un câble semi-rigide est connecté en lieu et place de l'appareil de mesure, et le système de mesure est court-circuité afin de déterminer le niveau de référence. Mesurer le niveau de référence à chaque température et l'utiliser pour déterminer IA à chaque température.

Cette technique d'utilisation de l'affaiblissement d'insertion prend pour hypothèse que le couplage est identique des deux côtés du résonateur. Les boucles de couplage sont difficiles à fabriquer, l'orientation de la boucle est difficile à contrôler et tous les mouvements de la tige de saphir pendant le mesurage ne sont pas connus. Ces effets dépendants de l'assemblage dépendent également de la température. Cette éventuelle asymétrie de couplage peut donner lieu à d'importantes erreurs de calcul du facteur de couplage si le couplage est important (IA <~ 10 dB). Si le couplage est suffisamment faible (IA > 20 dB), l'asymétrie du couplage devient moins importante.

2) Une autre technique d'extraction de la valeur Q à vide implique de mesurer les facteurs de répartition de la réflexion à la fréquence de résonance des deux côtés du résonateur.

$$Q_u = Q_L(1 + \beta_1 + \beta_2) \tag{3}$$

$$\beta_1 = \frac{1 - |S_{11}|}{|S_{11}| + |S_{22}|} \tag{4}$$

$$\beta_2 = \frac{1 - |S_{22}|}{|S_{11}| + |S_{22}|} \tag{5}$$

Dans les Équations (4) et (5), S_{11} et S_{22} sont les facteurs de répartition de la réflexion (voir la Figure 4) et sont mesurés en unités de puissance linéaires, pas en dB relatif. β_1 et β_2 sont les facteurs de couplage.

Cette technique d'utilisation des facteurs de répartition de la réflexion présente deux avantages. Elle n'exige pas d'étape supplémentaire d'étalonnage du niveau de référence et donne une mesure des valeurs de couplage des deux côtés du résonateur. Cette technique présente également deux inconvénients. Elle ne fonctionne que pour une résonance à bande étroite (ce qui est heureusement le cas) et est limitée par la plage dynamique de l'analyseur de réseau dans le mesurage des facteurs de réflexion [15] [16].

Une combinaison des deux techniques est utile pour «doubler» la vérification.

f) Les valeurs f_0 et Q_u mesurées pour cette courte tige sont appelées f_{01} et Q_{u1} pour la résonance du mode TE_{011}. En faisant lentement varier la température du cryoréfrigérateur, la dépendance vis-à-vis de la température de f_{01} et Q_{u1} doit être mesurée.

g) À l'issue du mesurage de la dépendance vis-à-vis de la température de f_{01} et Q_{u1}, l'appareil de mesure doit être chauffé jusqu'à la température ambiante.

h) Ensuite, remplacer le résonateur TE_{011} dans l'appareil par le résonateur TE_{013} à température ambiante, refroidir l'appareil à une température inférieure à la température critique, puis mesurer la dépendance vis-à-vis de la température de f_0 et Q_u de son mode de résonance TE_{013}, appelés f_{03} et Q_{u3}, comme pour le cas du résonateur TE_{011}. Si la longueur de la tige de saphir du résonateur TE_{013} est précisément trois fois supérieure à celle du résonateur TE_{011}, la valeur f_{03} du résonateur TE_{013} doit coïncider avec la valeur f_{01} du résonateur TE_{011}. S'il est convenablement conçu, la différence entre f_{01} et f_{03} est souvent très faible (<~ 0,25 %). Il peut être considéré que f_0 de l'équation (9) peut être remplacé par f_{01} ou f_{03}.

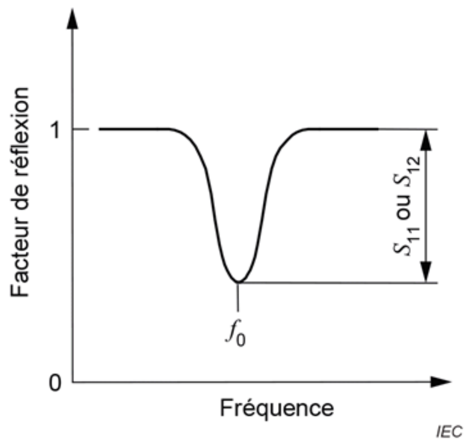

Figure 4 – Facteurs de répartition de la réflexion (S_{11} et S_{22})

6.5 Détermination de la résistance de surface du supraconducteur et ε' et tan δ des tiges de saphir normalisées

Calculer la dépendance vis-à-vis de la température de la résistance de surface de R_s des films supraconducteurs, puis ε' et tan δ des tiges de saphir normalisées à l'aide de la dépendance vis-à-vis de la température de Q_{u1} et Q_{u3}. Q_{u1} et Q_{u3} peuvent être calculés à l'aide des équations (1) et (2). Si les températures mesurées pour Q_{u3} se révèlent être sensiblement différentes de celles de Q_{u1}, une interpolation peut être utilisée pour préparer des valeurs de température ajustées pour l'une aux mêmes températures pour l'autre. Les Équations (6) à (12) sont établies dans la cavité de type ouvert, mais si la taille du film supraconducteur est trois fois plus importante que le diamètre de la tige de saphir, ces équations peuvent être utilisées pour une cavité de type fermé.

$$R_s = \frac{30\pi^2 \times 3}{(3-1)} \left(\frac{2h_0}{\lambda 0} \right)^3 \frac{\varepsilon' + W}{1+W} \left(\frac{1}{Q_{u1}} - \frac{1}{Q_{u3}} \right) \quad (6)$$

$$\varepsilon' = \left(\frac{\lambda 0}{\pi d} \right)^2 \left(u^2 + v^2 \right) + 1 \quad (7)$$

$$\tan \delta = \frac{1 + \frac{W}{\varepsilon'}}{(3-1)} \left(\frac{3}{Q_{u3}} - \frac{1}{Q_{u1}} \right) \quad (8)$$

où

$$\lambda_0 = \frac{c}{f_0} \quad (9)$$

$$W = \frac{J_1^2(u)}{K_1^2(v)} \frac{K_0(v)K_2(v) - K_1^2(v)}{J_1^2(u) - J_0(u)J_2(u)} \quad (10)$$

$$v^2 = \left(\frac{\pi d}{\lambda_0}\right)^2 \left[\left(\frac{3\lambda_0}{2h_0}\right)^2 - 1\right] \tag{11}$$

$$u\frac{J_0(u)}{J_1(u)} = -v\frac{K_0(v)}{K_1(v)} \tag{12}$$

Dans les équations, λ_0 est la longueur d'onde de résonance en espace libre, c est la vitesse de la lumière dans le vide (c = 2,997 9 × 10^8 m/s), h_0 est la hauteur de la courte tige diélectrique normalisée. La valeur u^2 est donnée par l'Équation (12) transcendantale utilisant la valeur de v^2, où $J_n(u)$ est la fonction de Bessel de premier ordre, et $K_n(v)$ la fonction de Bessel modifiée de second ordre. Les dérivées des équations sont décrites à l'Article A.3.

En règle générale, le facteur de dilatation thermique des tiges doit être connu pour déterminer la dépendance de leur taille vis-à-vis de la température. Toutefois, les effets de dilatation thermique des tiges de saphir peuvent être négligés pour l'incertitude type relative cible de la résistance de surface R_s (20 %).

Il est à noter que la résistance de surface R_s mesurée signifie qu'il s'agit de la résistance de surface efficace si l'épaisseur du film est deux fois inférieure à la profondeur de pénétration en fonction de la température.

7 Incertitude de la méthode d'essai

7.1 Résistance de surface

La résistance de surface (R_s) doit être déterminée à partir de la valeur Q mesurée par la technique du résonateur diélectrique.

Un analyseur de réseau vectoriel (voir le Tableau 3) doit être utilisé pour enregistrer la dépendance de l'affaiblissement vis-à-vis de la fréquence. L'enregistrement obtenu doit permettre de déterminer Q selon une incertitude relative de 10^{-2}.

Tableau 3 – Spécifications pour l'analyseur de réseau vectoriel

Plage dynamique de S_{21}	supérieure à 60 dB
Résolution de fréquence	inférieure à 1 Hz
Incertitude d'affaiblissement	inférieure à 0,1 dB
Limitation de puissance d'entrée	inférieure à 10 dBm

Les résonateurs diélectriques doivent être équipés de deux tiges diélectriques avec un faible tan δ inférieur à 2 × 10^{-7} à 77 K et un rayon inférieur à 1/3 du rayon de l'éprouvette de supraconducteur. Le saphir est le meilleur candidat pour les tiges (voir le Tableau 4). Les définitions terminologiques du Tableau 4 sont représentées à la Figure 5.

Tableau 4 – Spécifications pour les tiges de saphir

Diamètre	±0,05 mm
Hauteur	±0,05 mm
Planéité	inférieure à 0,005 mm
Rugosité de surface	surface supérieure et inférieure: inférieure à 10 nm en valeur efficace surface cylindrique: inférieure à 0,001 mm en valeur efficace
Perpendicularité	dans les limites de 0,1 degré
Axe	parallèle à l'axe *c* à 0,3° près

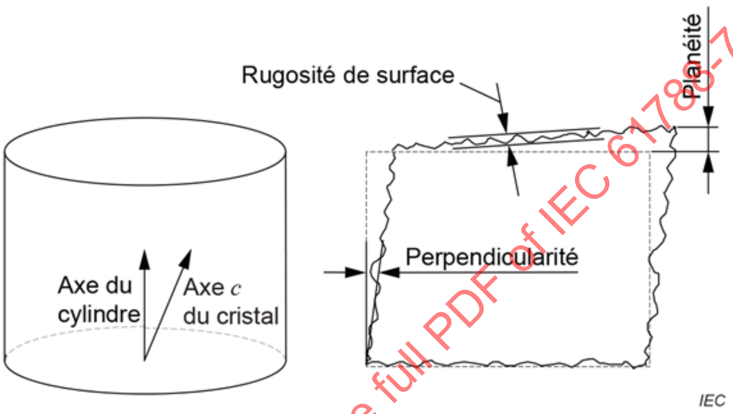

Figure 5 – Définitions terminologiques du Tableau 4

La technique décrite prend pour hypothèse qu'une hauteur simple et triple de tiges de saphir peut être fabriquée avec le même tan δ. Toutefois, la variation du tan δ entre des tiges identiques d'un point de vue nominal, découpées dans la même boule et polies selon la même technique, peut être large de deux ordres d'amplitude. À ce jour, la plus faible variation du tan δ entre des tiges de saphir identiques d'un point de vue nominal présente un facteur de quatre. Par conséquent, l'incertitude du tan δ mesuré est importante. La variation du tan δ de la présente tige de saphir est à l'origine d'une incertitude supplémentaire jusqu'à au moins 10 % dans le mesurage de la résistance de surface. Cela limite l'incertitude cible de la présente technique à 5 %. Si la reproductibilité des tiges de saphir est améliorée ou si une méthode de sélection des tiges de saphir normalisées est établie, une incertitude cible peut être améliorée.

7.2 Température

L'appareil de mesure est refroidi à la température spécifiée par tous les moyens lors de l'essai. Un choix pertinent consisterait à plonger l'appareil dans un cryogène liquide. Cette technique est rapide et simple, et permet d'obtenir une température connue et stable. Malheureusement, la plupart des matériaux HTS sont endommagés par la condensation de l'humidité qui se produit lorsque l'échantillon est retiré du cryogène. De plus, les incertitudes générées par la présence d'un mélange de gaz et de liquide à l'intérieur de la cavité, et l'inaptitude à mesurer R_s en fonction de la température plaident en faveur d'autres méthodes de refroidissement. Ces limitations peuvent être contournées par l'immersion d'un caisson à vide dans le cryogène liquide. Si le caisson à vide peut être rempli avec du gaz, un refroidissement rapide et des températures uniformes sont obtenus. Si des éléments chauffants sont associés à l'appareil, la dépendance du matériau HTS vis-à-vis de la température peut être mesurée. Un troisième choix, très bon également, consiste à utiliser un cryoréfrigérateur. Dans ce cas, le résonateur est placé sous vide et refroidi par conduction à l'aide d'un boîtier métallique. Les gradients de température avec l'appareil doivent être évités.

Un cryostat doit être prévu avec l'environnement nécessaire à la mesure de R_s, et l'éprouvette doit être mesurée à l'état stable et isotherme. Par hypothèse, la température de l'éprouvette est identique à la température du porte-éprouvette. La température du porte-éprouvette doit être consignée à ±0,5 K, mesurée au moyen d'un capteur de température approprié.

La différence entre la température de l'éprouvette et la température du porte-éprouvette doit être réduite le plus possible à l'aide de blindages présentant une bonne conductivité thermique.

7.3 Structure de l'éprouvette et du support

La structure du support doit assurer un maintien adapté de l'éprouvette. Les deux films doivent être parallèles et doivent présenter une stabilité mécanique tout au long du mesurage, plus particulièrement dans un cryoréfrigérateur et sur une plage de températures étendue. Le parallélisme des deux films peut être obtenu à l'aide d'une tige de saphir satisfaisant aux spécifications décrites dans le Tableau 4.

7.4 Protection de l'éprouvette

La condensation de l'humidité et les rayures du film détériorent les propriétés de supraconduction. Il convient de prévoir des mesures de protection pour les éprouvettes. Les revêtements en polytétrafluoroéthylène (PTFE) ou en polyméthylméthacrylate (PMMA) n'ont aucun impact sur les mesurages, et peuvent donc être utilisés pour la protection. Une épaisseur de matériau de revêtement inférieure à quelques micromètres est recommandée.

7.5 Incertitude de la résistance de surface mesurée par la méthode normalisée à deux résonateurs

Pour la méthode de résonance diélectrique, le tan δ des tiges de saphir du mode TE_{011} et celui du mode TE_{013} sont par hypothèse absolument égaux. Si le tan δ des deux tiges de saphir est différent, la résistance de surface ne peut pas être calculée à l'aide de l'Équation (6). Les effets d'un écart de tan δ sur la résistance de surface ont été vérifiés (voir l'Annexe B). L'incertitude de la résistance de surface hyperfréquences des supraconducteurs par la méthode du résonateur diélectrique dépend de la taille, de la constante diélectrique, du tan δ des tiges de saphir et de l'incertitude du Q mesuré du résonateur. L'incertitude type composée relative est inférieure à 20 % (voir l'Annexe B)

8 Rapport d'essai

8.1 Identification de l'éprouvette d'essai

L'éprouvette d'essai doit être identifiée, si possible, par les éléments suivants:

a) nom du fabricant de l'éprouvette;
b) classification et/ou symbole;
c) numéro de lot;
d) composition chimique du film fin et du substrat;
e) épaisseur et rugosité du film fin;
f) technique du processus de fabrication.

8.2 Consignation des valeurs R_s

Les valeurs R_s à la fréquence mesurée et celles échelonnées à 10 GHz, accompagnées de leurs valeurs f_{01}, f_{03}, Q_{u1}, Q_{u3}, IA et/ou (β_1, β_2), ε' et tan δ correspondantes, et leur dépendance vis-à-vis de la température doivent être consignées.